

KP THEORY, PLANE-BIPARTITE NETWORKS IN THE DISK, AND RATIONAL DEGENERATIONS OF M-CURVES

SIMONETTA ABENDA AND PETR G. GRINEVICH

ABSTRACT. We associate real and regular algebraic-geometric data to the class of multi-line soliton solutions of Kadomtsev-Petviashvili II (KP) equation whose asymptotic behavior in space-time has been recently classified using the combinatorial structure of the totally non-negative part of real Grassmannians $Gr^{\text{TNN}}(k, n)$. In our construction we directly relate real and regular KP divisors on reducible M-curves to the classification of networks parametrizing a given positroid cell in $Gr^{\text{TNN}}(k, n)$.

2010 MSC. 37K40; 37K20, 14H50, 14H70.

KEYWORDS. Total positivity, KP hierarchy, real solitons, M-curves, Le-diagrams, planar bipartite networks in the disk, Baker-Akhiezer function.

CONTENTS

1. Introduction	2
2. The totally nonnegative Grassmannian	9
2.1. The planar oriented bipartite trivalent network \mathcal{N}_T associated to the Le-tableau	15
2.2. Planar bipartite networks \mathcal{N} and the totally non-negative Grassmannian	18
3. KP-II multi-line solitons	19
3.1. The heat hierarchy and the dressing transformation	19
3.2. Real finite-gap KP solutions and M-curves	23
4. Algebraic-geometric approach for KP soliton data in $Gr^{\text{TNN}}(k, n)$	26
4.1. The reducible rational curve $\Gamma(\mathcal{N})$	27
4.2. The KP divisor on $\Gamma(\mathcal{N})$	34
5. A system of vectors on the Le-network	41
5.1. A representation of the rows of the RREF matrix using the Le-tableau	41

This research has been partially supported by GNFM-INDAM and RFO University of Bologna, by the Russian Foundation for Basic Research, grant 17-01-00366, by the program “Fundamental problems of nonlinear dynamics”, Presidium of RAS. Partially this research was fulfilled during the visit of the second author (P.G.) to IHES, Universit Paris-Saclay, France in November 2017.

5.2.	Recursive construction of the row vectors $E^{(\tau)}[l]$ using the Le–diagram	43
6.	Proof of Theorem 4.1 on $\Gamma(\mathcal{N}_T)$	48
6.1.	A vacuum vertex wavefunction on the Le–network	50
6.2.	The vacuum vertex divisor	55
6.3.	The vacuum wavefunction on $\Gamma(\mathcal{N}_T)$ and its pole divisor	57
7.	Systems of vectors for general trivalent perfect bipartite oriented networks	63
7.1.	The system of vectors and its basic properties for fixed gauge and fixed orientation	64
7.2.	Rational representation of the components of E_e and null vectors	70
7.3.	The dependence of E_e on the gauge ray direction \mathfrak{l}	73
7.4.	The dependence of E_e on the orientation of the graph	74
8.	The effect of moves and reductions on the system of vectors	79
8.1.	(M1) The square move	80
8.2.	(M2) The unicolored edge contraction/uncontraction	81
8.3.	(M3) The middle edge insertion/removal	83
8.4.	(R1) The parallel edge reduction and (R2) the dipole reduction	83
8.5.	(R3) The leaf reduction	84
9.	The construction of the KP divisor on $\Gamma(\mathcal{N})$	85
9.1.	The modified network \mathcal{N}'	87
9.2.	The vacuum and the KP vertex wavefunctions	89
9.3.	The vacuum wavefunction $\hat{\phi}$ on $\Gamma(\mathcal{N})$	97
9.4.	The KP wavefunction $\hat{\psi}$ on $\Gamma(\mathcal{N})$ and the proof of Theorem 4.2.	101
10.	The combinatorial characterization of the reality and regularity conditions for both the vacuum and the KP divisors.	105
11.	The effect of Postnikov moves and reductions on the KP divisor	115
	References	120

1. INTRODUCTION

In this paper we continue our work [2] and we associate real and regular algebraic–geometric data to the class of multi–line soliton solutions of Kadomtsev–Petviashvili II (KP) equation whose asymptotic behavior in space–time has been successfully classified using the combinatorial structure of the totally non–negative part of real Grassmannians in a series of recent works

[6, 7, 9, 10, 12, 35, 36, 37, 38, 61]. In our text the notation **KP always means KP II**, with the heat conductivity operator in the Lax pair.

The motivation of our research is to connect two relevant approaches for constructing real regular exact solutions of KP equation, which can be used to model waves in the shallow water approximation (the surface tension is assumed to be negligible).

The simplest way to construct nonlinear superposition of line solitons is to use Darboux transformations [48], [21]. Relation between the regularity of real KP solutions and non-negativity of all maximal minors was first pointed out in [45]. The asymptotic structure of such solutions was studied in a series of paper, including [6, 7, 9, 10, 12, 35, 36, 37, 38, 61]. In this setting the multi-line soliton solution is encoded by the following soliton data: a set of ordered phases $\mathcal{K} = \{\kappa_1 < \dots < \kappa_n\}$ and a point in the totally non-negative part of a real Grassmannian, $[A] \in Gr^{\text{TNN}}(k, n)$. Moreover, a non-trivial result of [37] shows that if one considers only the first three real KP times x, y, t , i.e. one considers only the KP equation itself, but not the other members of the KP hierarchy, the total non-negativity remains necessary for the reality and regularity of multi-line solutions.

It is also well-known that, in principle, such solutions can be obtained by degenerating finite-gap solutions [51]. Let us remark that, using deeper degenerations, corresponding to the conditions on the wave functions analogous to those considered in [14], one can construct other interesting classes of solutions, including the rational ones. For additional information about singular spectral curves in soliton theory see [57].

According to [39, 40], finite-gap KP solutions are parametrized by the following algebraic-geometrical data: a finite genus g Riemann surface with a marked point, fixed local parameter near this point and non-special divisor of degree g . As it was pointed out by S.P. Novikov, in problems of real multi-soliton solutions it is natural to assume that we degenerate real quasi-periodic regular solutions. Real regular finite-gap KP solutions (let us recall that in our text KP always means KP II) correspond to the so-called M-curves (see, for instance, [30, 29, 50, 59]) with natural constraints on divisor positions [16]: by definition, this curve has $g + 1$ real ovals, one of them contains the marked point, and each other oval contains exactly one divisor point.

Therefore it is natural to assume that to any point of $Gr^{\text{TNN}}(k, n)$, one can associate an appropriate degenerate M-curve equipped with a proper divisor (of course, the curve is not unique). In our work we use the positroid stratification of $Gr^{\text{TNN}}(k, n)$, which is naturally related to the Gelfand-Serganova stratification of the complex Grassmannian $Gr(k, n)$ [25, 26]. Let us point

out, that the positivity conditions essentially simplify the problem; the geometrical structure of the strata for generic Grassmannians can be as complicated as essentially any algebraic variety [46].

In [45], it was shown that the dressed KP wavefunction carries a real k point divisor on a rational curve Γ_0 with n marked points corresponding to the phases \mathcal{K} and a marked point corresponding to the essential singularity of the KP wavefunction. However a soliton data in the main cell, $[A] \in Gr^{TP}(k, n)$, depends on $k(n - k)$ parameters. Therefore, under genericity assumption on the data, it is natural to expect that it may be realized from the rational degeneration of a real regular finite gap solution associated to an M-curve of genus $g \geq k(n - k)$. It is then natural, following the approach of [41] for degenerate finite-gap solutions, to look for a **reducible** (rational) curve.

In [2] we started from KP soliton data from the main cell, corresponding to the totally positive part of real Grassmannian, $Gr^{TP}(k, n)$, and we constructed a family of reducible (rational) M-curves of genus $g = k(n - k)$ and real regular divisors, generating these solutions. In the present paper we extend this construction to all points of $Gr^{TNN}(k, n)$. More precisely, we associate a canonical curve Γ to any planar graph in the disk, describing the corresponding cell in Postnikov's approach [52], and the points of the cell are parametrized by the positions of the real regular divisors.

Let us point out that in literature there are well-known relations of different nature between networks, algebraic curves and integrable systems: for dimer models with periodic boundary conditions (models on tori) the Riemann surfaces arise as the spectral curves for operators on networks on tori [34], and such spectral curves, which generically are regular, may be associated to classical or quantum integrable systems [27].

Another big area of activity is currently associated with the use of planar networks in the disk for studying scattering amplitudes in $N = 4$ super Yang-Mills on-shell diagrams, see [4], [5]. We have noticed an analogy between the momentum-helicity conservation relations in the trivalent planar networks in the approach of [4], [5], and the relations satisfied by the vacuum and dressed vertex wave functions in our approach. It is unclear to us whether our approach for KP may be interpreted as a scalar analog of a field theoretic model.

The concept of totally positive matrix was first introduced in [56]. The property of total positivity naturally arise in many applications, and usually is connected with some reality properties of the system. Important connections between positivity and oscillatory properties of mechanical

systems were found in [22], [23]. The extensions of positivity property to integral kernels were investigated in [33]. Extension of the total positivity to split reductive connected algebraic groups and flag manifolds was suggested in [43],[44]. The total positivity in classical and generalized sense is one of the basic concepts in the theory of cluster manifolds and cluster algebras [19, 20], see also the book [24]. Applications of the theory of total positivity in Lie groups to the study of homomorphisms of the fundamental group of a closed surface into a Lie group is considered in [17]. Non-negativity of systems of modified Bessel functions of the first kind, arising during the solution of non-linear differential equations in a model of overdamped Josephson junction was studied in [8]. Of course, this list of literature is far from being complete. For our applications we mainly follow [52].

The main results. The main construction follows the idea in [2]: on the reducible curve Γ we first construct a vacuum wavefunction which coincides with Sato vacuum wavefunction on a rational component Γ_0 and satisfies the following conditions: at the so-called Darboux source points such vacuum wave function coincides with appropriate generators of the Darboux transformation. The Darboux dressing corresponds to a special shift of divisor: we add zeroes at the Darboux source points and k -order pole at P_0 . Then the normalized dressed wavefunction is the Baker-Akhiezer function for the given soliton datum on Γ , and its divisor coincides with Sato divisor on Γ_0 and satisfies the reality and regularity conditions expected from the finite-gap theory. The main improvement of the present generalization to any soliton data in $Gr^{\text{TNN}}(k, n)$ comes from the fact that we directly relate our construction of real and regular divisors on reducible curves to the classification of networks parametrizing a given positroid cell in $Gr^{\text{TNN}}(k, n)$ in [52].

More precisely, for any fixed soliton data $(\mathcal{K}, [A])$, we choose a planar trivalent bipartite network in the disk \mathcal{N} move-reduction equivalent to the Le-network \mathcal{N}_T for $[A] \in Gr^{\text{TNN}}(k, n)$. To the graph of \mathcal{N} we naturally associate a unique reducible rational curve Γ using the following correspondence:

- (1) The boundary of the disk is the rational component Γ_0 containing the essential singularity of the KP wavefunction and the Sato divisor;
- (2) Each (bivalent or trivalent) vertex corresponds to a rational component of Γ . The black and white colors are related to the different analytic properties of the normalized KP wavefunction on the corresponding rational component. The divisor points are associated to white trivalent vertexes;

- (3) Each edge corresponds to a double point of Γ where different components are glued. Therefore, the trivalency assumption implies that each \mathbb{CP}^1 component carries three marked points and we may avoid the introduction of parameters marking double points;
- (4) Faces of the network correspond to ovals of Γ ;
- (5) The perfect orientation of the graph is associated to a well-defined choice of coordinates on the rational components of Γ .

In particular, to the Le-graph \mathcal{N}_T of a $|D|$ dimensional positroid cell in $Gr^{\text{TNN}}(k, n)$, we associate a real plane curve $\Gamma(\mathcal{N}_T)$ with $|D| + 1$ ovals, which is the rational degeneration of an M-curve of genus $g = |D|$. If the soliton data belong to the top cell $Gr^{\text{TP}}(k, n)$, then $|D| = k(n - k)$ and the curve $\Gamma(\xi)$ constructed in [2] corresponds to a particular desingularization of $\Gamma(\mathcal{N})$ which reduces the number of rational components to $k + 1$.

We directly relate the construction of both the vacuum and the dressed wavefunction on $\Gamma(\mathcal{N})$ to the network \mathcal{N} .

As a first step, on \mathcal{N} we construct systems of **edge** vectors satisfying linear relations at the vertexes. Each component of a given edge vector is computed by summing the weights of all paths starting at the given edge and ending at the same boundary sink vertex. We introduce gauge rays to compute generalized winding numbers and to count the boundary sources crossed by each path. Any such system of edge vectors satisfies appropriate boundary conditions and we thoroughly investigate its dependence on the choice of the gauge ray direction and on the orientation of the network. We also explain how the edge vectors change if we transform the network to a move-reduction equivalent one.

In the special case of the Le-network \mathcal{N}_T with Postnikov natural orientation, we also provide a recursive construction of one such system of vectors; such recursion generalizes the algebraic construction of systems of vectors in [2] for soliton data in $Gr^{\text{TP}}(k, n)$.

The second step consists in the construction of a vertex vacuum wavefunction $\Phi(\vec{t})$ and of its dressing $\Psi(\vec{t})$ on the network for any given system of vectors. We modify the original network adding an univalent internal vertex next to each boundary source vertex using Postnikov move (M2) in order that the vacuum vertex wavefunction satisfies Sato boundary conditions on Γ_0 and in order to associate an edge vector to each Darboux point. To prove the invariance of the KP divisor we also add an univalent internal vertex next to each boundary sink vertex. Then, using the linear relations at the vertexes, we associate to each trivalent white vertex of the modified network \mathcal{N}' a vacuum and a dressed divisor number.

Both \mathcal{N} and \mathcal{N}' have $g + 1$ faces, the number of trivalent white vertexes is $g - k$ in the original network \mathcal{N} , and $g + n - k$ in the modified network \mathcal{N}' . Therefore both the vacuum and the dressed network divisors have degree $g + n - k$.

Using the correspondence between edges at vertexes and marked points on rational components of Γ , we build a meromorphic vacuum normalized wavefunction $\hat{\phi}(P, \vec{t})$ and a meromorphic KP normalized wavefunction $\hat{\psi}(P, \vec{t})$ on $\Gamma \setminus \{P_0\}$ imposing that at all marked points they respectively coincide with the vacuum and the dressed vertex wavefunctions. Therefore, by construction both wavefunctions satisfy the compatibility conditions at all double points for all times \vec{t} . Thanks to the linear relations at the vertexes, both $\hat{\phi}(P, \vec{t})$ and $\hat{\psi}(P, \vec{t})$ have the following analytic properties:

- (1) On Γ_0 they coincide respectively with Sato vacuum and Sato dressed normalized wavefunctions for all \vec{t} ;
- (2) On each rational component corresponding to a bivalent vertex or a trivalent black vertex both $\hat{\phi}$ and $\hat{\psi}$ are independent of the spectral parameter for all \vec{t} ;
- (3) On each rational component corresponding to a trivalent white vertex both $\hat{\phi}$ and $\hat{\psi}$ are meromorphic of degree less than or equal to one in the spectral parameter, for all \vec{t} ;
- (4) In the vacuum network divisor the $n - k$ vacuum network divisor numbers corresponding to the Darboux sink vertexes are trivial; therefore we define an effective degree g vacuum divisor $\mathcal{D}_{\text{vac}, \Gamma(\mathcal{N})}$ on Γ depending on the given orientation of the network and such that for almost all \vec{t} , $(\hat{\phi}(P, \vec{t}) + \mathcal{D}_{\text{vac}, \Gamma(\mathcal{N})} \geq 0$;
- (5) In the dressed network divisor the n dressed network divisor numbers corresponding to the Darboux sources and sink vertexes are trivial; therefore we define an effective degree g KP divisor $\mathcal{D}_{\text{KP}, \Gamma}$ as the set of points in Γ which correspond to the union of the Sato divisor and of the reduced dressed network divisor, obtained eliminating the n points corresponding to the trivial Darboux sink and source network divisor numbers. By construction, for almost all \vec{t} , $(\hat{\psi}(P, \vec{t}) + \mathcal{D}_{\text{KP}, \Gamma} \geq 0$;
- (6) The pole divisors of both the vacuum and the dressed normalized wavefunctions are independent of \vec{t} and belong to the union of all ovals.

The KP divisor $\mathcal{D}_{\text{KP}, \Gamma}$ depends only on the soliton data $(\mathcal{K}, [A])$ and the network chosen to construct Γ (Theorem 4.2). The invariance on $\mathcal{D}_{\text{KP}, \Gamma}$ on the gauge ray direction and the orientation of the network used in the construction follows from the properties of the system of vectors defined on Γ : a change in the orientation of the network simply corresponds to a change of coordinate of the double points and of the KP pole divisor in the corresponding rational

component of Γ , which leaves invariant their relative positions. Instead, the vacuum divisor $\mathcal{D}_{\text{vac},\Gamma(\mathcal{N})}$ depends also on the base I in the matroid of $[A]$ and on the positions of the Darboux source points.

We finally check that the KP divisor $\mathcal{D}_{\text{KP},\Gamma}$ satisfies the reality and regularity conditions, *i.e.* that each finite oval contains exactly one divisor point in three different ways:

- (1) Directly in the case of general networks using the combinatorial characterization of the dressed network divisor;
- (2) Indirectly in the general case by proving that, in each finite oval, the total number of vacuum divisor points and of Darboux source points is odd, while the total number of vacuum divisor points, of Darboux source points plus k is even in the infinite oval;
- (3) Indirectly in the general case, using the direct proof in the case $\Gamma = \Gamma(\mathcal{N}_T)$ and then using the properties of transformation of the divisor points due to Postnikov moves and reductions.

Plan of the paper: We did our best to make the paper self-contained. In sections 2 and 3, we briefly present a review of the necessary results respectively for totally non-negative Grassmannians and KP soliton theory necessary in the rest of the paper. Section 4 contains the main construction and the statements of the principal theorems.

Sections 5 and 6 contain respectively the construction of the system of vectors on the Le-network \mathcal{N}_T based on the algebraic recursion which generalizes [2] and the proof of Theorem 4.1 in the case of $\Gamma(\mathcal{N}_T)$. We have decided to leave this case separate both because the reducible curve $\Gamma(\mathcal{N}_T)$ is the rational degeneration of a smooth \mathbb{M} -curve of minimal genus g equal to the dimension of the positroid cell and also to evidence the relations with the construction in [2].

In section 7 we construct and characterize systems of edge vectors on any network \mathcal{N} in the move-reduction equivalence class of the Le-network \mathcal{N}_T . In sections 9 and 10, we use such systems of vectors to generalize the construction of the vacuum and the KP wavefunctions on any $\Gamma(\mathcal{N})$ and characterize the reality and regularity properties of the KP divisor.

In section 8 we explain how edge vectors depend on Postnikov moves and reductions and then in section 11, we use the above to characterize the dependence of the vacuum and the dressed divisors on moves and reductions.

Notations: We use the following notations throughout the paper:

- (1) k and n are positive integers such that $k < n$;
- (2) for $s \in \mathbb{N}$ let $[s] = \{1, 2, \dots, s\}$; if $s, j \in \mathbb{N}$, $s < j$, then $[s, j] = \{s, s+1, s+2, \dots, j-1, j\}$;

- (3) $\vec{t} = (t_1, t_2, t_3, \dots)$, where $t_1 = x$, $t_2 = y$, $t_3 = t$;
- (4) $\theta(\zeta, \vec{t}) = \sum_{s=1}^{\infty} \zeta^s t_s$,
- (5) we denote the real phases $\kappa_1 < \kappa_2 < \dots < \kappa_n$ and $\theta_j \equiv \theta(\kappa_j, \vec{t})$.

2. THE TOTALLY NONNEGATIVE GRASSMANNIAN

In this section we fix the algebraic setting.

We first recall some useful definitions and theorems from [52] to make the paper self-contained. For more details on the topological properties of $Gr^{TNN}(k, n)$ and on generalizations of total positivity to reductive groups we refer to [43, 44, 47, 53, 54].

In Section 2.1 we associate to each Le-diagram D a unique bipartite trivalent oriented network \mathcal{N}_T , adapting the Postnikov rules [52] to our purposes. Using the graph associated to \mathcal{N}_T , in Section 4.1 we construct a curve $\Gamma(\mathcal{N}_T)$, which is a rational degeneration of a smooth M-curve of genus equal to the dimension $|D|$ of the corresponding positroid cell.

In Section 2.2 we recall some results from [52] concerning the class of planar bipartite trivalent networks \mathcal{N} in the disk associated to a given point in $Gr^{TNN}(k, n)$ which we use to generalize the construction of an effective KP divisor on $\Gamma(\mathcal{N})$, the rational degeneration of a smooth M-curve of genus $g \geq |D|$.

Definition 2.1. *The totally non-negative part of $Gr(k, n)$. The totally non-negative Grassmannian $Gr^{TNN}(k, n)$ is the subset of the Grassmannian $Gr(k, n)$ with all Plücker coordinates non-negative, i.e. it may be defined as the following quotient: $Gr^{TNN}(k, n) = GL_k^+ \backslash Mat_{kn}^{TNN}$. Here GL_k^+ is the group of $k \times k$ matrices with positive determinant, and Mat_{kn}^{TNN} is the set of real $k \times n$ matrices A of rank k such that all maximal minors are non-negative, i.e. $\Delta_I(A) \geq 0$, for all k -element subsets $I \subset [n]$.*

The totally positive Grassmannian $Gr^{TP}(k, n) \subset Gr^{TNN}(k, n)$ is the subset of $Gr(k, n)$ whose elements may be represented by $k \times n$ matrices with all strictly positive maximal minors $\Delta_I(A)$.

It is well-known that $Gr(k, n)$ is decomposed into a disjoint union of Schubert cells Ω_λ indexed by partitions $\lambda \subset (n-k)^k$ whose Young diagrams fit inside the $k \times (n-k)$ rectangle. A refinement of this decomposition was proposed in [25], [26]. Intersecting these strata with $Gr^{TNN}(k, n)$ one obtains the totally non-negative Grassmann cells [52] with the following property: each cell is birationally equivalent to an open octant of appropriate dimension, and this birational map is also a topological homeomorphism.

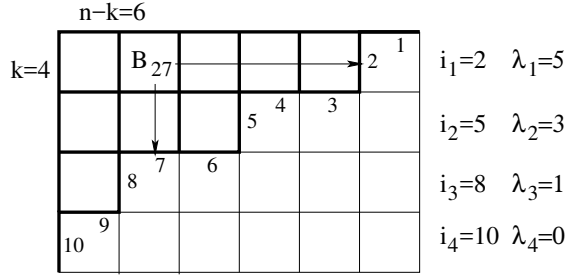


FIGURE 1. The Young diagram associated to the partition $(5, 3, 1, 0)$, $k = 4$, $n = 10$.

Let us recall these constructions. The Schubert cells are indexed by partitions, or, equivalently by pivot sets. To each partition $\lambda = (\lambda_1, \dots, \lambda_k)$, $n - k \geq \lambda_1 \geq \lambda_2 \dots \geq \lambda_k \geq 0$, $\lambda_j \in \mathbb{Z}$ there is associated a pivot set $I(\lambda) = \{1 \leq i_1 < \dots < i_k \leq n\}$ defined by the following relations:

$$(1) \quad i_j = n - k + j - \lambda_j, \quad j \in [k].$$

Each Schubert cell is the union of all Grassmannian points sharing the same set of pivot columns, since the pivot columns are invariant with respect to left multiplication by $k \times k$ invertible matrices. In particular, any $k \times n$ matrix representing a given point in Ω_λ with pivot set I can be transformed by row operations to the canonical echelon form, i.e. a matrix A such that $A_{i_l}^l = 1$ for $l \in [k]$ and all the entries to the left of these 1's are zero.

The Young diagram associated to the Schubert cell Ω_λ is a collection of boxes arranged in k rows, aligned on the left such that the j -th row contains λ_j boxes, $j \in [k]$.

Remark 2.1. *In this paper we use the **ship battle** rule to enumerate the boxes of the Young diagram of a given partition λ . Let $I = I(\lambda)$ be the pivot set of the k vertical steps in the path along the SE boundary of the Young diagram proceeding from the NE vertex to the SW vertex of the $k \times (n - k)$ bound box, and let $\bar{I} = [n] \setminus I$ be the non-pivot set is. Then the box B_{ij} corresponds to the pivot element $i \in I$ and the non-pivot element $j \in \bar{I}$ (see Figure 1 for an example).*

The refined decomposition of $Gr(k, n)$ into matroid strata[25] is defined by the following rule: each stratum is composed by the points of the Grassmannian which share the same set of non-zero Plücker coordinates. Each Plücker coordinate is indexed by a base, i.e. a k -element subset in $[n]$, and, for a given stratum, the set of these bases forms a matroid \mathcal{M} , i.e. for all $I, J \in \mathcal{M}$ for all $i \in I$ there exists $j \in J$ such that $I \setminus \{i\} \cup \{j\} \in \mathcal{M}$. Then the stratum $\mathcal{S}_{\mathcal{M}} \subset Gr(k, n)$ is defined as

$$\mathcal{S}_{\mathcal{M}} = \{[A] \in Gr(k, n) : \Delta_I(A) \neq 0 \iff I \in \mathcal{M}\}$$

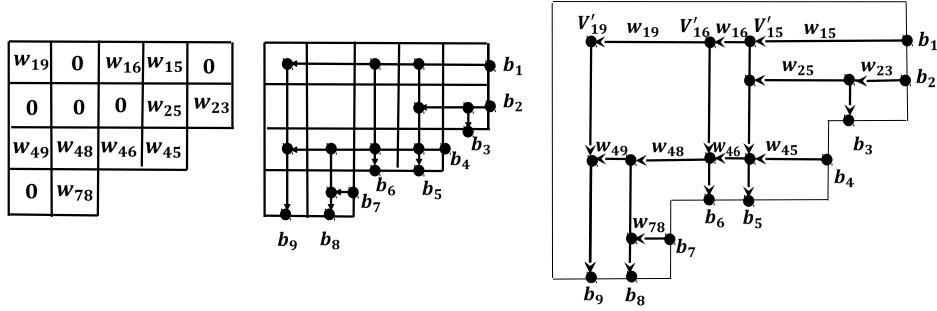


FIGURE 3. The Le -diagram and the Le -network of Example 2.2. The horizontal edges are oriented from right to left while the vertical ones from top to bottom.

- (2) G contains only vertical edges oriented downward and horizontal edges oriented to the left;
- (3) for any internal vertex v , the graph G contains the line going down from v till it reaches the boundary at some boundary sink, and the line going to the right of v till it reaches the boundary at some boundary source;
- (4) All pairwise intersections of such lines are also vertexes of G ;
- (5) The graph may contain isolated boundary vertexes which are assigned to be sources or sinks.

A Le -network associated to the Le -graph G is obtained assigning positive weights w_e to all oriented horizontal edges e and unit weight to all vertical edges.

The construction of the Le -graph associated to a given Le -diagram is as follows [52]. The boundary of the Young diagram of λ gives the lattice path of length n from the upper right corner to the lower left corner of the rectangle $k \times (n - k)$. Place a vertex in the middle of each step in the lattice path and mark the vertexes by b_1, \dots, b_n proceeding NE to SW. The vertexes b_i , $i \in I \equiv I(\lambda)$ corresponding to vertical steps are the sources of the network and the remaining vertexes b_j , $j \in \bar{I}$, corresponding to horizontal steps are the sinks. Connect the upper right corner to the lower left corner by another path to obtain a simple close curve containing the Young diagram. For each box of the Le -diagram (i, j) filled by 1 draw an internal vertex V_{ij} in the middle of the box and draw the vertical line which goes downwards from V_{ij} to the boundary sink and the horizontal line which goes to the right from V_{ij} to the boundary source.

By the Le-property any intersection of such lines is also a vertex. Orient all edges to the left and downwards.

To obtain a Le-network from a Le-tableaux of shape λ one constructs the Le-graph from the corresponding Le-diagram, assigns the weight $w_{ij} > 0$ from the box B_{ij} to the horizontal edge e which enters V_{ij} and assigns unit weights $w_e = 1$ to all vertical edges. Call the network \mathcal{N}_T . The correspondence between the Le-tableau and the Le-network is illustrated in Figure 3.

The map $T \mapsto \mathcal{N}_T$ gives the isomorphism $\mathbb{R}_{>0}^{|D|} \simeq \mathbb{R}_{>0}^{E(G)}$ between the set of Le-tableaux T with fixed Le-diagram D and the set of Le-networks (modulo gauge transformations) with fixed graph G corresponding to the diagram D as above.

Definition 2.5. [52] *Boundary measurement map.* For each Le-diagram D fitted in a $k \times (n - k)$ rectangle, define the boundary measurement map $Meas_D : T \mapsto Gr^{TNN}(k, n)$ as follows: $\Delta_J(Meas_D(T)) = \sum_{A \in \mathcal{A}_J(\mathcal{N}_T)} w(A)$, where

- (1) J is any k -element subset of $[n]$;
- (2) \mathcal{N}_T is the Le-network corresponding to the Le-tableau T and the boundary source set is labeled by I ;
- (3) $\mathcal{A}_J(\mathcal{N}_T)$ is the collection of non-intersecting directed path families $A = \{A_i\}_{i \in I}$ in \mathcal{N}_T from the boundary sources I to the boundary destinations J^\dagger . For any $i \in I \cap J$ the only path to the destination i is path without edges from i to itself, equipped with the weight 1.
- (4) $w(A) = \prod_{i \in I} w(A_i)$;
- (5) the weight of a path A_i in the family A is the product of the weights w_e of the edges $e \in A_i$: $w(A_i) = \prod_{e \in A_i} w_e$.

Theorem 2.1. (Theorem 6.5 [52]) For each Le-diagram as in Definition 2.5 the map $Meas_D$ is a well-defined map to the Grassmannian, i.e. the collection $\Delta_J(Meas_D(T))$ satisfy Plücker relations, moreover it is a subtraction-free parametrization of a certain totally nonnegative Grassmann cell $\mathcal{S}_M^{TNN} = Meas_D(\mathbb{R}_{>0}^{|D|}) \subset Gr^{TNN}(k, n)$. The Le-diagram has shape λ if and only if $\mathcal{S}_M^{TNN} \subset \Omega_\lambda$. The dimension of \mathcal{S}_M^{TNN} is $|D|$. Finally, for D of shape λ the map $Meas_D$ is I -polynomial, with $I = I(\lambda)$.

Given a Le-tableau T with pivot set I it is possible to reconstruct both the matroid and the representing matrix in reduced row echelon form using the Lindström lemma.

[†]We remark that the path collection is the same for all Le-tableau T associated with the given Le-diagram D . Nevertheless, it is convenient to keep the reference to T in $\mathcal{A}_J(\mathcal{N}_T)$, since all paths carry weights.

Proposition 2.1. [52] *Let \mathcal{N} be a network associated to the Le-diagram D and let I be the pivot set. For any k -elements subset $J \subset [n]$, let $K = I \setminus J$ and $L = J \setminus I$. Then the maximal minor $\Delta_J(A)$ of the matrix $A = A(\mathcal{N})$ is given by the following subtraction-free polynomial expression in the edge weights w_e :*

$$\Delta_J(A) = \sum_Q \prod_{i=1}^r w(Q_i),$$

where the sum is over all non-crossing collections $Q = (Q_1, \dots, Q_r)$ of paths joining the boundary vertexes b_i , $i \in K$ with boundary vertexes b_j , $j \in L$.

Let $i_r \in I$, where $r \in [k]$ and $j \in [n]$. Then the element A_j^r of the matrix A in reduced row echelon form (RREF) associated to the Le-network \mathcal{N} is

$$(2) \quad A_j^r = \begin{cases} 0 & j < i_r, \\ 1 & j = i_r, \\ (-1)^{\sigma_{i_r j}} \sum_{P: i_r \rightarrow j} \left(\prod_{e \in P} w_e \right) & j > i_r, \end{cases}$$

where the sum is over all paths P from the boundary source b_{i_r} to the boundary sink b_j , $j \in \bar{I}$, and $\sigma_{i_r j}$ is the number of pivot elements $i_s \in I$ such that $i_r < i_s < j$.

Example 2.2. *Let us consider the Le-diagram D and Le-network as in Figure 3. Then $I = (1, 2, 4, 7)$ and the matrix in reduced row echelon form is*

$$A = \begin{pmatrix} 1 & 0 & 0 & 0 & w_{15} & w_{15}(w_{16} + w_{46}) & 0 & -w_{15}w_{48}(w_{16} + w_{46}) & -w_{15}w_{48}w_{49}(w_{16} + w_{46}) - w_{15}w_{16}w_{19} \\ 0 & 1 & w_{23} & 0 & -w_{23}w_{25} & -w_{23}w_{25}w_{46} & 0 & w_{23}w_{25}w_{46}w_{48} & w_{23}w_{25}w_{46}w_{48}w_{49} \\ 0 & 0 & 0 & 1 & w_{45} & w_{45}w_{46} & 0 & -w_{45}w_{46}w_{48} & -w_{45}w_{46}w_{48}w_{49} \\ 0 & 0 & 0 & 0 & 0 & 0 & 1 & w_{78} & 0 \end{pmatrix}.$$

The same example is used in [38] to illustrate the combinatorial properties of the KP-soliton tropical asymptotics in the limit $t \rightarrow -\infty$.

Given any representative matrix A of a given point in $Gr^{\text{TNN}}(k, n)$, the boundary measurement map is given in terms of its Plücker coordinates $\{\Delta_I(A)\}$ by the conditions that $\Delta_I(A) \neq 0$ and

$$M_{ij} = \frac{\Delta_{(I \setminus \{i\}) \cup \{j\}}}{\Delta_I}, \quad \forall i \in I, \quad j \in \bar{I}.$$

The boundary measurement is invariant under the following gauge transformation of the weights w_e [52]: pick a collection of positive real numbers t_v , for any internal vertex $v \in \mathcal{N}$ and assume that $t_b = 1$ for each boundary vertex b . Let \mathcal{N}' be the network with the same directed graph as \mathcal{N} and weights $w'_e = w_e t_u t_v^{-1}$ for each directed edge $e = (u, v)$. Then \mathcal{N}' has the same boundary measurement as the network \mathcal{N} .

Remark 2.2. Reducible positroid cells *A totally non-negative cell $\mathcal{S}_{\mathcal{M}}^{TNN} \subset Gr^{TNN}(k, n)$ is reducible if its Le-diagram contains either rows or columns filled by 0s [52].*

If the j -th column of the Le-diagram is filled by zeroes, then there is no path in the Le-network with destination j , the RREF matrix A has the j -th column filled by zeroes. One may then represent the same point in a totally non-negative cell $\mathcal{S}_{\mathcal{M}'}^{TNN} \subset Gr^{TNN}(k-1, n)$, by eliminating the j -th column from the Le-diagram and the j -th column from the matrix A .

If the r -th line of the Le-diagram is filled by zeroes, then there is no path in the Le-network starting from the boundary source b_{i_r} , the r -th row of A contains just the pivot element. One may then represent the same point in a totally non-negative cell $\mathcal{S}_{\mathcal{M}'}^{TNN} \subset Gr^{TNN}(k-1, n-1)$, by eliminating the r -th row of the Le-diagram, eliminating the r -th row and the i_r -th columns from the matrix A and changing the sign of all elements of A_j^i with $i < r$ and $j > i_r$.

2.1. The planar oriented bipartite trivalent network \mathcal{N}_T associated to the Le-tableau.

In section 4.1, we model the construction of a rational degeneration of an M-curve on the Le-network: vertexes of the graph correspond to copies of \mathbb{CP}^1 and the gluing rules are ruled by its edges. Moreover, we associate an unique universal curve to each positroid cell. For this purpose we require a construction without parameters, therefore we require that each copy of \mathbb{CP}^1 associated to an internal vertex has three marked points. Moreover, the recursive construction of the wavefunction and the characterization of its divisor is technically simpler if modeled on a bipartite graph where black and white vertexes alternate. For the above reasons we follow Postnikov's rules to transform the Le-network \mathcal{N}_T into a planar bipartite perfect network with internal vertexes of degree at most three, and we continue to denote it with \mathcal{N}_T , since this transformation is well-defined.

Definition 2.6. Perfect graph. *Planar directed graph is a **perfect graph** if each internal vertex in G is either the initial vertex of exactly one edge or the final vertex of exactly one edge, and if each boundary vertex has degree one.*

Any planar directed network may be transformed into a network with a perfect graph with only trivalent internal vertexes without changing the boundary measurements M_{ij} . For the Le-graph the only transformation concerns degree four internal vertexes to a couple of trivalent vertexes of opposite colour as in [52] (see Figure 4).

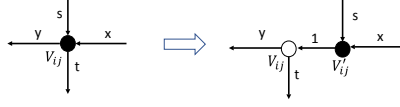


FIGURE 4. All internal vertexes of the Le -network are transformed to trivalent vertexes, preserving the boundary measurement map.

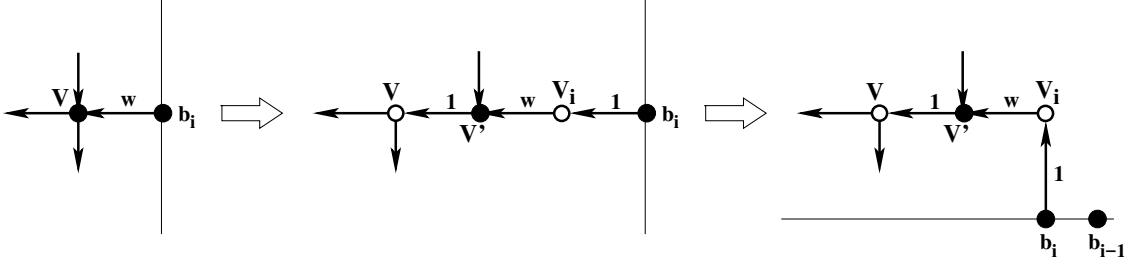


FIGURE 5. Transformation of graph at the boundary source b_i .

Following Postnikov [52], we assign black color to each internal vertex with exactly one outgoing edge and white color to each trivalent internal vertex with exactly one incoming edge. We also assign black color to all boundary vertexes.

We then transform the perfect trivalent network associated to the Le -diagram D into a **bi-partite network** \mathcal{N}_T with the following rules:

- (1) All internal vertexes corresponding to the same row in D lie on a horizontal line;
- (2) If the box B_{ij} of D is filled with 1, we transform the vertex V_{ij} in Figure 4[left] into a couple of one black vertex V'_{ij} and one white vertex V_{ij} ; we then assign unit weight to the horizontal edge joining the black vertex V'_{ij} to the white vertex V_{ij} and we keep invariant all other weights to preserve the boundary measurement map (see Figure 4[right]);
- (3) We assign black colour to all boundary vertexes. If the boundary source b_i is isolated, we add a horizontal edge of unit weight ending at a white vertex V_i . If the boundary source b_i is not isolated, we add a white vertex V_i to the edge of weight w starting at such boundary source, we assign unit weight to the edge joining b_i to V_i and weight w to the other edge of V_i (see Figure 5 middle);
- (4) We continuously deform the contour of the disk in such a way that all of the boundary sources and boundary sinks lay on the same horizontal line and the edge outcoming from

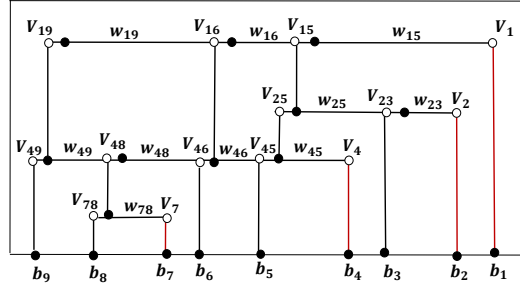


FIGURE 6. The bipartite Le -network for Example 2.2 (see Figure 3). The weights refer to the perfect orientation associated to the pivot base $[1, 2, 4, 7]$ of the matroid: the red vertical edges are oriented upwards, all black vertical edges are oriented downwards, while all horizontal edges are oriented from right to left.

the boundary source or sink is vertical, while leaving invariant the positions of all internal vertexes (see Figure 5 right).

In Figure 6 we show the bipartite Le -network for Example 2.2.

Remark 2.3. Let \mathcal{N}_T be the bipartite Le -network associated to the Le -diagram D . Then in \mathcal{N}_T

- (1) Each black vertex has **at most** one vertical edge;
- (2) Each white vertex has **exactly** one vertical edge;
- (3) For any $r \in [k]$, all vertexes associated to a given line r of D included the white source vertex V_{i_r} lie on the same horizontal line;
- (4) The total number of white vertexes is $|D| + k$;
- (5) If D is irreducible, then the total number of trivalent white vertexes is $|D| - k$, while the total number of trivalent black vertexes is $|D| - n + k$.

For any $r \in [k]$, we denote N_r the number of boxes filled with 1 in the r -th row of the Le -diagram D . By construction we have the following identities

(3)

$$N_r \equiv \# \{ \text{boxes } B_{i_r j} : j \in \bar{I} \} = \# \{ \text{white vertexes } V_{i_r j} : j \in \bar{I} \} = \# \{ \text{black vertexes } V_{i_r j} : j \in \bar{I} \}$$

$$|D| \equiv \sum_{i_r \in I} N_r = \# \{ \text{white vertexes } V_{i_r j} : i \in I, j \in \bar{I} \} = \# \{ \text{black vertexes } V_{i_r j} : i \in I, j \in \bar{I} \}.$$

Indeed, by construction, the number of white vertexes in each line of the bipartite Le -network is $1 + N_r$, since there is one such vertex for any box $B_{i_r j}$ filled by 1, $j \in \bar{I}$, and one white vertex is associated to the boundary source b_{i_r} . We also introduce an index to simplify the counting of boxes filled by ones. For any fixed $r \in [k]$, let $1 \leq j_1 < j_2 \cdots < j_{N_r} \leq n$ be the non-pivot

indexes of the boxes $B_{i_r j_s}$, $s \in \hat{N}_r$, filled by one in the r -th row. Then for any $r \in [k]$, we define the index

$$(4) \quad \chi_l^{i_r} = \begin{cases} 1 & \text{if there exists } s \in [N_r] \text{ such that } l = j_s, \\ 0 & \text{if } B_{i_r l} \text{ is filled by 0 or } l < i_r. \end{cases}$$

2.2. Planar bipartite networks \mathcal{N} and the totally non-negative Grassmannian. Any planar directed network in the disk may be transformed into a perfect network with trivalent internal vertexes without changing the boundary measurement [52].

In the next theorem we recall the invariance of the boundary measurement map w.r.t. changes of orientation in a perfect network. We shall relate such theorem to the invariance of effective divisor of the KP wavefunction in Section 4.

Theorem 2.2. [52] *Let $\mathcal{N} = (G, w)$ and $\mathcal{N}' = (G', w')$ be two perfect networks with k sources and $n - k$ sinks such that:*

- (1) *The graphs G and G' are isomorphic as undirected graphs;*
- (2) *Each internal vertex v of degree bigger than 2 has the same colour in both networks \mathcal{N} and \mathcal{N}' ;*
- (3) *If e is an edge that has the same orientation both in \mathcal{N} and \mathcal{N}' , then $w_e = w'_e$. If the edge e has opposite orientation in \mathcal{N} and \mathcal{N}' then $w_e = (w'_e)^{-1}$.*

Then the boundary measurement map Meas maps both networks to the same point in the Grassmannian $Gr(k, n)$.

Since the boundary measurement map is independent of the orientation of the graph, Postnikov[52] introduces weights on faces of \mathcal{N} to give an invariant formulation of such theorem. More precisely he introduces **plabic networks**, i.e planar bicolored undirected graphs with positive weights assigned to faces and boundary vertexes of unit degree.

A plabic network is called **perfectly orientable** if there exists an orientation of \mathcal{N} such that each white internal vertex possesses exactly one incoming edge and each internal black vertex exactly one outgoing edge. The plabic network is said to be **of type** (k, n) if it has n boundary vertexes and

$$(5) \quad k = \frac{1}{2} \left(n + \sum_{V_b} (\deg(V_b) - 2) + \sum_{V_w} (2 - \deg(V_w)) \right),$$

where the first sum runs on all black internal vertexes V_b and the second one on all white internal vertexes V_w .

Let f be a face of an oriented network with weights on the edges. The exterior boundary of f consists of some edges, say e_1, \dots, e_s . If f is not simply connected, then it has an hole in correspondence of each isolated component inside f . Let e_{s+1}, \dots, e_l be the edges of such holes. Orient clockwise the exterior boundary of f and counterclockwise the boundaries of such holes. Let I_f^+ be the subset of the edges e_1, \dots, e_l whose orientation in \mathcal{N} agrees with that of the face and I_f^- its complement. Then the **face weight** y_f of the face f in \mathcal{N} is

$$(6) \quad w(f) = \prod_{e \in I_f^+} w(e) \cdots \prod_{e \in I_f^-} w(e)^{-1}.$$

For an example see Figure 7. The weight of the face is invariant w.r.t. changes of orientation of \mathcal{N} according to Theorem 2.2.

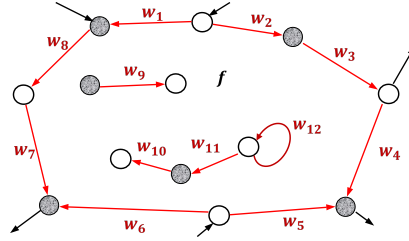


FIGURE 7. An example of computation of the face weight: $f = w_1^{-1}w_2w_3w_4w_5^{-1}w_6w_7^{-1}w_8^{-1}(w_9^{-1}w_9)(w_{10}^{-1}w_{11}^{-1}w_{12}w_{11}w_{10})$.

3. KP-II MULTI-LINE SOLITONS

In this section, we review the characterization of the real bounded regular multiline soliton solutions in the general class of KP-soliton solutions via Darboux transformations, Sato's dressing transformations and finite gap-theory. The KP-II equation [32]

$$(7) \quad (-4u_t + 6uu_x + u_{xxx})_x + 3u_{yy} = 0,$$

is the first non-trivial flow of an integrable hierarchy [11, 15, 31, 49, 55]. In the following we denote $\vec{t} = (t_1 = x, t_2 = y, t_3 = t, t_4, \dots)$.

3.1. The heat hierarchy and the dressing transformation. Multiline solitons may be realized starting from the soliton data $(\mathcal{K}, [A])$, where \mathcal{K} is a set of real ordered phases $\kappa_1 < \dots < \kappa_n$, $A = (A_j^i)$ is a $k \times n$ real matrix of rank k and $[A]$ denotes the point in the finite dimensional real Grassmannian $Gr(k, n)$ corresponding to A , which we parametrize using the maximal $k \times k$ minors of A (Plücker embedding).

Following [48], see also [21], let us consider k linear independent solutions

$$(8) \quad f^{(i)}(\vec{t}) = \sum_{j=1}^n A_j^i e^{\theta_j}, \quad i \in [k],$$

to the heat hierarchy[‡]

$$(9) \quad \partial_y f = \partial_x^2 f, \quad \partial_{t_l} f = \partial_x^l f, \quad l = 2, 3, \dots,$$

and define their Wronskian

$$(10) \quad \tau(\vec{t}) = Wr(f^{(1)}, \dots, f^{(k)}) \equiv \det \begin{vmatrix} f^{(1)} & \dots & f^{(k)} \\ \partial_x f^{(1)} & \dots & \partial_x f^{(k)} \\ \vdots & \ddots & \vdots \\ \partial_x^{n-1} f^{(1)} & \dots & \partial_x^{n-1} f^{(k)} \end{vmatrix} = \sum_I \Delta_I(A) \prod_{\substack{i_1 < i_2 \\ i_1, i_2 \in I}} (\kappa_{i_2} - \kappa_{i_1}) e^{\sum_{i \in I} \theta_i}$$

where the sum is over all k -element ordered subsets I in $[n]$, *i.e.* $I = \{1 \leq i_1 < i_2 < \dots < i_k \leq n\}$ and $\Delta_I(A)$ are the maximal minors of the matrix A , *i.e.* the Plücker coordinates for the corresponding point in the finite dimensional Grassmannian $Gr(k, n)$.

Then

$$(11) \quad u(\vec{t}) = 2\partial_x^2 \log(\tau(\vec{t}))$$

is a regular multi-line soliton solution to the KP equation (7) bounded for all real x, y, t if and only if $\Delta_I(A) \geq 0$, for all I [38]. In such case $A \in Mat_{k,n}^{\text{TNN}}$, the set of real $k \times n$ matrices of maximal rank k with non-negative maximal minors $\Delta_I(A)$. Let GL_k^+ be the group of $k \times k$ matrices with positive determinants. Since left multiplication by $k \times k$ matrices with positive determinants preserves the KP multisoliton solution $u(\vec{t})$ in (11), the soliton datum is $[A]$ the equivalence class of A , *i.e.* a point in the totally non-negative Grassmannian [52]

$$Gr^{\text{TNN}}(k, n) = GL_k^+ \backslash Mat_{k,n}^{\text{TNN}}.$$

Any given soliton solution is associated to an infinite set of soliton data $(\mathcal{K}, [A])$ and there exists a unique minimal pair (k, n) , such that the soliton solution can be realized with n phases $\kappa_1 < \dots < \kappa_n$, $[A] \in Gr^{\text{TNN}}(k, n)$ but not with $n - 1$ phases and $[A'] \in Gr^{\text{TNN}}(k', n')$ and either $(k', n') = (k, n - 1)$ or $(k', n') = (k - 1, n - 1)$.

[‡]We remark that the class of solutions to (9) that we consider in this paper is not the general one.

Definition 3.1. Regular and irreducible soliton data We call $(\mathcal{K}, [A])$ regular soliton data if $\mathcal{K} = \{\kappa_1 < \dots < \kappa_n\}$ and $[A] \in Gr^{TNN}(k, n)$, that is if the KP soliton solution as in (11) is real regular and bounded for all $(x, y, t) \in \mathbb{R}^3$.

Moreover we call the regular soliton data $(\mathcal{K}, [A])$ irreducible if $[A]$ is a point in the irreducible part of the real Grassmannian, i.e. if the reduced row echelon matrix A has the following properties:

- (1) Each column of A contains at least a non-zero element;
- (2) Each row of A contains at least one nonzero element in addition to the pivot.

If either (1) or (2) occur, we call the soliton data $(\mathcal{K}, [A])$ reducible.

Remark 3.1. If (1) in Definition 3.1 is violated for column l , then the phase κ_l does not appear in the solution (11). Then, one may remove such phase from \mathcal{K} , remove the zero column from A (see Remark 2.2) and realize the soliton in $Gr^{TNN}(k, n - 1)$.

If (2) in Definition 3.1 is violated for the row l , the heat hierarchy solution $f^{(l)}(\vec{t})$ contains only the phase κ_{i_l} , where i_l is the pivot index, and such phase is missing in all other heat hierarchy solutions, associated to RREF matrix. Therefore $f^{(l)}(\vec{t})$ is factored out in (10), and again, the corresponding phase is missing in (11). So one may eliminate such phase from \mathcal{K} , remove the corresponding row and pivot column from A , change all signs in the new matrix to the right of the removed column and above the removed row and realize the soliton in $Gr^{TNN}(k - 1, n - 1)$ (compare with Remark 2.2).

The class of solutions associated to irreducible regular soliton data has remarkable asymptotic properties both in the (x, y) plane at fixed time t and in the tropical limit ($t \rightarrow \pm\infty$), which have been successfully related to the combinatorial classification of the irreducible part $Gr^{TNN}(k, n)$ for generic choice of the phases \mathcal{K} in a series of papers (see [6, 7, 9, 10, 12, 35, 36, 37, 38, 61] and references therein).

According to Sato theory [55], the wavefunction associated to soliton data $(\mathcal{K}, [A])$, $[A] \in \mathcal{S}_{\mathcal{M}}^{TNN} \subset Gr^{TNN}(k, n)$ can be obtained from the dressing (inverse gauge) transformation of the vacuum (zero-potential) eigenfunction $\phi^{(0)}(\zeta, \vec{t}) = \exp(\theta(\zeta, \vec{t}))$, which solves

$$(12) \quad \partial_x \phi^{(0)}(\zeta, \vec{t}) = \zeta \phi^{(0)}(\zeta, \vec{t}), \quad \partial_{t_l} \phi^{(0)}(\zeta, \vec{t}) = \zeta^l \phi^{(0)}(\zeta, \vec{t}), \quad l \geq 2,$$

via the dressing (*i.e.* gauge) operator

$$W(\vec{t}) = 1 - \sum_{j=1}^{\infty} \mathfrak{w}_j(\vec{t}) \partial_x^{-j},$$

under the condition that W satisfies Sato equations $\partial_{t_l} W = B_l W - W \partial_x^l$, $l \geq 1$, where $B_l = (W \partial_x^l W^{-1})_+$ is the differential part of the operator $W \partial_x^l W^{-1}$. Then

$$L = W \partial_x W^{-1} = \partial_x + \frac{u(\vec{t})}{2} \partial_x^{-1} + \dots, \quad u(\vec{t}) = 2 \partial_x \mathfrak{w}_1(\vec{t}), \quad \psi^{(0)}(\zeta; \vec{t}) = W \phi^{(0)}(\zeta; \vec{t})$$

are respectively the KP-Lax operator, the KP-potential (KP solution) and the KP-eigenfunction, *i.e.*

$$L \psi^{(0)}(\zeta; \vec{t}) = \zeta \psi^{(0)}(\zeta; \vec{t}), \quad \partial_{t_l} \psi^{(0)}(\zeta; \vec{t}) = B_l \psi^{(0)}(\zeta; \vec{t}), \quad l \geq 2,$$

where $B_l = (W \partial_x^l W^{-1})_+ = (L^l)_+$.

The dressing transformation associated to the line solitons (11) corresponds to the following choice of the dressing operator

$$W = 1 - \mathfrak{w}_1(\vec{t}) \partial_x^{-1} - \dots - \mathfrak{w}_k(\vec{t}) \partial_x^{-k},$$

where $\mathfrak{w}_1(\vec{t}), \dots, \mathfrak{w}_k(\vec{t})$ are the solutions to the following linear system of equations

$$(13) \quad \partial_x^k f^{(i)} = \mathfrak{w}_1 \partial_x^{k-1} f^{(i)} + \dots + \mathfrak{w}_k f^{(i)}, \quad i \in [k].$$

In such case, $\mathfrak{w}_1(\vec{t}) = \partial_x \tau / \tau$, $u(\vec{t}) = 2 \partial_x \mathfrak{w}_1(\vec{t}) = 2 \partial_x^2 \log(\tau)$,

$$(14) \quad \mathfrak{D}^{(k)} \equiv B_k = (L^k)_+ = L^k = \partial_x^k - \mathfrak{w}_1(\vec{t}) \partial_x^{k-1} - \dots - \mathfrak{w}_k(\vec{t}),$$

and $\partial_{t_k} W = 0$. The KP-eigenfunction associated to this class of solutions is

$$\psi^{(0)}(\zeta; \vec{t}) = W \phi^{(0)}(\zeta; \vec{t}) = \left(1 - \frac{\mathfrak{w}_1(\vec{t})}{\zeta} - \dots - \frac{\mathfrak{w}_k(\vec{t})}{\zeta^k} \right) e^{\theta(\zeta; \vec{t})},$$

or, equivalently,

$$(15) \quad \mathfrak{D}^{(k)} \phi^{(0)}(\zeta; \vec{t}) = W \partial_x^k \phi^{(0)}(\zeta; \vec{t}) = \left(\zeta^k - \zeta^{k-1} \mathfrak{w}_1(\vec{t}) - \dots - \mathfrak{w}_k(\vec{t}) \right) \phi^{(0)}(\zeta; \vec{t}) = \zeta^k \psi^{(0)}(\zeta; \vec{t}).$$

We observe that $\mathfrak{w}_1, \dots, \mathfrak{w}_k$ is the solution to the linear system (13) if and only if $\mathfrak{D}^{(k)} f^{(i)} \equiv W \partial_x^k f^{(i)} = 0$, $i \in [k]$. Moreover, if the above identity holds, then $\partial_{t_l} (W_k f^{(i)}) = 0$, for all $l \in \mathbb{N}$, that is, by construction, the k -th order Darboux transformation is associated with the k eigenfunctions $f^{(1)}(\vec{t}), \dots, f^{(k)}(\vec{t})$, of the KP Lax Pair with zero potential for the infinite eigenvalue.

Definition 3.2. Sato divisor *Let the regular soliton data be $(\mathcal{K}, [A])$, $\mathcal{K} = \{\kappa_1 < \dots < \kappa_n\}$, $[A] \in Gr^{TNN}(k, n)$. We call Sato divisor at time \vec{t} , $\mathcal{D}_S^{(k)}(\vec{t})$, the set of roots of the characteristic equation associated to the Dressing transformation*

(16)

$$\mathcal{D}_S^{(k)}(\vec{t}) = \{\gamma_{S,j}(\vec{t}), j \in [k] : (\gamma_{S,j}(\vec{t}))^k - (\gamma_{S,j}(\vec{t}))^{k-1}\mathfrak{w}_1(\vec{t}) - \dots - \gamma_{S,j}(\vec{t})\mathfrak{w}_{k-1}(\vec{t}) - \mathfrak{w}_k(\vec{t}) = 0\}.$$

Remark 3.2. Sato divisor for reducible regular soliton data *Suppose that the r -th row of the RREF matrix A of the regular soliton data $(\mathcal{K}, [A])$, $\mathcal{K} = \{\kappa_1 < \dots < \kappa_n\}$, $[A] \in Gr^{TNN}(k, n)$, contains only the pivot element: $A_j^r = \delta_{j,i_r}$ for some $i_r \in [r, n]$. Then, for all \vec{t} , $\kappa_{i_r} \in \mathcal{D}_S(\vec{t})$, that is the characteristic polynomial associated to the Darboux differential operator satisfies*

$$(17) \quad \zeta^k - \zeta^{k-1}\mathfrak{w}_1(\vec{t}) - \dots - \mathfrak{w}_k(\vec{t}) = (\zeta - \kappa_{i_r}) \left(\zeta^{k-1} - \zeta^{k-2}\mathfrak{w}'_1(\vec{t}) - \dots - \mathfrak{w}'_{k-1}(\vec{t}) \right),$$

and

$$(18) \quad D' = W'\partial_x^{k-1} = \partial_x^{k-1} - \partial_x^{k-2}\mathfrak{w}'_1(\vec{t}) - \dots - \mathfrak{w}'_{k-1}(\vec{t})$$

is the Darboux transformation associated to the reduced soliton data $(\mathcal{K}', [A'])$, with $\mathcal{K}' = \mathcal{K} \setminus \{\kappa_{i_r}\}$, $[A'] \in Gr^{TNN}(k-1, n-1)$ and A' is obtained from A as in Remark 3.1.

3.2. Real finite-gap KP solutions and M-curves. Periodic and quasiperiodic solutions of the KP equation (7) are constructed using the finite-gap approach [39, 40]. The spectral data for this construction are: a finite genus g compact Riemann surface Γ with a marked point P_0 , a local parameter $1/\zeta$ near P_0 and a non-special divisor $\mathcal{D} = \gamma_1 + \dots + \gamma_g$ of degree g in Γ .

The Baker-Akhiezer function $\hat{\psi}(P, \vec{t})$, $P \in \Gamma$, is defined by the following analytic properties:

- (1) For any fixed \vec{t} the function $\hat{\psi}(P, \vec{t})$ is meromorphic in P on $\Gamma \setminus P_0$.
- (2) On $\Gamma \setminus P_0$ the function $\hat{\psi}(P, \vec{t})$ is regular outside the divisor points γ_j and has at most first order poles at the divisor points. Equivalently, if we consider the line bundle $\mathcal{L}(\mathcal{D})$ associated to \mathcal{D} , then for each fixed \vec{t} the function $\hat{\psi}(P, \vec{t})$ is a holomorphic section of $\mathcal{L}(\mathcal{D})$ outside P_0 .
- (3) $\hat{\psi}(P, \vec{t})$ has an essential singularity at the point P_0 with the following asymptotic:

$$\hat{\psi}(\zeta, \vec{t}) = e^{\zeta x + \zeta^2 y + \zeta^3 t + \dots} \left(1 - \chi_1(\vec{t})\zeta^{-1} - \dots - \chi_k(\vec{t})\zeta^{-k} - \dots \right).$$

For generic data these properties define an unique function, which is common eigenfunction for all KP hierarchy auxiliary linear operators $-\partial_{t_j} + B_j$, where $B_j = (L^j)_+^{\S}$, and the Lax operator

^{\S}here $()_+$ denotes the differential part

L is

$$L = \partial_x + \frac{u(\vec{t})}{2} \partial_x^{-1} + u_2(\vec{t}) \partial_x^{-2} + \dots$$

Therefore all these operators commute and the potential $u(\vec{t})$ satisfies the KP hierarchy. In particular, the KP equation arises for Zakharov-Shabat commutation representation [60] as the compatibility for the second and the third operator:

$$(19) \quad [-\partial_y + B_2, -\partial_t + B_3] = 0,$$

with $B_2 \equiv (L^2)_+ = \partial_x^2 + u$, $B_3 = (L^3)_+ = \partial_x^3 + \frac{3}{4}(u\partial_x + \partial_x u) + \tilde{u}$ and $\partial_x \tilde{u} = \frac{3}{4} \partial_y u$.

The Its-Matveev formula represents the KP hierarchy solution $u(\vec{t})$ in terms of the Riemann theta-functions associated with Γ (see, for example, [13]). After fixing a canonical basis of cycles $a_1, \dots, a_g, b_1, \dots, b_g$ and a basis of normalized holomorphic differentials $\omega_1, \dots, \omega_g$ on Γ , that is $\oint_{a_j} \omega_l = 2\pi i \delta_{jl}$, $\oint_{b_j} \omega_l = B_{lj}$, $j, l \in [g]$, the KP solution takes the form

$$(20) \quad u(\vec{t}) = 2\partial_x^2 \log \theta \left(\sum_j t_j U^{(j)} + z_0 \right) + c_1,$$

where θ is the Riemann theta function and $U^{(j)}$, are vectors of the b -periods of the following normalized meromorphic differentials, holomorphic on $\Gamma \setminus \{P_0\}$ and with principal parts $\hat{\omega}^{(j)} = d(\zeta^j) + O(1)$, at P_0 (see [39, 16]).

For physical applications the real regular solutions are the most relevant. The necessary and sufficient conditions on spectral data generating real regular KP hierarchy solutions for all real \vec{t} under the assumption that Γ is smooth were found in [16]:

- (1) Γ possesses an antiholomorphic involution $\sigma : \Gamma \rightarrow \Gamma$, $\sigma^2 = \text{id}$, which has the maximal possible number of fixed components (real ovals). This number is equal to $g + 1$, therefore (Γ, σ) is an M-curve.
- (2) P_0 lies in one of the ovals, and each other oval contains exactly one divisor points. The oval containing P_0 is called “infinite” and all other ovals are called “finite”.

The set of real ovals divides Γ into two connected components. Each of these components is homeomorphic to a sphere with $g + 1$ holes. In Figure 8(left) we show an example for $g = 2$.

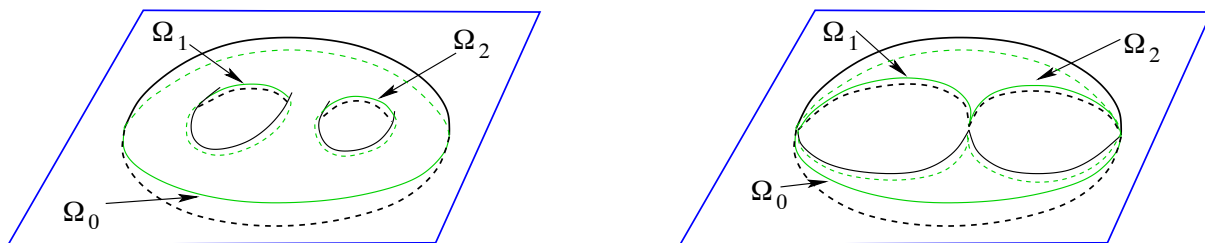


FIGURE 8. Left: a regular M-curve, $g = 2$, 3 real ovals (painted green), involution σ is reflection, orthogonal to the blue plane. Right: degeneration of a genus 2 M-curve, 3 real ovals (painted green).

Soliton KP solutions can be obtained from the finite-gap ones by proper degenerations of the spectral curve [40], [15]. The sufficiency part of the Theorem from [16] remains valid if the spectral curve Γ degenerates in such a way that the divisor remains in the finite ovals at a finite distance from the essential singularity [16]. But this condition is not necessary for degenerate curves.

Let us recall that in our construction the real part of the rational M-curve is represented by planar diagram. We assume that each real oval corresponds to a face of this diagram (see [2] for additional details). In this paper we construct the rational M-curves in Section 4 from the graphs associated with the given point of the totally-nonnegative Grassmannian $Gr^{TNN}(k, n)$. Each face of the graph corresponds to real oval. Having this in mind, we define the Baker-Akhiezer function associated with a given soliton data.

Definition 3.3. Real regular algebraic-geometrical data associated with a given soliton solution. Assume that we have a reducible connected curve Γ with a marked point P_0 , a local parameter $1/\zeta$ near P_0 , a non-special divisor \mathcal{D} on $\Gamma \setminus P_0$ and a normalized Baker-Akhiezer function $\hat{\psi}$ associated to such data. Assume also that we have fixed soliton data $(\mathcal{K}, [A])$, where \mathcal{K} is a collection of real phases $\kappa_1 < \kappa_2 < \dots < \kappa_n$, $[A] \in Gr^{TNN}(k, n)$.

$\hat{\psi}$ is the KP wave function on (Γ, P_0, ζ) associated to the soliton data $(\mathcal{K}, [A])$ if the irreducible component Γ_0 of Γ containing P_0 is \mathbb{CP}^1 , and the restriction of $\hat{\psi}$ to Γ_0 coincides with Sato normalized dressed wave function for the soliton data $(\mathcal{K}, [A])$.

Let $|D|$ be the dimension of the positroid cell to which $[A]$ belongs. Assume, in addition, that the curve Γ possesses $g + 1$ ovals, with $g \geq |D|$, that it may be obtained from a rational degeneration

of a smooth M-curve of genus g , and that the antiholomorphic involution preserves the maximum number of the ovals in the limit. Assume that the divisor \mathcal{D} has degree \mathfrak{d} , with $\mathfrak{d} = g$. Then we say that the divisor \mathcal{D} satisfies the reality and regularity conditions if P_0 belongs to one of the fixed ovals and the boundary of each other finite oval contains exactly one divisor point. In such case, the normalized Baker–Akhiezer function takes real values in the local parameter for any real \vec{t} and its pole divisor is contained in \mathcal{D} .

Of course, the algebraic-geometric data for a given soliton data $(\mathcal{K}, [A])$ are not unique. We can construct infinitely many curves generating the same soliton solutions.

In [2], to any soliton datum in $Gr^{\text{TP}}(k, n)$, we have associated a curve Γ , which is the rational degeneration of a smooth M-curve of minimal genus $k(n - k)$ and a degree $k(n - k)$ divisor satisfying the reality conditions of Dubrovin and Natanzon’s theorem. In Figure 8(right) we show the rational degeneration of the genus $g = 2$ curve, which we associate to soliton data in $Gr^{\text{TP}}(1, 3)$ and $Gr^{\text{TP}}(2, 3)$ [1], [2]. In the next Section we show how the construction from [2] may be extended to soliton data in arbitrary positroid strata in $Gr^{\text{TNN}}(k, n)$.

4. ALGEBRAIC-GEOMETRIC APPROACH FOR KP SOLITON DATA IN $Gr^{\text{TNN}}(k, n)$

Since $Gr^{\text{TNN}}(k, n)$ is topologically the closure of $Gr^{\text{TP}}(k, n)$, one can try to extend **indirectly** the construction of [2] to soliton data in $Gr^{\text{TNN}}(k, n)$ simply considering the latter as the limit of a sequence of soliton data in $Gr^{\text{TP}}(k, n)$.

In the following we present a **direct** construction of algebraic geometric data associated to points in $Gr^{\text{TNN}}(k, n)$ which is naturally related to the characterization of positroid cells in [52].

Let us recall that the rational curve associated to Sato dressing is \mathbb{CP}^1 . We denote it Γ_0 . This curve is equipped with a finite number of marked points: the ordered real phases $\kappa_1 < \dots < \kappa_n$, and the essential singularity P_0 of the wave function. The normalized wave function $\hat{\psi}$ on $\Gamma_0 \setminus \{P_0\}$ coincides with the normalized Sato wavefunction

$$(21) \quad \hat{\psi}(P, \vec{t}) = \frac{\mathfrak{D}^{(k)}\phi^{(0)}(P; \vec{t})}{\mathfrak{D}^{(k)}\phi^{(0)}(P; \vec{t}_0)} = \frac{\psi^{(0)}(P; \vec{t})}{\psi^{(0)}(P; \vec{t}_0)}, \quad \forall P \in \Gamma_0 \setminus \{P_0\}.$$

The dressing operator, defines the real k point divisor (Sato divisor) $\mathcal{D}_S^{(k)}(\vec{t})$. To fix ideas, let us suppose that the soliton data $(\mathcal{K}, [A])$ be regular and irreducible and that $[A] \in Gr^{\text{TNN}}(k, n)$ belongs to a positroid cell of dimension $|D|$ (see [52] and Section 2). Irreducibility implies that $|D| \geq \max\{k, n - k\}$. As a consequence, in general, the Sato divisor does not parametrize the

whole positroid cell to which $[A]$ belongs to, so that, in general, we cannot expect to reconstruct the soliton data $[A]$ from the Sato divisor.

In the present paper, we do the following

Main construction Assume we are given a real regular bounded multiline KP soliton solution generated by the following soliton data:

- (1) A set of n real ordered phases $\mathcal{K} = \{\kappa_1 < \kappa_2 < \cdots < \kappa_n\}$;
- (2) A point $[A] \in \mathcal{S}_{\mathcal{M}}^{\text{TNN}} \subset \text{Gr}^{\text{TNN}}(k, n)$, where $\mathcal{S}_{\mathcal{M}}^{\text{TNN}}$ is a positroid stratum of dimension $|D|$.

Our purpose is to associate an algebro-geometric data to this soliton data.

As the first step we choose \mathcal{N} , a planar connected orientable bipartite trivalent perfect network in the disk in Postnikov equivalence class for $[A]$. Of course, this choice is not unique, and this is in perfect agreement with the fact that the same soliton solution can be obtained from different degenerate algebro-geometrical data. In particular, following Postnikov [52], one can choose the maximally reduced network $\mathcal{N} = \mathcal{N}_T$, but any other network from the Postnikov equivalence class for $[A]$ can be used as well.

At the second step we associate the following algebraic-geometrical objects to each triple $(\mathcal{K}, [A], \mathcal{N})$:

- (1) A reducible curve $\Gamma = \Gamma(\mathcal{N})$ which is the rational degeneration of a smooth M-curve of genus $g \geq |D|$, where $g + 1$ is the number of faces of \mathcal{N} . In our approach, the curve Γ_0 is one of the irreducible components of Γ . The marked point P_0 belongs to the intersection of Γ_0 with an oval (infinite oval);
- (2) A unique real and regular degree g non-special KP divisor $\mathcal{D}_{\text{KP}, \Gamma}(\mathcal{K}, [A])$ such that any finite oval contains exactly one divisor point and $\mathcal{D}_{\text{KP}, \Gamma}(\mathcal{K}, [A]) \cap \Gamma_0$ coincides with Sato divisor;
- (3) A unique KP wave-function $\hat{\psi}$ as in Definition 3.3 such that
 - (a) Its restriction to $\Gamma_0 \setminus \{P_0\}$ coincides with the normalized Sato wave function (15);
 - (b) Its pole divisor has degree $\mathfrak{d} \leq g$ and is contained in $\mathcal{D}_{\text{KP}, \Gamma}(\mathcal{K}, [A])$.

In particular, if $\mathcal{N} = \mathcal{N}_T$ is the trivalent bipartite Le-network, then $\Gamma(\mathcal{N}_T)$ is the rational degeneration of on M-curve of minimal genus $|D|$ and has exactly $|D| + 1$ ovals and $\mathfrak{d} = g = |D|$.

4.1. The reducible rational curve $\Gamma(\mathcal{N})$. For a given network \mathcal{N} of $[A]$, the curve $\Gamma(\mathcal{N})$ is obtained by gluing a finite number of curves $\Gamma_j = \mathbb{CP}^1$ corresponding to vertexes in \mathcal{N} , at pairs of points corresponding to edges in \mathcal{N} . We also fix a local affine coordinate ζ_j on Γ_j (which is a

global coordinate at the affine part of the corresponding component, see Definition 4.2), therefore we have complex conjugation $\zeta_j \rightarrow \bar{\zeta}_j$ at each component. The points of Γ_j with real ζ_j form the real part of Γ_j . By construction (see Definition 4.2), the coordinates at each pair of glued points P, Q , are real. Therefore, we can topologically represent the real part of $\Gamma(\mathcal{N})$ as a union of circles (ovals), which correspond to the faces of \mathcal{N} .

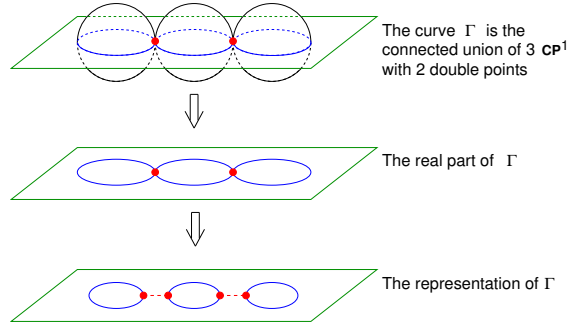


FIGURE 9. *The model of reducible rational curve.*

Following [2], we use the following representation for real rational curves (see Fig. 9). Instead of drawing the curve we draw only the real part of it, i.e. we replace each $\Gamma_j = \mathbb{CP}^1$ by a circle. Then we schematically represent the real part of the curve by drawing these circles separately and connecting the glued points by dashed lines. The property that our curve is a rational M-curve is equivalent to the following: the schematic picture is planar.

Definition 4.1. *The curve $\Gamma(\mathcal{N})$. The curve $\Gamma = \Gamma(\mathcal{N})$ for a given planar connected oriented trivalent bipartite network \mathcal{N} in the disk representing the soliton datum $[A] \in \mathcal{S}_{\mathcal{M}}^{TNN}$, is constructed in the following way. Without loss of generality we assume that:*

- (1) *The n boundary vertexes have degree one with edge of unit weight and we deform the boundary of the network in such a way that all boundary vertexes lie at a common straight interval;*
- (2) *Each non-isolated boundary source vertex b_{i_r} is joined by its unit edge to an internal bivalent white vertex which we denote V_{i_r} , $r \in [k]$. In section 9, we assume that also each non-isolated boundary sink b_{j_l} is joined by its unit edge to an internal bivalent white vertex.*

The curve $\Gamma = \Gamma(\mathcal{N})$ is associated to the graph of \mathcal{N} according to the following Table 1, after reflecting the graph w.r.t. a line orthogonal to the one containing the boundary vertexes (we reflect the graph to have the natural increasing order of the phases on $\Gamma_0 \subset \Gamma(\mathcal{N})$):

TABLE 1. The graph of \mathcal{N} vs the degenerate rational curve

<i>Graph</i>	<i>Degenerate M-curve</i>
<i>Boundary of disk</i>	<i>Copy of \mathbb{CP}^1 denoted Γ_0</i>
<i>Boundary vertex b_l</i>	<i>Marked point κ_l on Γ_0</i>
<i>Black vertex V'_{ij}</i>	<i>Copy of \mathbb{CP}^1 denoted Σ_{ij}</i>
<i>White vertex V_{ij}</i>	<i>Copy of \mathbb{CP}^1 denoted Γ_{ij}</i>
<i>Internal Edge</i>	<i>Double point</i>
<i>Face</i>	<i>Oval</i>

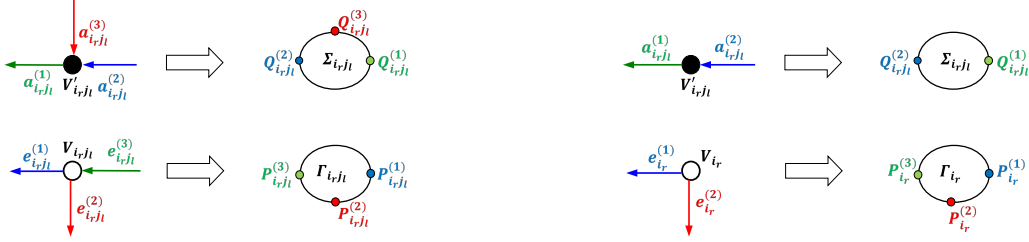


FIGURE 10. Left: the rule for the marked points on the copies Γ_{i_r, j_l} and Σ_{i_r, j_l} and for the edges of trivalent white and black vertexes. Right: the rule for the marked points on the copies of \mathbb{CP}^1 and for the edges of a bivalent white vertex associated to a boundary source b_{i_r} .

More precisely:

- (1) We denote Γ_0 the copy of \mathbb{CP}^1 corresponding to the boundary of the disk and mark on it the points $\kappa_1 < \dots < \kappa_n$ corresponding to the boundary vertexes b_1, \dots, b_n on \mathcal{N} ;
- (2) A copy of \mathbb{CP}^1 corresponds to any internal vertex of \mathcal{N} . We use the symbol Γ_s (respectively Σ_s) for the copy of \mathbb{CP}^1 corresponding to the white vertex V_s (respectively the black vertex V'_s). In particular, if $\mathcal{N} = \mathcal{N}_T$ we denote Γ_{ij} (resp. Σ_{ij}) the copy of \mathbb{CP}^1 corresponding to V_{ij} (resp. V'_{ij});
- (3) To any edge at an internal vertex, we associate a marked point on the copy of \mathbb{CP}^1 corresponding to such vertex. The edges at an internal vertex are numbered in increasing order anticlockwise with the following rule: the unique edge pointing inward at a white vertex is numbered 3 while the unique edge pointing outward at a black vertex is numbered

1. On the corresponding copies of \mathbb{CP}^1 the marked points are numbered clockwise using the mirror rule (see Figure 10[left]);
- (4) Let Γ_{i_r} be the copy of \mathbb{CP}^1 associated to the bivalent white vertex V_{i_r} corresponding to the boundary source vertex b_{i_r} , $r \in [k]$. For technical reasons we need to mark three points on each such copy of \mathbb{CP}^1 : two of them correspond to the edges at V_{i_r} and the third is the Darboux zero point. We number the marked points on Γ_{i_r} and the edges on V_{i_r} as in Figure 10[right,bottom]. Such enumeration rule is justified in sections 6 and 9 where we modify \mathcal{N} to \mathcal{N}' adding an internal source in correspondence to any boundary source.
- (5) If a boundary sink vertex b_{j_l} is joined to a bivalent white vertex V_{j_l} then we number its edges according to the rule of item (3) above (Figure 10[right, top]);
- (6) Gluing rules between copies of \mathbb{CP}^1 are ruled by edges: we glue copies of \mathbb{CP}^1 in pairs at the marked points corresponding to the end points of the edge (see Figure 11);
- (7) The faces of \mathcal{N} correspond to the ovals of Γ . In particular in the case of $\Gamma = \Gamma(\mathcal{N}_T)$, we label the ovals $\Omega_0, \Omega_{i_r j_s}$, $r \in [k]$, $s \in [N_r]$, following the enumeration rule of the faces of \mathcal{N}_T .

Remark 4.1. Universality of the reducible rational curve. Let us point out, that, for any fixed network \mathcal{N} , the construction of $\Gamma = \Gamma(\mathcal{N})$ does **not** introduce any parameter ξ . Therefore it provides an **universal** curve $\Gamma = \Gamma(\mathcal{S}; \mathcal{N})$ for the whole positroid cell \mathcal{S} . In section 6, we show that the points of \mathcal{S} are parametrized by the divisor positions at the finite ovals in the case $\mathcal{N} = \mathcal{N}_T$, and we generalize such result to any \mathcal{N} in Section 9.

The number of copies of \mathbb{CP}^1 used to construct $\Gamma(\mathcal{N})$ is **excessive** in the sense that the number of ovals and the KP divisor is invariant if we eliminate all copies of \mathbb{CP}^1 corresponding to bivalent vertexes (see Section 11).

In particular, we illustrate the case of the bipartite Le-graph in Example 4.1, see Figure 11.

Remark 4.2. Comparison with the construction in [2]. In [2], to any given soliton datum $(\mathcal{K}, [A])$, $[A] \in Gr^{TP}(k, n)$, we associate a curve obtained gluing $k + 1$ copies of \mathbb{CP}^1 at double points whose position is ruled by a parameter $\xi \gg 1$. We then control the asymptotic leading behavior in ξ of the vacuum wavefunction via an algebraic construction using the positivity properties of a specific representative matrix of $[A]$. In this approach the number of \mathbb{CP}^1 components is much smaller, but we have to introduce extra parameters marking the positions of the glued

points. In practice one can obtain such curve from the universal one by a proper desingularization of some double point.

Example 4.1. The degenerate rational curve $\Gamma(\mathcal{N}_T)$: Let $(\mathcal{K}, [A])$, with $\mathcal{K} = \{\kappa_1 < \dots < \kappa_n\}$ and $[A] \in \mathcal{S}_{\mathcal{M}}^{TNN}$ a point in $Gr^{TNN}(k, n)$ corresponding to the matroid \mathcal{M} . Moreover let $1 \leq i_1 < \dots < i_k \leq n$ be the pivot indexes (i.e the lexicographically minimal base of \mathcal{M}) and, for any $r \in [k]$, let $1 \leq j_1 < j_2 < \dots < j_{N_r} \leq n$ be the non-pivot indexes of the boxes B_{i_r, j_s} with index $\chi_{j_s}^{i_r} = 1$, $s \in [N_r]$, as in (4). Take $2n + k + 1$ copies of $\mathbb{C}\mathbb{P}^1$ and denote them as $\Gamma_0, \Sigma_{i_r, j_s}, \Gamma_{i_r, j_s}, \Gamma_{i_r}$, for $r \in [k]$, $s \in [N_r]$. Orient clockwise the real part of each copy of $\mathbb{C}\mathbb{P}^1$ and fix the following marked points:

- (1) Γ_0 has n ordered real marked points $\kappa_1 < \dots < \kappa_n$ and a marked point P_0 such that $\zeta^{-1}(P_0) = 0$;
- (2) For any $r \in [k]$ and $s \in [N_r]$:
 - (a) Σ_{i_r, j_s} has 2 real marked points $Q_{i_r, j_s}^{(1)}, Q_{i_r, j_s}^{(2)}$, either if $r = 1$ for all $s \in [N_1]$, or $r > 1$ and the j_s -th column of the Le-diagrams contains only zeroes above the box B_{i_r, j_s} ; otherwise Σ_{i_r, j_s} has 3 real ordered marked points which we denote $Q_{i_r, j_s}^{(1)}, Q_{i_r, j_s}^{(2)}, Q_{i_r, j_s}^{(3)}$ (see Figure 10[top, left]);
 - (b) each copy Γ_{i_r, j_s} has 3 real ordered marked points which we denote $P_{i_r, j_s}^{(1)}, P_{i_r, j_s}^{(2)}, P_{i_r, j_s}^{(3)}$ (see Figure 10[bottom, left]);
 - (c) each copy Γ_{i_r} has 3 real ordered marked points which we denote $P_{i_r}^{(1)}, P_{i_r}^{(2)}, P_{i_r}^{(3)}$ (see Figure 10[bottom, right]).

Then Γ is the connected union of all these copies of $\mathbb{C}\mathbb{P}^1$,

$$\Gamma = \Gamma_0 \bigsqcup_{r=1}^k \left(\Gamma_{i_r} \sqcup \left(\bigsqcup_{s=1}^{N_r} \Gamma_{i_r, j_s} \sqcup \Sigma_{i_r, j_s} \right) \right)$$

according to the following gluing rules (see also Figure 11):

- (1) **Horizontal gluing rules for fixed $r \in [k]$:**
 - (a) If, for some $r \in [k]$, $N_r = 0$, then $P_{i_r}^{(1)} \in \Gamma_{i_r}$ is not glued to any other marked point;
 - (b) If, for some $r \in [k]$, $N_r > 0$, then $P_{i_r}^{(1)} \in \Gamma_{i_r}$ is glued to $Q_{i_r, j_1}^{(2)} \in \Sigma_{i_r, j_1}$;
 - (c) For any $s \in [N_r - 1]$, $P_{i_r, j_s}^{(1)} \in \Gamma_{i_r, j_s}$ is glued to $Q_{i_r, j_{s+1}}^{(2)} \in \Sigma_{i_r, j_{s+1}}$;
 - (d) $P_{i_r, j_{N_r}}^{(1)} \in \Gamma_{i_r, j_{N_r}}$ is not glued to any other marked point;
 - (e) For any $s \in [N_r]$, $P_{i_r, j_s}^{(3)} \in \Gamma_{i_r, j_s}$ is glued to $Q_{i_r, j_s}^{(1)} \in \Sigma_{i_r, j_s}$;
 - (f) $P_{i_r, j}^{(3)} \in \Gamma_{i_r}$ is not glued to any other marked point.

- (1) Γ possesses $|D| + 1$ ovals which we label $\Omega_0, \Omega_{i_r j_s}, r \in [k], s \in [N_r]$. Moreover the ovals are uniquely identified by the following properties:
- (a) Ω_0 is the unique oval whose boundary contains both κ_1 and κ_n ;
 - (b) For any $r \in [k], s \in [2, N_r], \Omega_{i_r j_s}$ is the unique oval whose boundary contains both $P_{i_r j_s}^{(2)} \in \Gamma_{i_r j_s}$ and $P_{i_r j_{s-1}}^{(2)} \in \Gamma_{i_r j_{s-1}}$;
 - (c) For any $r \in [k], \Omega_{i_r j_1}$ is the unique oval whose boundary contains both $P_{i_r j_1}^{(2)} \in \Gamma_{i_r j_1}$ and $P_{i_r}^{(2)} \in \Gamma_{i_r}$.
- (2) Γ is the rational degeneration of a regular M-curve of genus $|D|$ equal to the dimension of the matroid \mathcal{M} and possessing $|D| + 1$ ovals.

Proof. The only un-trivial statement is the one concerning the genus of the perturbed curve. It is not restrictive to assume that the soliton data be irreducible in $Gr^{\text{TNN}}(k, n)$ [¶].

By definition, Γ is represented by $d = 2|D| + k + 1$ complex projective lines which intersect generically in $d(d-1)/2$ double points. The regular curve is obtained keeping all such double points fixed except those corresponding to the edges in \mathcal{N}_T , which are perturbed creating regular gaps and keeping the number of ovals fixed to $|D| + 1$. The total number of desingularized double points corresponds to the total number of internal edges in \mathcal{N}_T . The number of horizontal edges is $2|D|$, since for any fixed $r \in [k]$ we have $2N_r + 1$ copies of $\mathbb{C}\mathbb{P}^1$ and $\sum_r N_r = |D|$, while the number of vertical edges is $|D| + k$, since by construction each white vertex has a vertical edge. Then Γ has degree d and is the rational degeneration of a regular Riemann surface of genus

$$g = \frac{(d-1)(d-2)}{2} - d(d-1)/2 + 3|D| + k = 3|D| + k - d + 1 = |D|,$$

and $|D| + 1$ ovals.

Alternatively, we may obtain the genus of the smooth curve by the following formula $g = N - d + 1 = 3|D| + k - (2|D| + k + 1) + 1 = |D|$, where N is the number of desingularized double points and d is the number of components, i.e. copies of $\mathbb{C}\mathbb{P}^1$.

The regular M-curve is the normalization of this nodal plane curve. □

[¶]Indeed, if this is not the case, we may preliminarily reduce the dimension of the Grassmannian eliminating all isolated boundary vertexes. The elimination of an isolated boundary source corresponds to the elimination of a row filled by zeros in the Le-diagram, and corresponds to the identification of the positroid cell of dimension $|D|$ as a realizable matroid in $Gr(k-1, n-1)$. The elimination of an isolated boundary sink is equivalent to the elimination of a column filled by zeros in the Le-diagram and corresponds to the identification of the positroid cell of dimension $|D|$ as a realizable matroid in $Gr(k-1, n)$. We remark that these reductions leave invariant the number of faces of the Le-graph and so the number of ovals of the reducible curve.

In Figure 12 we show such continuous deformation for the reduced bipartite Le–network of Example 2.2 (see Section 8.1). We remark that in this case the degree of the curve $d = 14$ (since we represent Γ as an union of two quadrics and 10 lines). The sum of the δ -s of all singular point of Γ is $\Delta = 89$. The perturbed regular curve is obtained by perturbing 21 ordinary intersection points (for each of them $\delta = 1$), which correspond to the double points in the topological representation in Figure 12. The normalized perturbed regular curve has then genus [28]

$$g = \frac{(d-1)(d-2)}{2} - \Delta + 21 = 10 = |D|.$$

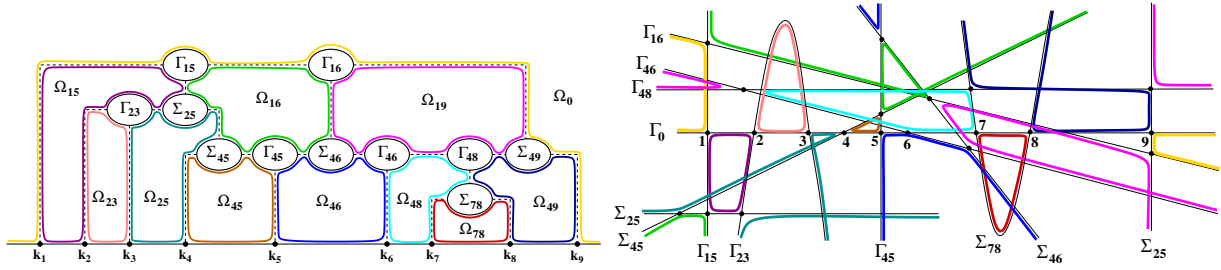


FIGURE 12. The topological model of the oval structure (left) is the partial normalization of the planar nodal curve (right) for the reduced curve Γ .

Remark 4.3. The genus of $\Gamma(\mathcal{N})$. In the general case of the curve $\Gamma(\mathcal{N})$ associated to a planar oriented bipartite trivalent perfect network \mathcal{N} with $g + 1$ faces, $\Gamma(\mathcal{N})$ is the rational degeneration of a smooth M–curve of genus g . If \mathcal{N} is associated to $[A] \in \mathcal{S}_{\mathcal{M}}^{\text{TNN}} \subset \text{Gr}^{\text{TNN}}(k, n)$ of dimension $|D|$, then $g \geq |D|$ (see [52]). See also Remark 9.2 in Section 7 for the relation between the number of vertexes and edges with g, k, n .

4.2. The KP divisor on $\Gamma(\mathcal{N})$. Throughout this section we fix the soliton data $(\mathcal{K}, [A])$, with $\mathcal{K} = \{\kappa_1 < \dots < \kappa_n\}$ and $[A] \in \mathcal{S}_{\mathcal{M}}^{\text{TNN}} \subset \text{Gr}^{\text{TNN}}(k, n)$, a positroid cell of dimension $|D|$. \mathcal{N}_T denotes the bipartite Le–network constructed in section 2.1 and $\Gamma(\mathcal{N}_T)$ is the curve as in Example 4.1. \mathcal{N} denotes any planar connected oriented bipartite trivalent perfect network associated to $[A]$. $\Gamma(\mathcal{N})$ is the reducible rational curve associated to \mathcal{N} via Definition 4.1 and is the rational degeneration of a smooth M–curve of genus $g \geq |D|$. Finally we denote $I = \{1 \leq i_1 < \dots < i_k \leq n\}$ the base of the given orientation of \mathcal{N} and $f^{(r)}(\vec{t})$, $r \in [k]$, the corresponding set of linearly independent heat hierarchy solutions associated to the generalized RRE representation of $[A]$ with pivot columns in I .

In this section we state the main results of our paper:

- (1) As a first step of the construction we show, that to a given data $(\mathcal{K}, [A], I, \mathcal{N})$, where I is a base in the matroid \mathcal{M} , we associate a unique degree g effective real and regular **vacuum** divisor and a unique real and regular **vacuum** wavefunction on $\Gamma(\mathcal{N})$ satisfying appropriate boundary conditions (Theorem 4.1);
- (2) Then we apply the Darboux dressing to such vacuum wave function and define the normalized dressed divisor $\mathcal{D}_{\text{KP},\Gamma}$, which, by construction is effective and of degree g . In Theorem 4.2 we prove that $\mathcal{D}_{\text{KP},\Gamma}$ does not depend on the base I .
- (3) Therefore, the curve $\Gamma(\mathcal{N})$ can be used as the spectral curve for the given soliton data, $\mathcal{D}_{\text{KP},\Gamma}$ is the KP divisor, and, by construction, it satisfies the reality and regularity conditions of Definition 3.3 (see Theorem 4.3).
- (4) In particular, on $\Gamma(\mathcal{N}_T)$ the KP real and regular divisor has minimal degree $\mathfrak{d}(\mathcal{N}_T) = |D|$. As a byproduct, on $\Gamma(\mathcal{N}_T)$ we obtain a local bijection between KP divisors on $\Gamma(\mathcal{N}_T)$ and points in the positroid cell $\mathcal{S}_{\mathcal{M}}^{\text{TNN}}(k, n)$.

Remark 4.4. *In Theorem 10.1 and Corollary 10.1 in Section 10 we prove that we may use indexes for pair of edges at trivalent white vertexes of the network to uniquely reconstruct the position of each divisor point of $\mathcal{D}_{\text{KP},\Gamma}$ in the ovals.*

We start introducing local affine coordinates on each copy of \mathbb{CP}^1 and we use the same symbol ζ for any such affine coordinate to simplify notations.

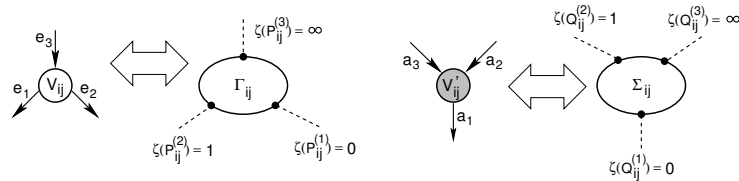


FIGURE 13. *Local coordinates on the components Γ_{ij} and Σ_{ij} (reflection w.r.t. the vertical line): the marked point $P_s \in \Gamma_{ij}$ corresponds to the edge e_s at the white vertex V_{ij} and the marked point $Q_s \in \Gamma_{ij}$ corresponds to the edge a_s at the black vertex V'_{ij} .*

Definition 4.2. Local affine coordinate on $\Gamma(\mathcal{N})$ *On each copy of \mathbb{CP}^1 the local coordinate ζ is uniquely identified by the following properties:*

- (1) *On Γ_0 , $\zeta^{-1}(P_0) = 0$ and $\zeta(\kappa_1) < \dots < \zeta(\kappa_n)$. To abridge notations, we identify the ζ -coordinate with the marked points $\kappa_j = \zeta(\kappa_j)$, $j \in [n]$;*

(2) On the component Γ_{ij} corresponding to the internal white vertex V_{ij} :

$$\zeta(P_{ij}^{(1)}) = 0, \quad \zeta(P_{ij}^{(2)}) = 1, \quad \zeta(P_{ij}^{(3)}) = \infty,$$

while on the component Σ_{ij} corresponding to the internal black vertex V'_{ij} :

$$\zeta(Q_{ij}^{(1)}) = 0, \quad \zeta(Q_{ij}^{(2)}) = 1, \quad \zeta(Q_{ij}^{(3)}) = \infty,$$

see Figure 13.

We start defining the desired properties for both the vacuum divisor and the vacuum wavefunction on $\Gamma(\mathcal{N})$ in the following Definitions.

Definition 4.3. *Real and regular vacuum divisor on $\Gamma = \Gamma(\mathcal{N})$, compatible with a base I .* Let $\mathcal{D}_{\text{vac},\Gamma}$ be a degree g divisor on $\Gamma \setminus \Gamma_0$. Let Ω_0 be the infinite oval containing the marked point $P_0 \in \Gamma_0$ and let us call finite the remaining g ovals of Γ . Let $I = \{i_1, \dots, i_k\}$, $1 \leq i_1 < i_2 < \dots < i_k \leq n$, and $P_3^{(i_r)}$, $r \in [k]$, be the corresponding Darboux source points in Γ .

Then, we call $\mathcal{D}_{\text{vac},\Gamma}$ a real and regular vacuum divisor compatible with I if:

- (1) $\mathcal{D}_{\text{vac},\Gamma}$ is contained in the union of all the ovals of Γ ;
- (2) The total number of vacuum divisor poles plus the number of Darboux source points contained in any finite oval is $1 \pmod{2}$;
- (3) The total number of vacuum divisor poles plus the number of Darboux source points contained in Ω_0 plus k is $0 \pmod{2}$.

Definition 4.4. *A real and regular vacuum wavefunction on $\Gamma = \Gamma(\mathcal{N})$ for a base I :* Let I be a base in the matroid associated to $[A]$. Let $\mathcal{D}_{\text{vac},\Gamma}$ be a degree g real and regular divisor on $\Gamma \setminus \Gamma_0$ for the base I as in Definition 4.3. We call vacuum wavefunction associated to $(\mathcal{K}, [A], I, \mathcal{D}_{\text{vac},\Gamma})$, any function $\hat{\phi}(P, \vec{t})$ regular for all $\vec{t} = (t_1 = x, t_2 = y, t_3 = t, t_4, \dots)$ and meromorphic of degree $\mathfrak{d} \leq g$ on $\Gamma \setminus \{P_0\}$ with the following properties:

- (1) For all $P \in \Gamma \setminus \Gamma_0$ the function $\hat{\phi}(P, \vec{t})$ satisfies all equations (12) of the vacuum hierarchy;
- (2) There exists \vec{t}_0 such that $\hat{\phi}(P, \vec{t}_0) = 1$ at all points $P \in \Gamma \setminus \{P_0\}$;
- (3) The restriction of $\hat{\phi}$ to $\Gamma_0 \setminus \{P_0\}$ coincides with the following normalization of Sato's wavefunction, $\hat{\phi}(\zeta(P), \vec{t}) = e^{\theta(\zeta, \vec{t} - \vec{t}_0)}$, where $\theta(\zeta, \vec{t}) = \sum_{l \geq 1} t_l \zeta^l$;
- (4) $\hat{\phi}(\zeta(P), \vec{t})$ is real for real values of the local coordinate ζ and for all real \vec{t} on each component of Γ ;
- (5) $\hat{\phi}$ takes compatible values at pairs of glued points $P, Q \in \Gamma$, for all \vec{t} : $\hat{\phi}(P, \vec{t}) = \hat{\phi}(Q, \vec{t})$;

- (6) $\hat{\phi}(P_{i_r}^{(3)}, \vec{t}) \equiv f^{(r)}(\vec{t})$ at each Darboux source point $P_{i_r}^{(3)}$, $r \in [k]$, for all \vec{t} ;
- (7) $\hat{\phi}(\zeta, \vec{t})$ is either constant or meromorphic of degree one w.r.t. to the spectral parameter on each copy of \mathbb{CP}^1 corresponding to a trivalent white vertex of \mathcal{N} or to a boundary source vertex V_{i_r} , $r \in [k]$;
- (8) $\hat{\phi}(\zeta, \vec{t})$ is constant w.r.t. to the spectral parameter on each other copy of \mathbb{CP}^1 ;
- (9) For any fixed \vec{t} we have $(\hat{\phi}(P, \vec{t})) + \mathcal{D}_{\text{vac}, \Gamma} \geq 0$ on $\Gamma \setminus P_0$, where (f) denotes the divisor of f . Equivalently, for any fixed \vec{t} on $\Gamma \setminus P_0$ the function $\hat{\phi}(\zeta, \vec{t})$ is regular outside the points of $\mathcal{D}_{\text{vac}, \Gamma}$ and at each of these points either it has a first order pole or is regular.

Theorem 4.1. Existence and uniqueness of a real and regular vacuum wavefunction satisfying Definition 4.4 on $\Gamma(\mathcal{N})$. Let $\Gamma(\mathcal{N})$ be the curve for a planar connected oriented bipartite trivalent network \mathcal{N} associated to $[A]$. Let $A = (A_i^j)_{i \in [k], j \in [n]}$ be the RREF representative matrix of $[A]$ with respect to the base I corresponding to the given orientation of \mathcal{N} .

Then to such data $(\mathcal{K}, [A], I, \mathcal{N})$ we associate:

- (1) A **unique** real and regular vacuum divisor $\mathcal{D}_{\text{vac}, \Gamma} = \mathcal{D}_{\text{vac}, \Gamma}(I)$ as in Definition 4.3. In particular the divisor has the following properties:
 - (a) $\mathcal{D}_{\text{vac}, \Gamma}$ is contained in the union of all the ovals of Γ ;
 - (b) The total number of vacuum divisor poles plus the number of Darboux source points contained in any finite oval is 1 mod 2;
 - (c) The total number of vacuum divisor poles plus the number of Darboux source points contained in Ω_0 plus k is 0 mod 2.
 - (2) A **unique** real and regular vacuum wavefunction $\hat{\phi}(P, \vec{t}) = \hat{\phi}(P, \vec{t}|I)$ as in Definition 4.4 such that, at each Darboux source point $\hat{\phi}(P, \vec{t})$ coincides with the heat hierarchy solution associated to the r -th row of the representative matrix A ,
- $$(22) \quad \hat{\phi}(P_{i_r}^{(3)}, \vec{t}) \equiv \sum_{l=1}^n A_l^r \exp(\theta_l(\vec{t})), \quad r \in [k], \forall \vec{t}.$$

In section 6 we prove Theorem 4.1 in the special case $\Gamma(\mathcal{N}_T)$ parametrized by the coordinates on $\Gamma(\mathcal{N}_T)$ corresponding to the canonical acyclic orientation of \mathcal{N}_T . More precisely, we construct a unique vacuum wavefunction on $\Gamma(\mathcal{N}_T)$ using the algebraic recursion settled in Section 5.2. We first define a unique vertex vacuum wavefunction (v.v.w.) at the edges of \mathcal{N}_T using the system of vectors in Theorem 5.1. Then, by construction, the normalized v.v.w. possesses a degree $|D|$ divisor with the required reality and regularity conditions (see Lemma 6.2). We then construct the degree $|D|$ real and regular vacuum wavefunction on Γ imposing that it takes the value of the

normalized v.v.w. at the marked points (double points and Darboux points) which correspond to the edges (see Theorem 6.1).

Let $g + 1$ denote the number of faces of \mathcal{N} . The proof of Theorem 4.1 in the general case $\Gamma = \Gamma(\mathcal{N})$ is carried out in several steps:

- (1) In section 7 we generalize the construction of systems of vectors to **any** planar bipartite trivalent perfectly oriented network \mathcal{N} and explain the dependence of the system of vectors on the change of orientation in the network.
- (2) Then, in Section 9, we preliminarily modify the connected oriented network \mathcal{N} to \mathcal{N}' in order to identify each Darboux (source and sink) point in Γ with a convenient edge in \mathcal{N}' . This modification is a technical tool to control the dependence of the divisor on the orientation of the network;
- (3) In section 9.2, we construct a unique vacuum vertex wavefunction $\phi(\vec{t})$ for any given orientation of \mathcal{N}' . Its normalization $\hat{\phi}(\vec{t})$ is invariant w.r.t changes of orientation of the closed cycles of \mathcal{N}' , i.e. it is associated to a **base** of the matroid \mathcal{M} .
- (4) We use the system of linear relations satisfied by the vertex vacuum wavefunction at all internal vertexes, to assign a real vacuum divisor point to any trivalent white vertex of \mathcal{N}' in section 9.2. The position of the divisor point depends on the base I .
- (5) The vacuum wavefunction and the vacuum divisor on $\Gamma(\mathcal{N})$ are constructed in section 9.3 along similar lines as in the case of $\Gamma(\mathcal{N}_T)$.
- (6) By construction each vacuum divisor point belongs to an oval. The position of each vacuum pole and the number of vacuum poles in each oval are encoded in a set of indexes assigned to the vacuum vertex wavefunction.
- (7) An alternative proof of the construction follows from the direct construction on $\Gamma(\mathcal{N}_T)$ in Section 6 and the fact that Postnikov moves and reductions preserve the parity of divisor poles in the ovals (see Sections 8 and 11).

Definition 4.5. *The dressing of the vacuum wavefunction on Γ . Let Γ and $\hat{\phi}$ be as in Theorem 4.1 for given soliton data $(\mathcal{K}, [A])$. Then the corresponding Darboux transformed wavefunction is defined by:*

$$(23) \quad \psi(P, \vec{t}) = \mathfrak{D}^{(k)} \hat{\phi}(P, \vec{t}), \quad P \in \Gamma \setminus \{P_0\}, \forall \vec{t},$$

where $\mathfrak{D}^{(k)}$ is the k -th order ordinary differential operator associated to such soliton data as in (14).

Let us define the non-effective divisor $\mathcal{D}_{\text{dr},\Gamma}$ by

$$(24) \quad \mathcal{D}_{\text{dr},\Gamma} = \mathcal{D}_{\text{vac},\Gamma} + kP_0 - \sum_{r=1}^k P_{i_r}.$$

Let the initial condition \vec{t}_0 be such that $\mathfrak{D}^{(k)}\hat{\phi}(P, \vec{t}_0) \neq 0$ at all double points $P \in \Gamma$. We define the normalized dressed wavefunction $\hat{\psi}(P, \vec{t})$ as

$$(25) \quad \hat{\psi}(P, \vec{t}) = \frac{\psi(P, \vec{t})}{\psi(P, \vec{t}_0)}.$$

Let us also define the normalized dressed divisor by:

$$(26) \quad \mathcal{D}_{\text{KP},\Gamma} = \mathcal{D}_{\text{dr},\Gamma} + (\psi(P, \vec{t}_0)).$$

Remark 4.5. In case of reducible soliton data $[A]$ in $Gr^{TNN}(k, n)$ with s isolated boundary sources we have two Darboux dressings: the reducible k -th order dressing operator and the reduced $(k-s)$ -order dressing operator. In the Definition above we use the k -th order reducible operator, the normalized dressed wave function will be the same for both dressings as well as the $\mathcal{D}_{\text{KP},\Gamma}$ divisor.

Lemma 4.1. (1) For any \vec{t} we have the following inequality on $\Gamma \setminus P_0$:

$$(27) \quad (\psi(P, \vec{t})) + \mathcal{D}_{\text{dr},\Gamma} \geq 0.$$

(2) The number of poles minus the number of zeroes for $\mathcal{D}_{\text{dr},\Gamma}$ (counted with multiplicities, if necessary) at each finite oval is odd and at the infinite oval it is even.

The first property follows directly from the definition of $\psi(P, \vec{t})$. The second statement simply follows from properties of the vacuum wave function constructed in Theorem 4.1, namely properties (6) in Definition 4.4, (2)-(3) in Definition 4.3 and formula (24).

Lemma 4.2. (1) For any \vec{t} we have the following inequality on $\Gamma \setminus P_0$:

$$(28) \quad (\hat{\psi}(P, \vec{t})) + \mathcal{D}_{\text{KP},\Gamma} \geq 0.$$

(2) The divisor $\mathcal{D}_{\text{KP},\Gamma}$ is effective and has degree g .

(3) All poles of $\mathcal{D}_{\text{KP},\Gamma}$ lie at the finite ovals, and each finite oval contains exactly one pole of $\mathcal{D}_{\text{KP},\Gamma}$.

The first statement follows immediately from the definition of $\hat{\psi}(P, \vec{t})$ and $\mathcal{D}_{\text{KP}, \Gamma}$. The second statement follows immediately from (26). The third statement follows from the fact that $\psi(P, \vec{t}_0)$ is real at all real ovals and from Lemma 4.1.

Theorem 4.2. Invariance of $\mathcal{D}_{\text{KP}, \Gamma}$. *Let $\hat{\phi}_1(P, \vec{t})$, $\hat{\phi}_2(P, \vec{t})$ be the vacuum KP wavefunctions constructed on $\Gamma(\mathcal{N})$ respectively using bases I_1 and I_2 in the matroid of $[A]$. Then $\mathcal{D}_{\text{KP}, \Gamma}(I_1) = \mathcal{D}_{\text{KP}, \Gamma}(I_2)$, therefore the normalized Darboux transformed wavefunctions coincide on $\Gamma(\mathcal{N})$ for all \vec{t} , that is*

$$(29) \quad \frac{\mathfrak{D}^{(k)} \hat{\phi}_2(P, \vec{t})}{\mathfrak{D}^{(k)} \hat{\phi}_2(P, \vec{t}_0)} = \frac{\mathfrak{D}^{(k)} \hat{\phi}_1(P, \vec{t})}{\mathfrak{D}^{(k)} \hat{\phi}_1(P, \vec{t}_0)}, \quad \forall P \in \Gamma, \forall \vec{t}.$$

In particular the KP divisor $\mathcal{D}_{\text{KP}, \Gamma} = \mathcal{D}_{\text{KP}, \Gamma}(\mathcal{K}, [A], \mathcal{N})$ does not depend on the orientation of \mathcal{N} used in the construction.

The proof of this statement requires the introduction of dressed divisor $\mathcal{D}_{\text{dr}, \mathcal{N}'}$ on a modified network \mathcal{N}' , and it is carried out in Section 9.2.

Theorem 4.3. The effective divisor on $\Gamma(\mathcal{N})$. *Assume that $\hat{\phi}$ is the real and regular vacuum wavefunction on $\Gamma = \Gamma(\mathcal{N})$ as in Theorem 4.1 for given soliton data $(\mathcal{K}, [A])$ and base I . Let $\hat{\psi}$ be the normalized dressed wavefunction as in Definition 4.5.*

Then $\hat{\psi}$ is the KP wave function on $\Gamma(\mathcal{N})$ for the soliton data $(\mathcal{K}, [A])$, and the divisor $\mathcal{D}_{\text{KP}, \Gamma}$ satisfies the reality and regularity conditions of Definition 3.3.

Moreover if $\mathcal{N} = \mathcal{N}_T$ then the degree of the effective pole divisor of $\hat{\psi}$ coincides with the dimension of the positroid cell of $[A]$, that is $\mathfrak{d} = |D|$, where \mathfrak{d} is the degree of the pole divisor of $\hat{\psi}$.

The proof of the Theorem easily follows from Lemmas 4.1, 4.2 and Theorems 4.1, 4.2. Moreover, by construction, the Darboux transformation creates the Sato divisor on Γ_0 .

We provide a direct proof of the above Theorem in Section 10 by associating a set of indexes to each pair of edges at an internal vertex, for the dressed vertex wavefunction. Using such indexes we directly prove that $\mathcal{D}_{\text{KP}, \Gamma}$ is a real and regular divisor on $\Gamma(\mathcal{N}_T)$, and we control the positions of the poles.

Finally, in Section 11 we provide an alternative proof based on the effect of Postnikov moves and reductions on the position of the divisor poles.

Remark 4.6. *The last statement in the case of the Le-network \mathcal{N}_T follows from the construction in section 6. The case of $\Gamma = \Gamma(\mathcal{N}_T)$ is important for many reasons. First of all, this M-curve is*

a rational degeneration of a curve having the minimal possible genus under genericity assumption of soliton data for given cell. Next, in this case we have a recursion to construct the divisor. In addition, the set of poles of $\hat{\psi}$ for generic \vec{t} exactly coincides with $\mathcal{D}_{\text{KP},\Gamma}$.

5. A SYSTEM OF VECTORS ON THE LE-NETWORK

In [2] we associate the representation of the rows of a certain representative matrix of a point $Gr^{\text{TP}}(k, n)$ as a linear combination of a minimal set of vectors to the behavior of the vacuum wave function at double points and Darboux points. In this section we use the Le-network \mathcal{N}_T to express each row of the RREF representative matrix as a linear combination with positive coefficients of a minimal number of some basic row vectors. This construction is a generalization of the Principal Algebraic Lemma in [2].

In Section 5.2 we present a recursive construction of these basic vectors which generalizes the algebraic construction in [2] and then we use this recursion to construct a vacuum wave function on the spectral curve $\Gamma(\mathcal{N}_T)$ in Section 6.3.

Systems of vectors for a generic planar bipartite network \mathcal{N} in the disk associated to a given point of $Gr^{\text{TN}}(k, n)$ are introduced in Section 7.

5.1. A representation of the rows of the RREF matrix using the Le-tableau. Let \mathcal{N}_T be the planar bipartite trivalent perfect network associated to the Le-tableau T for the given point $[A] \in Gr^{\text{TN}}(k, n)$ and A be the representative matrix in RREF of $[A]$.

Below, we derive an useful formula expressing each row r of the RREF matrix as a linear combination with **positive coefficients** $c_{l_s}^r$ of $N_r + 1$ vectors $E^{(r)}[l_s]$, $s \in [0, N_r]$, computed using the bipartite Le-graph. Each coefficient $c_{l_s}^r$ is the weight of the directed path from the boundary source b_{i_r} to the internal white vertex V_{i_r, l_s} . The j -th component of the vector $E^{(r)}[l_s]$ is the sum of the weights of all possible paths starting downwards at V_{i_r, l_s} and zig-zagging to the destination b_j , and its sign depends on the number of boundary sources passed before reaching the destination (see Lemma 5.1).

Let us fix $r \in [k]$ and let $i_r \in I$ be the corresponding pivot index. Let $l \in \bar{J}$ such that the box $B_{i_r, l}$ contains a 1 and let $V_{i_r, l}$ be the corresponding white vertex. Let us consider all paths P starting at b_{i_r} , moving horizontally from V_{i_r} to $V_{i_r, l}$, moving downwards at $V_{i_r, l}$ and then zig-zagging towards any possible destination $j \in \bar{I}$. Clearly the set of such path may be non-empty only for $j \geq l$; moreover, for $l = j$, there is exactly one such path from b_{i_r} to b_l . For $j \in \bar{I}$ and

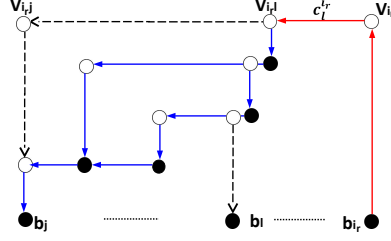


FIGURE 14. The coefficient $c_l^{i_r}$ is the weight of the red path from the source b_{i_r} to the white internal vertex $V_{i,l}$, while $E_j^{(r)}[l]$, the j -th component of the vector $E^{(r)}[l]$, is the sum of all the blue paths starting downwards at the internal vertex $V_{i,l}$ and zig-zagging to the boundary sink b_j .

$j \geq l$, let us define

$$(30) \quad \begin{aligned} \mathcal{P}_{lj}^{(r)} &= \{ P_{lj}^{(r)} : b_{i_r} \mapsto b_j : P_{lj}^{(r)} \text{ moves downwards at the white vertex } V_{i,r,l} \}, \\ \bar{\mathcal{P}}_{lj}^{(r)} &= \{ \bar{P}_{lj}^{(r)} : V_{i,r,l} \mapsto b_j : \bar{P}_{lj}^{(r)} \text{ moves downwards at the white vertex } V_{i,r,l} \}, \end{aligned}$$

and denote by $P_{i_r,l}$ the path from the source b_{i_r} to the white vertex $V_{i,r,l}$. Then for any $P_{lj}^{(r)} \in \mathcal{P}_{lj}^{(r)}$ there exists a unique path $\bar{P}_{lj}^{(r)} \in \bar{\mathcal{P}}_{lj}^{(r)}$ such that

$$P_{lj}^{(r)} = P_{i_r,l} \sqcup \bar{P}_{lj}^{(r)}.$$

Define

$$(31) \quad c_l^i \equiv \prod_{e \in P_{i_r,l}} w_e.$$

Then the weight of the path $P_{lj}^{(r)}$ is

$$w(P_{lj}^{(r)}) = \prod_{e \in P_{lj}^{(r)}} w_e = c_l^i \left(\prod_{e \in \bar{P}_{lj}^{(r)}} w_e \right) = c_l^i w(\bar{P}_{lj}^{(r)})$$

and for any $j \in \bar{I}$, $j > i_r$, the matrix entry in reduced row echelon form as in (2), may be re-expressed as

$$A_j^{r,i} = (-1)^{\sigma_{i_r,j}} \sum_{s=1}^{N_r} c_{l_s}^i \sum_{\substack{\bar{P}_{l_s j}^{(r)} \in \bar{\mathcal{P}}_{l_s j}^{(r)}}} w(\bar{P}_{l_s j}^{(r)}) = (-1)^{\sigma_{i_r,j}} \sum_{l \leq j} c_l^i \sum_{\substack{\bar{P}_{lj}^{(r)} \in \bar{\mathcal{P}}_{lj}^{(r)}}} w(\bar{P}_{lj}^{(r)}).$$

Notice that in the sum above the set of paths may be not empty only if the box $B_{i_r,l}$ has index $\chi_l^{i_r} = 1$.

Finally, for any $r \in [k]$, $i_r \in I$, $l \in \bar{I}$, $l > i_r$ and such that $\chi_l^{i_r} = 1$, let us define the row vector $E^{(r)}[l] = (E_1^{(i)}[l], \dots, E_n^{(i)}[l])$, with

$$(32) \quad E_j^{(r)}[l] = \begin{cases} 0 & \text{if } j < l \text{ or } j \in I, \\ (-1)^{\sigma_{i_r j}} \sum_{\bar{P}_{l_j}^{(r)} \in \bar{\mathcal{P}}_{l_j}^{(r)}} w(\bar{P}_{l_j}^{(r)}) & \text{if } l, j \in \bar{I} \text{ and } j \geq l, \end{cases}$$

where $\sigma_{i_r j}$ is the number of pivot elements in the open interval $]i_r, j[$. In the expression above the entry $E_j^{(r)}[l] = 0$ if there is no path moving downwards at the vertex $V_{i_r, l}$ and reaching destination b_j . Finally we associate to the boundary source a vector

$$(33) \quad E^{(r)}[i] = (0, \dots, 0, 1, 0, \dots, 0),$$

with non zero entry in the i_r -th column. Then the following Lemma holds true.

Lemma 5.1. *Let A be the reduced row echelon form matrix representing a given point in the matroid stratum $\mathcal{S}_{\mathcal{M}}^{TNN} \subset Gr^{TNN}(k, n)$ and let D be the corresponding Le-diagram. Let $E^{(r)}[i]$, $E^{(r)}[l]$, c_l^i as in (31), (32) and (33), with $r \in [k]$, $i_r \in I$, $l \in \bar{I}$, such that the box $B_{i_r, l}$ is filled by 1. Then, the r -th row of A is*

$$(34) \quad A[r] = E^{(r)}[i] + \sum_{s=1}^{N_r} c_{l_s}^r E^{(r)}[l_s],$$

where the sum runs over the indexes $l_s \in \bar{I}$ such that the index in (4) is $\chi_{l_s}^{i_r} = 1$.

The proof is trivial and is omitted.

5.2. Recursive construction of the row vectors $E^{(r)}[l]$ using the Le-diagram. In the previous Section an explicit construction of the system of vectors $E^{(r)}[l]$ was provided. But we also require a recursive representation for this system, and we provide it in Theorem 5.1 using the Le-tableau. At this aim, for any $r \in [k]$, we complete such vectors into a basis in \mathbb{R}^n , introducing an $n \times n$ matrix $\hat{E}^{(r)}$. We pass from the basis associated to the $(r+1)$ -th row to the one associated to the r -th row applying transition matrices $C^{[r, r+1]}$: $\hat{E}^{(r)} = C^{[r, r+1]} \hat{E}^{(r+1)}$, for all $r \in [k-1]$. Each transition matrix $C^{[r, r+1]}$ keeps track of empty and non-empty boxes of the $(r+1)$ -th line of the Le-tableau, and is upper triangular by definition. The choice of signs in $C^{[r, r+1]}$ in (35) keeps track of the sign changes when passing a pivot column. We also complete the set of coefficients c_l^r defined in (31) to row vectors $\hat{c}^{(r)}$.

The recursion in Theorem 5.1 is based on addition of rows to the Le-diagram starting from the bottom line and may be considered a straightforward corollary to the Lindström lemma in

the case of acyclic graphs. It may be also considered as the combinatorial version of Theorem 5 in [2] in the case of points in $Gr^{\text{TP}}(k, n)$ for a different choice of the basic vectors and of the representative matrix.

The recursion in Theorem 5.1 is generalized in Section 7 where we give general rules to construct well defined systems of vectors on any network.

The relevance of Theorem 5.1 is in its natural relation with the recursive computation of the value of the vacuum wavefunction at the marked points in section 6.1, where we use such vectors and coefficients to define a vacuum vertex wavefunction on the bipartite Le-network \mathcal{N}_T .

Theorem 5.1. (The recursive algebraic construction) *Let $[A] \in \mathcal{S}_{\mathcal{M}}^{\text{TNN}} \subset Gr^{\text{TNN}}(k, n)$ with pivot set $I = I(\lambda) = \{1 \leq i_1 < i_2 < \dots < i_k \leq n\}$. Let D and \mathcal{N}_T respectively be the Le-diagram and its oriented bipartite network. Define the following collections of $n \times n$ invertible matrices $\hat{E}^{(r)}$, $n \times n$ transition matrices $C^{[r-1, r]}$ and row vectors $\hat{c}^{(r)}$, $r \in [k]$, associated to G_L as follows:*

- (1) $\hat{E}^{(k)}$ is the $n \times n$ identity matrix and we denote its row vectors as $\hat{E}^{(k)}[l]$, $l \in [n]$;
- (2) For $r \in [k]$, define the $n \times n$ transition matrix $C^{[r-1, r]}$ as follows:

$$(35) \quad C_j^{[r-1, r], l} = \begin{cases} \delta_j^l, & \text{if } l \in [1, i_r[, \quad j \in [n], \\ -\hat{w}_{i_r j}^{(r)}, & \text{if } l = i_r, \quad j \in [i_r, n], \quad \chi_j^{i_r} = 1, \\ -\hat{w}_{l j}^{(r)}, & \text{if } l, j \in \bar{I} \cap]i_r, n], \quad j \geq l, \quad \chi_j^{i_r} \chi_l^{i_r} = 1, \\ -\delta_j^l, & \text{if } l \in I \cap]i_r, n], \quad j \in [n], \\ -\delta_j^l, & \text{if } l \in \bar{I} \cap]i_r, n], \quad \chi_l^{i_r} = 0, \quad j \in [n], \\ 0 & \text{otherwise,} \end{cases}$$

where

- (a) for $l, j \in \bar{I} \cap]i_r, n]$, $j \geq l$, $\hat{w}_{l j}^{(r)}$ is the weight of the directed horizontal path from the black vertex $V'_{i_r, l}$ to the white vertex $V_{i_r, j}$. In particular $\hat{w}_{i_r}^{(r)} = 1$;
- (b) for $l = i_r$, $\hat{w}_{i_r i_r}^{(r)} = 1$;
- (c) for $l = i_r$ and $j \in \bar{I}$, $\hat{w}_{i_r j}^{(r)}$ is the weight of the directed horizontal path from the black vertex $V'_{i_r, l}$ to the white vertex $V_{i_r, j}$.

- (3) The matrices $\hat{E}^{(r-1)}$ are recursively computed as r decreases from k to 2, by

$$(36) \quad \hat{E}^{(r-1)} = C^{[r-1, r]} \hat{E}^{(r)}.$$

(4) For any $r \in [k]$, the l -element of the row vector $\hat{c}^{(r)}$, $l \in [n]$, is

$$(37) \quad \hat{c}_l^{(r)} = \begin{cases} 1 & \text{if } l = i_r, \\ c_l^r & \text{if } \chi_l^{i_r} = 1, \\ 0 & \text{otherwise,} \end{cases}$$

with c_l^r as in (31).

Then

(1) For $r \in [k-1]$ $\hat{E}^{(r)}$ is the $n \times n$ matrix such that

$$(38) \quad \hat{E}^{(r)}[l] = \begin{cases} \hat{E}^{(k)}[l] & \text{if } l \leq i_r, \\ (-1)^{\sigma_{sr}} A[s] & \text{if } l = i_s, \text{ and } s \in]r, k], \\ E^{(r)}[l] & \text{if } l \in \bar{I} \cap]i_r, n], \text{ and } \chi_l^r = 1, \end{cases}$$

with $E^{(r)}[l]$ as in (32) and $\sigma_{sr} = \#\{i_t \in I, r \leq t < s\}$;

(2) For any $r \in [k]$,

$$(39) \quad A[r] = \sum_{l=1}^n \hat{c}_l^r \hat{E}^{(r)}[l] \equiv E^{(r)}[i_r] + \sum_{s=1}^{N_r} c_{l_s}^r E^{(r)}[l_s],$$

where the second sum is over the indexes such that $\chi_{l_s}^{i_r} = 1$.

Remark 5.1. Changing the orientation of the graph Any change of orientation in \mathcal{N}_T corresponds to a specific choice of the base in the matroid \mathcal{M} associated to $[A]$ (see [52]). Such change induces a well defined change of the basis of vectors $\hat{E}^{[r]}$ in each row, i.e. a well defined linear recombination of the rows of the representative matrix of $[A]$. In section 7, we explain how the system of vectors depend on the orientation for **any** network associated to $[A]$. In section 9.4 we associate any change of orientation to a well defined change of position of the Darboux points on the curve Γ and so to a well-defined change in the vacuum divisor (see Theorem 4.2) which does **not** affect the effective KP divisor (see Theorem 4.2). For this reason we do not discuss here the effect on the basis of vectors due to a change of orientation in the graph.

Proof. (39) follows immediately from Lemma 5.1 and (38). The first statement in (38), $\hat{E}^{(r)}[l] = \hat{E}^{(k)}[l]$ for $l \leq i_r$, $r \in [k]$ follows from the definition of the transition matrix (35). The remaining statements in (38) follow by induction in the index r as it decreases from k to 1.

Let $r = k$. Then the transition matrix $C^{[k-1,k]}$

- (1) Leaves invariant all canonical basis vectors $\hat{E}^{(k)}[l]$ with $l < i_k$;
- (2) If $l = i_k$, $C^{[k-1,k]}$ transforms the canonical basis vector $\hat{E}^{(k)}[i_k]$ to $-A[k]$;

- (3) If $l \in \bar{I} \cap]i_k, n]$ and $\chi_l^{i_k} = 0$, $\hat{E}^{(k-1)}[l] = -\hat{E}^{(k)}[l]$;
(4) If $l \in \bar{I} \cap]i_k, n]$ and $\chi_l^{i_k} = 1$, the components of $\hat{E}^{(k-1)}[l]$ are then

$$\hat{E}_j^{(k-1),l} = \begin{cases} 0 & \text{if } j < l, \\ -1 & \text{if } j = l, \\ 0 & \text{if } j > l \text{ and } \chi_j^{i_k} = 0, \\ -\hat{w}_{lj}^{(k)} & \text{if } j > l \text{ and } \chi_j^{i_k} = 1. \end{cases}$$

It is straightforward to verify that $\hat{E}^{(k-1)}[l] = E^{(k-1)}[l]$, if $l = i_{k-1}$ or $\chi_l^{i_{k-1}} = 1$, for $l \geq i_{k-1}$. Indeed if both $\chi_l^{i_{k-1}} = 1$ and $\chi_l^{i_k} = 1$, the white vertex $V_{i_{k-1}l}$ is joined to the black vertex $V'_{i_k l}$ by an edge of weight 1 so that by definition $\hat{E}^{(k-1)}[l] = E^{(k-1)}[l]$. If $\chi_l^{i_{k-1}} = 1$ and $\chi_l^{i_k} = 0$, the white vertex $V_{i_{k-1}l}$ is joined to the boundary vertex b_l by an edge of unit weight and $\hat{E}^{(k-1)}[l] = E^{(k-1)}[l]$.

Let us now suppose to have verified (38), for any $s \in [r, k]$ and let's verify it for $s = r - 1$. By definition

$$(40) \quad \hat{E}^{(r-1)} = C^{[r-1,r]} \hat{E}^{(r)} = C^{[r-1,r]} C^{[r,r+1]} \hat{E}^{(r+1)} = \dots = \left(\prod_{s=r}^k C^{[s-1,s]} \right) \hat{E}^{(k)}.$$

Let $l \in \bar{I} \cap]i_{r-1}, n]$ be fixed. If $\chi_l^{i_{r-1}} = 0$, then there is no contribution to $A[r-1]$ from the vector $\hat{E}^{(r-1)}[l]$ since the coefficient $\hat{c}_l^{r-1} = 0$. Suppose now that $\chi_l^{i_{r-1}} = 1$ and consider the set $S = \{s \in [r, k] : \chi_l^{i_s} = 1\}$. If $S = \emptyset$, then the white vertex $V_{i_{r-1}l}$ is joined directly to the boundary sink b_l by an edge of unit weight and

$$\hat{E}^{(r-1)}[l] = (-1)^{k-r+1} \hat{E}^{(k)}[l] = (-1)^{k-r+1} E^{(k)}[l] = E^{(r-1)}[l].$$

Otherwise, let $\bar{s} = \min S$. In this case moving downwards from the white vertex $V_{i_{r-1}l}$ the first black vertex that we meet is $V'_{i_{\bar{s}}l}$ and such edge has unit weight. Then, using (40), we have

$$\hat{E}^{(r-1)}[l] = (-1)^{\bar{s}-r+1} \hat{E}^{(\bar{s})}[l] = (-1)^{\bar{s}-r+1} E^{(\bar{s})}[l] = E^{(r-1)}[l].$$

Finally let $l = i_r$. In such case

$$\hat{E}^{(r-1)}[i_r] = C^{[r-1,r]}[i_r] \hat{E}^{(r)} = - \sum_{j=1}^n \hat{c}_j^r \hat{E}^{(r)}[j] = -A[r].$$

since, by definition $C_j^{[r-1,r],i_r} = -\hat{c}_j^r$ and \hat{c}_j^r is non zero if and only if $j = i_r$ or $j \in \bar{I} \cap]i_r, n]$ is such that $\chi_j^{i_r} = 1$.

□

On each component Γ_{i_r} , $r \in [k]$ we have three marked points, but only two edges at the corresponding vertex V_{i_r} . Since in our construction marked points on the curve correspond to edges of the network, we modify \mathcal{N}_T to create an edge $e_{i_r}^{(3)}$ corresponding to the Darboux point $P_{i_r}^{(3)} \in \Gamma_{i_r}$.

To obtain a vacuum vertex wavefunction which coincides with Sato vacuum wavefunction at each boundary edge, we also modify the orientation of edges at V_{i_r} .

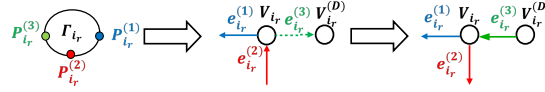


FIGURE 15. The modified graph \mathcal{N}'_T is obtained adding an edge $e_{i_r}^{(3)}$ at each pivot vertex V_{i_r} and a white vertex $V_{i_r}^{(D)}$. The orientation in \mathcal{N}'_T is the same as in the initial network \mathcal{N}_T except at the edge $e_{i_r}^{(2)}$.

Definition 6.1. *The planar oriented trivalent bipartite network \mathcal{N}'_T :*

Denote \mathcal{N}'_T the network obtained from \mathcal{N}_T adding a unit edge $e_{i_r}^{(3)}$ at each pivot vertex V_{i_r} in the position corresponding to the Darboux point $P_{i_r}^{(3)} \in \Gamma_{i_r}$ and let $V_{i_r}^{(D)}$ be the white vertex at the other end of $e_{i_r}^{(3)}$. Such move corresponds to Move (M2) - unicolored edge contraction/uncontraction in [52] and leaves the boundary measurement invariant. Then orient all edges as in \mathcal{N}_T except the edges $e_{i_r}^{(2)}$, $r \in [k]$, which point from V_{i_r} to b_{i_r} in \mathcal{N}'_T and orient $e_{i_r}^{(3)}$, $r \in [k]$, from $V_{i_r}^{(D)}$ to V_{i_r} (see Figure 15). In practice, in \mathcal{N}'_T the Darboux vertexes $V_{i_r}^{(D)}$, $r \in [k]$, are the internal sources while all boundary vertexes b_j , $j \in [n]$, are sinks.

In section 6.1, we define and characterize a vacuum vertex wavefunction on \mathcal{N}'_T using the recursion settled in Theorem 5.1. The vertex vectors and the vacuum vertex wavefunction satisfy linear relations at each trivalent black or white vertex (see Definition 6.2 and Figures 16-17), which are of the same type as those imposed by momentum conservation at trivalent vertexes of on-shell diagrams in [4, 5] (see also Section 7 and compare Figures 16 with formulas (4.54) and (4.55) in [4]). In our construction, such linear relations form a consistent set of relations both on \mathcal{N}_T and on \mathcal{N}'_T for the v.v.w. and its Darboux transform (see Remark 6.2 and Section 7 for the general case \mathcal{N}).

In Lemma 6.2 we use such linear relations to associate a $|D|$ -dimensional vacuum vertex divisor on \mathcal{N}'_T . This divisor fulfils all the properties of reality and regularity settled in Definition 4.4. In

section 6.3 we define the real and regular vacuum wavefunction on Γ so that the vacuum divisor coincides with the vacuum vertex divisor on \mathcal{N}'_T (see Theorem 6.1).

Remark 6.1. Data and notations in this section. *To the data fixed at the preamble of this Section we associate:*

- (1) For the Le-diagram D and the Le-tableau T , N_r , $r \in [k]$, denotes the number of filled boxes in the row r of the Le diagram, χ_j^i is the index of the box $B_{i,j}$ (see (3) and (4)). The pivot indexes are denoted $1 \leq i_1 < \dots < i_k \leq n$ and, for any $r \in [k]$, $1 \leq j_1 < j_2 < \dots < j_{N_r} \leq n$ are the non-pivot indexes of the boxes B_{i_r, j_s} of index $\chi_{j_s}^{i_r} = 1$, $s \in [N_r]$, in the Le-diagram
- (2) The oriented bipartite trivalent Le-network \mathcal{N}'_T , where $|D|$ is the dimension of $\mathcal{S}_{\mathcal{M}}^{TNN}$. The index $j_0 \equiv 0$ is associated to the pivot vertexes, $V_{i_r,0} \equiv V_{i_r}$, and to any quantity referring to them. The edges $e_{i_r, j_l}^{(m)}$, $m \in [3]$, are enumerated with the indexes of its ending white vertex V_{i_r, j_l} , $r \in [k]$ and $l \in [0, N_r]$ (see Figures 10 and 15). Finally, the vertexes $V_{i_r, j_{N_r}}$ have two edges which we label $e_{i_r, j_l}^{(2)}$ and $e_{i_r, j_l}^{(3)}$;
- (3) The families of matrices $\hat{E}^{(r)}$ and vectors $\hat{c}^{(r)}$, $r \in [k]$, as in Theorem 5.1 associated to the RREF matrix A representing $[A]$.

Finally, $\mathfrak{E}_\theta(\vec{t}) = (e^{\theta_1(\vec{t})}, \dots, e^{\theta_n(\vec{t})})$, where $\theta_j(\vec{t}) = \sum_{l \geq 1} \kappa_j^l t_l$ and $\vec{t} = (t_1 = x, t_2 = y, t_3 = t, t_4, \dots)$ are the KP times, and $\langle \cdot, \cdot \rangle$ denotes the usual scalar product. In the statements of Theorems and in the Definitions of this section we do not explicitly mention such data.

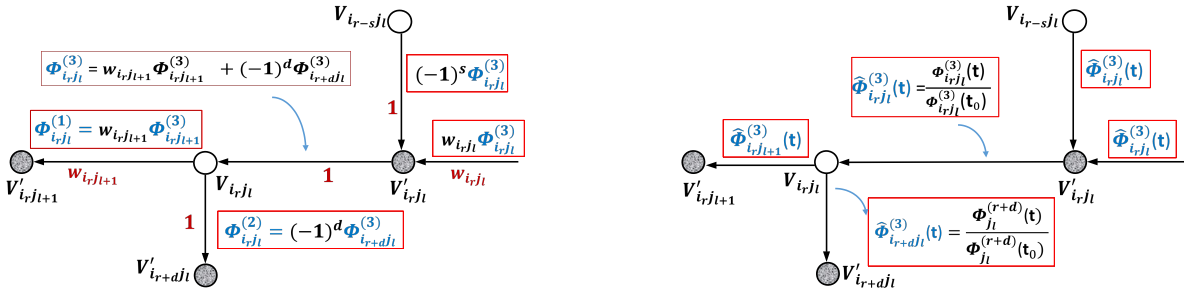


FIGURE 16. Left: the linear relations for the v.v.w. $\Phi_{i_r, j_l}^{(m)}(\vec{t})$ at white and black vertexes. Right: the normalized v.v.w. $\hat{\Phi}_{i_r, j_l}^{(m)}(\vec{t})$ takes the same value at all the edges at a given black vertex V'_{i_r, j_l} and different values at the edges at a given trivalent white vertex V_{i_r, j_l} .

6.1. A vacuum vertex wavefunction on the Le-network. By construction, for each fixed $r \in [k]$ and $l \in [0, N_r]$ we may assign the vector $E^{(r)}[j_l]$ to the vertical edge ending at the white

vertex $V_{i_r j_l}$. We now introduce a simple rule to assign a vector at each horizontal edge in such a way that, if we move along the graph in the opposite direction w.r.t. its orientation along all edges except the pivot edges, where we move up, we obtain the r -th row of the RREF matrix A when we reach the edge $e_{i_r}^{(3)}$. When we pass a black vertex, we multiply the vector of its left horizontal edge by the weight of the right horizontal edge. When we pass a white vertex, we sum up the vectors of its left and vertical vertexes.

In section 7, we associate consistent systems of vectors to any orientation of any network \mathcal{N} associated to the given point $[A]$.

Definition 6.2. Vertex vectors (v.v.) and vacuum vertex wavefunction (v.v.w.) on \mathcal{N}'_T . Let the soliton data and the notations be fixed as in Remark 6.1. To each edge of \mathcal{N}'_T , we associate a vertex vector (v.v.) and a vertex vacuum wavefunction (v.v.w.) depending on \vec{t} as follows:

(1) For any $r \in [k]$, to the vertical edge $e_{i_r}^{(2)}$ joining the boundary source vertex b_{i_r} to the white vertex V_{i_r} , we assign v.v. and v.v.w.

$$(41) \quad \mathfrak{E}_{i_r}^{(2)} = \hat{E}^{(k)}[i_r], \quad \Phi_{i_r}^{(2)}(\vec{t}) \equiv \prec \hat{E}^{(k)}[i_r], \mathfrak{E}_\theta(\vec{t}) \succ = e^{\theta_{i_r}(\vec{t})};$$

(2) For any fixed $r \in [k]$ and $l \in [N_r]$, to the vertical edge $e_{i_r j_l}^{(2)}$ at $V_{i_r j_l}$ we assign

$$(42) \quad \mathfrak{E}_{i_r j_l}^{(2)} = \hat{E}^{(r)}[j_l], \quad \Phi_{i_r j_l}^{(2)}(\vec{t}) \equiv \prec \mathfrak{E}_{i_r j_l}^{(2)}, \mathfrak{E}_\theta(\vec{t}) \succ;$$

(3) For any $r \in [k]$, to the horizontal edge $e_{i_r j_{N_r}}^{(3)}$ joining $V_{i_r j_{N_r}}$ and $V'_{i_r j_{N_r}}$ we assign:

$$(43) \quad \mathfrak{E}_{i_r j_{N_r}}^{(3)} = \mathfrak{E}_{i_r j_{N_r}}^{(2)}, \quad \Phi_{i_r j_{N_r}}^{(3)}(\vec{t}) \equiv \prec \mathfrak{E}_{i_r j_{N_r}}^{(3)}, \mathfrak{E}_\theta(\vec{t}) \succ = \Phi_{i_r j_{N_r}}^{(2)}(\vec{t})$$

(4) For any $r \in [k]$, $l \in [N_r - 1]$, to the horizontal edge $e_{i_r j_l}^{(1)}$ joining $V_{i_r j_l}$ and $V'_{i_r j_{l+1}}$ we assign

$$(44) \quad \mathfrak{E}_{i_r j_l}^{(1)} = w_{i_r j_l} \mathfrak{E}_{i_r j_{l+1}}^{(3)}, \quad \Phi_{i_r j_l}^{(1)}(\vec{t}) \equiv \prec \mathfrak{E}_{i_r j_l}^{(1)}, \mathfrak{E}_\theta(\vec{t}) \succ = w_{i_r j_l} \Phi_{i_r j_{l+1}}^{(3)}(\vec{t}),$$

where $w_{i_r j_l}$ is the weight of $e_{i_r j_l}^{(1)}$;

(5) For any $r \in [k]$, to the horizontal edge $e_{i_r}^{(1)}$ joining V_{i_r} and $V'_{i_r j_1}$ we assign

$$(45) \quad \mathfrak{E}_{i_r}^{(1)} = w_{i_r j_1} \mathfrak{E}_{i_r j_1}^{(3)}, \quad \Phi_{i_r}^{(1)}(\vec{t}) \equiv \prec \mathfrak{E}_{i_r}^{(1)}, \mathfrak{E}_\theta(\vec{t}) \succ = w_{i_r j_1} \Phi_{i_r j_1}^{(3)}(\vec{t}),$$

where $w_{i_r j_1}$ is the weight of $e_{i_r}^{(1)}$;

(6) For any $r \in [k]$, $l \in [N_r - 1]$, to the edge $e_{i_r j_l}^{(3)}$ joining $V_{i_r j_l}$ and $V'_{i_r j_l}$ we assign

$$(46) \quad \mathfrak{E}_{i_r j_l}^{(3)} = \mathfrak{E}_{i_r j_l}^{(1)} + \mathfrak{E}_{i_r j_l}^{(2)}, \quad \Phi_{i_r j_l}^{(3)}(\vec{t}) \equiv \prec \mathfrak{E}_{i_r j_l}^{(3)}, \mathfrak{E}_\theta(\vec{t}) \succ = \Phi_{i_r j_l}^{(1)}(\vec{t}) + \Phi_{i_r j_l}^{(2)}(\vec{t}),$$

i.e. the sum of the contributions from the edges to the left and below the white vertex $V_{i_r j_l}$;

(7) To the horizontal edge $e_{i_r}^{(3)}$ at the white source vertex V_{i_r} , $r \in [k]$, we associate the v.v. and the v.v.w.

$$(47) \quad \mathfrak{E}_{i_r}^{(3)} = \mathfrak{E}_{i_r j_1}^{(1)} + \mathfrak{E}_{i_r j_1}^{(2)}, \quad \Phi_{i_r}^{(3)}(\vec{t}) = \prec \mathfrak{E}_{i_r 0}^{(3)}, \mathfrak{E}_\theta(\vec{t}) \succ .$$

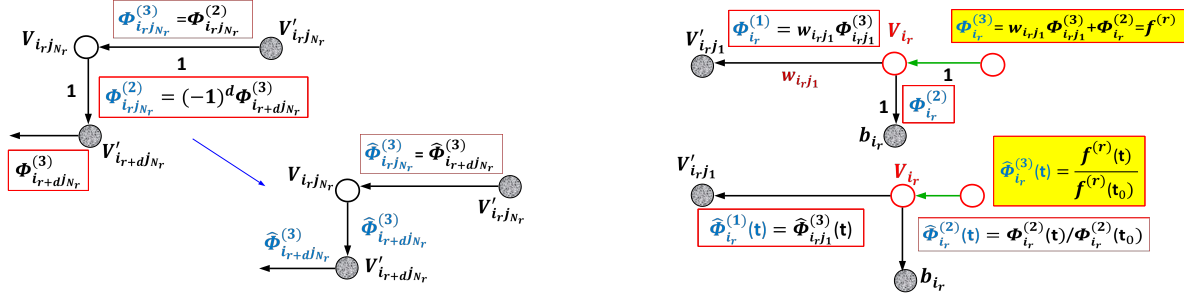


FIGURE 17. Same as in Fig. 17 at the bivalent white vertex $V_{i_r j_l}$ [left] and at the pivot vertex V_{i_r} [right].

We illustrate Definition 6.2 in Figures 16 and 17. For any $r \in [k]$, $l \in [N_r]$, Definition 6.2 implies:

- (1) the value of the v.v. (respectively of the v.v.w.) on the edge to the right of each white vertex $V_{i_r j_l}$ is the sum of the v.v. (respectively of the v.v.w.) on the edges to the left and below $V_{i_r j_l}$;
- (2) the value of the v.v. (respectively of the v.v.w.) on the edges to the right of and above each black vertex $V'_{i_r j_l}$ is the proportional to the value of the v.v. (respectively of the v.v.w.) on the edge to the left of $V'_{i_r j_l}$.

Comparing Theorem 5.1 and Definition 6.2, it is not difficult to prove that at the vertex V_{i_r} $\mathfrak{E}_{i_r}^{(3)} = A[r]$.

Lemma 6.1. *Let the soliton data and the notations be fixed as in Remark 6.1. Let the v.v. and v.v.w. be as in Definition 6.2. Then,*

- (1) for any $r \in [k]$ and $l \in [N_r]$, the vertex vector at the edge joining $V_{i_r j_l}$, $V'_{i_r j_l}$ is

$$(48) \quad \mathfrak{E}_{i_r j_l}^{(3)} = \sum_{s=l}^{N_r} \hat{c}_{j_s}^r \hat{E}^{(r)}[j_s];$$

(2) for any $r \in [k]$ the vertex vector at the edge $e_{i_r}^{(3)}$ is the r -th row of the RREF matrix representing $[A] \in Gr^{TNN}(k, n)$

$$(49) \quad \mathfrak{E}_{i_r j_l}^{(3)} = A[r],$$

and the v.v.w. is the r -th generator of the dressing transformation associated to the soliton data $(\mathcal{K}, [A])$.

$$(50) \quad \Phi_{i_r}^{(3)}(\vec{t}) = f^{(r)}(\vec{t}).$$

The proof of the Lemma easily follows comparing (48), (49) and (50) with (31), (36), (37) and (39) in Theorem 5.1 and with (41)–(47) in Definition 6.2.

As a consequence, both the vertex vectors and vertex wavefunction associated above to the bipartite Le–diagram may be recursively computed using Theorem 5.1 starting from the last row of the Le–diagram which corresponds to the index $r = k$ and moving up to $r = 1$. For simplicity, we illustrate the algorithm for the vertex vectors only (see also Figures 16 and 17 for the vertex wavefunction).

Algorithm for the vertex vectors: For any $r \in [k]$:

- (1) If $N_r = 0$, i.e. all the boxes of the r -th line of the Le–diagram contain zeros, assign to the white vertex V_r the vector $\hat{E}^{(r)}[i_r] \equiv \hat{E}^{(k+1)}[i_r]$ and proceed to (3);
- (2) Otherwise:
 - (a) Start from the leftmost white vertex of the line, $V_{i_r j_{N_r}}$ and assign to the edge joining $V_{i_r j_{N_r}}$ and $V'_{i_r j_{N_r}}$ the vertex vector

$$\mathfrak{E}_{i_r j_{N_r}}^{(3)} = \hat{E}^{(r)}[j_{N_r}]$$

- (b) For any l from $N_r - 1$ to 1, assign to the edge joining $V_{i_r j_l}$ and $V_{i_r j_{l+1}}$, the vector

$$\mathfrak{E}_{i_r j_l}^{(3)} = w_{i_r j_{l+1}} \mathfrak{E}_{i_r j_{l+1}}^{(3)} + \hat{E}^{(r)}[j_l].$$

- (c) At the white vertex V_r assign the vector

$$\mathfrak{E}_{i_r 0}^{(3)} = w_{i_r j_1} \mathfrak{E}_{i_r j_1}^{(3)} + \hat{E}^{(r)}[i_r] = A[r],$$

and go to (3).

- (3) If $r = 1$, just end. Otherwise set the counter to $r - 1$ and repeat the whole procedure.

Example 6.1. We illustrate such procedure for Example 2.2 (see Figure 6). At the horizontal edge joining V_{45} and V'_{45} we assign the vertex vector

$$\mathfrak{E}_{45}^{(3)} = E^{(3)}[5] + w_{46}\mathfrak{E}_{46}^{(3)} = (0, 0, 0, 0, 1, w_{46}, 0, -w_{46}w_{48}, -w_{46}w_{48}w_{49}),$$

since $\mathfrak{E}_{46}^{(3)} = E^{(3)}[6] + w_{48}\mathfrak{E}_{48}^{(3)} = E^{(3)}[6] + w_{48}(\hat{E}^{(3)}[8] + w_{49}\hat{E}^{(3)}[9])$, and the vertex wavefunction

$$\Phi_{45}^{(3)}(\vec{t}) = e^{\theta_5(\vec{t})} + w_{46}e^{\theta_6(\vec{t})} - w_{46}w_{48}e^{\theta_8(\vec{t})} - w_{46}w_{48}w_{49}e^{\theta_9(\vec{t})}.$$

At the horizontal edge joining V_{25} and V'_{25} we associate the vertex vector $\mathfrak{E}_{25}^{(3)} = E^{(2)}[5] = -\mathfrak{E}_{45}^{(3)}$ (compare with Example 5.1) and the vertex wavefunction $\Phi_{25}^{(3)}(\vec{t}) = -\Phi_{45}^{(3)}(\vec{t})$ for all times \vec{t} .

Remark 6.2. The v.v.w. is a solution of a linear system in \mathcal{N}'_T . The v.v.w. $\Phi(\vec{t})$ is a solution to the following linear system associated to the edges of \mathcal{N}'_T :

- (1) At each internal white vertex $V_{i_r j_l}$, $r \in [k]$, $l \in [0, N_r]$, let $\Phi_{i_r j_l}^{(3)}(\vec{t}) = \Phi_{i_r j_l}^{(1)}(\vec{t}) + \Phi_{i_r j_l}^{(2)}(\vec{t})$, where $\Phi_{i_r j_l}^{(m)}(\vec{t})$ is the value at $e_{i_r j_l}^{(m)}$. If the \bar{m} edge is absent at a white vertex $V_{i_r j_l}$ then we set $\Phi_{i_r j_l}^{(\bar{m})}(\vec{t}) \equiv 0$;
- (2) At each internal black vertex $V'_{i_r j_l}$, $r \in [k]$, $l \in [N_r]$, $H_{i_r j_l}^{(2)}(\vec{t}) = w_{i_r j_l} H_{i_r j_l}^{(1)}(\vec{t})$ and $H_{i_r j_l}^{(3)}(\vec{t}) = -(-1)^d H_{i_r j_l}^{(1)}(\vec{t})$, where $H_{i_r j_l}^{(m)}(\vec{t})$ is the value of the function at the edge $a_{i_r j_l}^{(m)}$ at $V'_{i_r j_l}$, and $d = d(i_r j_l)$ is the number of pivot indexes between i_r and j_l ;
- (3) The value of the function coincide for all \vec{t} , if the edges $e_{ij}^{(m)}$ and $a_{i'j'}^{(s)}$ coincide: $\Phi_{ij}^{(m)}(\vec{t}) = H_{i'j'}^{(s)}(\vec{t})$.

The above system forms a consistent system of linear relations: if we assign input values $\Phi_j^{(2)}(\vec{t})$ to each edge $e_j^{(2)}$ at a boundary vertex, $j \in [n]$, we obtain as output values the value of the v.v.w. at the k Darboux edges. Indeed, suppose that \mathcal{N}'_T corresponds to an irreducible positroid cell $\mathcal{S}_{\mathcal{M}}^{TNN} \subset Gr^{TNN}(k, n)$ of dimension $|D|$. Then, the number of variables is equal to the number of edges, $3|D| + 2k$ (we have $|D| + k$ vertical edges and $2|D| + k$ horizontal edges). The total number of equations at black vertexes is $2(|D| - n + k) + n - k = 2|D| - n + k$, since the total number of internal black vertexes is $|D|$ of which $|D| - n + k$ are trivalent. Any trivalent black vertex carries two equations, while each bivalent black vertex carries one condition. The total number of equations at white vertexes is $|D| + k$, since the total number of internal white vertexes is $|D| + 2k$, but the univalent Darboux vertexes on \mathcal{N}'_T do not carry any extra condition. Then we conclude that we may freely impose a value to $n = 3|D| + 2k - (2|D| - n + k) - (|D| + k)$ variables (edges).

The presence of an isolated boundary sink b_j implies the addition of an internal univalent vertex joined to b_j : we have a new variable (the univalent edge) and no extra condition. The presence of an isolated boundary source b_i implies the addition of a bivalent vertex V_i and of an univalent Darboux vertex $V_i^{(D)}$: we have two variables and one equation.

In section 7 we generalize the above relations to any network \mathcal{N} .

6.2. The vacuum vertex divisor. We now assign a vacuum vertex divisor to the bipartite Le-diagram \mathcal{N}'_T through the properties of Φ .

Remark 6.3. Choice of the initial time \vec{t}_0 . For any fixed $r \in [k]$, $l \in [0, N_r - 1]$, at both the horizontal edges at the white vertex $V_{i_r j_l}$, the vacuum vertex wavefunction takes the form

$$(51) \quad \Phi_{i_r j_l}^{(1)}(\vec{t}) = \sum_{s=i_r}^n a_s^{(1)[r]l} e^{\theta_s(\vec{t})}, \quad \Phi_{i_r j_l}^{(3)}(\vec{t}) = \sum_{s=i_r}^n a_s^{(3)[r]l} e^{\theta_s(\vec{t})},$$

and $a_s^{(1)[r]l} a_s^{(3)[r]l} \geq 0$, that is the coefficients associated to the same phase κ_s have the same sign since the latter depends only on the number of boundary sources in the open interval $]i_r, s[$. Moreover the highest index s such that $a_s^{(1)[r]l} \neq 0$ is the same as for $a_s^{(3)[r]l} \neq 0$ by construction. For this reason let $\vec{t}_0 = (x_0, 0 \dots)$ with $x_0 \in \mathbb{R}$ be such that:

- (1) for any $l \in [0, N_r]$, $r \in [k]$, the sign of both $\Phi_{i_r j_l}^{(1)}(\vec{t}_0)$ and $\Phi_{i_r j_l}^{(3)}(\vec{t}_0)$ are equal to the sign the highest non zero coefficient in (51);
- (2) for any $r \in [k]$ the sign of $\Phi_{i_r j_{N_r}}^{(3)}(\vec{t}_0)$ is equal to the sign of its highest non zero coefficient.

In practice we choose \vec{t}_0 in such a way that, for any fixed $r \in [k]$, the signs of the v.v.w. $\Phi_{i_r j_l}^{(1)}(\vec{t}_0)$, $\Phi_{i_r j_l}^{(3)}(\vec{t}_0)$, is the same at all horizontal edges, $l \in [0, N_r]$.

In the next Lemma, we normalize the v.v.w. previously defined and characterize the vacuum pole divisor associated to the set of white vertexes $V_{i_r j_l}$, $r \in [k]$, $l \in [0, N_r - 1]$.

Lemma 6.2. Let $(\mathcal{K}, [A])$ and the vacuum vertex wavefunction be as in the Definition 6.2 and let $\vec{t}_0 = (x_0, 0 \dots)$ be as in remark 6.3. Then the normalized v.v.w.

$$(52) \quad \hat{\Phi}_{i_r j_l}^{(m)}(\vec{t}) = \frac{\Phi_{i_r j_l}^{(m)}(\vec{t})}{\Phi_{i_r j_l}^{(m)}(\vec{t}_0)}, \quad l \in [0, N_r], r \in [k], m \in [3],$$

has the following properties:

- (1) $\hat{\Phi}_{i_r j_l}^{(m)}(\vec{t})$ is a regular function of \vec{t} for any $r \in [k]$, $l \in [0, N_r]$, $m \in [3]$;

- (2) For any $r \in [k]$, $j \in [N_r]$, the normalized v.v.w. takes the same value on all edges at the black vertex $V'_{i_r j_l}$, either bivalent or trivalent;
- (3) For any $r \in [k]$, the normalized v.v.w. takes the same value on both edges at the white vertex $V_{i_r j_{N_r}}$ for all times \vec{t} : $\hat{\Phi}_{i_r j_{N_r}}^{(2)}(\vec{t}) = \hat{\Phi}_{i_r j_{N_r}}^{(3)}(\vec{t})$;
- (4) For any fixed $r \in [k]$, $j \in [N_r - 1]$, the normalized v.v.w. takes different values on the edges at the white trivalent vertex $V_{i_r j_l}$ and

$$(53) \quad \gamma_{i_r j_l}^{(0)} = \frac{\Phi_{i_r j_l}^{(1)}(\vec{t}_0)}{\hat{\Phi}_{i_r j_l}^{(3)}(\vec{t}_0)} = \frac{\Phi_{i_r j_l}^{(1)}(\vec{t}_0)}{\Phi_{i_r j_l}^{(1)}(\vec{t}_0) + \hat{\Phi}_{i_r j_l}^{(2)}(\vec{t}_0)},$$

is the unique positive number such that

$$\hat{\Phi}_{i_r j_l}^{(3)}(\vec{t}) \equiv \gamma_{i_r j_l}^{(0)} \hat{\Phi}_{i_r j_l}^{(1)}(\vec{t}) + (1 - \gamma_{i_r j_l}^{(0)}) \hat{\Phi}_{i_r j_l}^{(2)}(\vec{t}), \quad \forall \vec{t};$$

- (5) For any $r \in [k]$, such that b_{i_r} is not an isolated boundary source, the normalized v.v.w. takes different values on the edges at the white trivalent vertex V_{i_r} and

$$(54) \quad \gamma_{i_r}^{(0)} = \frac{\Phi_{i_r}^{(1)}(\vec{t}_0)}{\hat{\Phi}_{i_r}^{(3)}(\vec{t}_0)} = \frac{\Phi_{i_r}^{(1)}(\vec{t}_0)}{\Phi_{i_r}^{(1)}(\vec{t}_0) + \hat{\Phi}_{i_r}^{(2)}(\vec{t}_0)},$$

is the unique positive number such that

$$\hat{\Phi}_{i_r}^{(3)}(\vec{t}) \equiv \gamma_{i_r}^{(0)} \hat{\Phi}_{i_r}^{(1)}(\vec{t}) + (1 - \gamma_{i_r}^{(0)}) \hat{\Phi}_{i_r}^{(2)}(\vec{t}), \quad \forall \vec{t};$$

- (6) If, for some $r \in [k]$, b_{i_r} is an isolated boundary source, the white vertex V_{i_r} is univalent and $\hat{\Phi}_{i_r}^{(3)}(\vec{t}) \equiv \hat{\Phi}_{i_r}^{(1)}(\vec{t}) = \exp(\theta_{i_r}(\vec{t} - \vec{t}_0))$, $\forall \vec{t}$;

- (7) The set of normalized v.v.w. $\hat{\Phi}_{i_r}^{(3)}(\vec{t})$ defined at the source vertexes V_{i_r} , $r \in [k]$,

- (a) Form a basis of heat hierarchy solutions which satisfy $\mathfrak{D}^{(k)} \hat{\Phi}_{i_r}^{(3)}(\vec{t}) \equiv 0$, for all $r \in [k]$, \vec{t} , with

$$(55) \quad \mathfrak{D}^{(k)} = W \partial_x^k \equiv \partial_x^k - \mathfrak{w}_1(\vec{t}) \partial_x^{k-1} - \mathfrak{w}_2(\vec{t}) \partial_x^{k-2} - \dots - \mathfrak{w}_k(\vec{t}),$$

the Darboux transformation and W the Sato dressing operator for $(\mathcal{K}, [A])$;

- (b) Generate the KP soliton solution $u(\vec{t})$ associated to $(\mathcal{K}, [A])$

$$u(\vec{t}) = 2\partial_{xx} \log(\tau(\vec{t})), \quad \tau(\vec{t}) = Wr_x(\hat{\Phi}_{i_1}^{(3)}(\vec{t}), \dots, \hat{\Phi}_{i_k}^{(3)}(\vec{t}))$$

where Wr_x denotes the Wronskian of $\hat{\Phi}_{i_r}^{(3)}(\vec{t})$, $r \in [k]$, with respect to $x = t_1$.

The proof is trivial and is omitted. We illustrate the above statement in Figures 16 and 17.

Definition 6.3. (*Pole divisor of the normalized vacuum vertex wavefunction*) Let $(\mathcal{K}, [A])$, D the Le-diagram associated to $[A]$, $\vec{t}_0 = (x_0, 0 \dots)$ and the normalized v.v.w. $\hat{\Phi}_{i_r j_l}^{(m)}(\vec{t})$, $l \in [0, N_r]$, $r \in [k]$, $m \in [3]$, be as in Lemma 6.2. We define the degree $|D|$ vacuum vertex pole divisor

$$(56) \quad \mathcal{D}_{\text{vac}, \mathcal{N}'_T} = \{\gamma_{i_r j_l}^{(0)}, r \in [k], l \in [0, N_r - 1]\},$$

where $\gamma_{i_r j_l}^{(0)}$ are as in (53) and (54).

Remark 6.4. The vacuum vertex divisor in Definition 6.3 is associated to the RREF representation A for the given regular soliton data $(\mathcal{K}, [A])$. A change of base in the matroid \mathcal{M} associated to such data induces a change in the values of the v.v.w. at each edge and so an untrivial change of the vacuum divisor points in (53) and (54). We postpone the discussion of this change of the vacuum divisor to section 9.4.

Example 6.2. Let's compute the normalized vacuum vertex wavefunction for Example 6.1. At the vertex V_{45} the normalized vertex vacuum wavefunction is

$$\hat{\Phi}_{45}^{(3)}(\vec{t}) = \frac{e^{\theta_5(\vec{t})} + w_{46}e^{\theta_6(\vec{t})} - w_{46}w_{48}e^{\theta_8(\vec{t})} - w_{46}w_{48}w_{49}e^{\theta_9(\vec{t})}}{e^{\theta_5(\vec{t}_0)} + w_{46}e^{\theta_6(\vec{t}_0)} - w_{46}w_{48}e^{\theta_8(\vec{t}_0)} - w_{46}w_{48}w_{49}e^{\theta_9(\vec{t}_0)}}.$$

At the vertex V_{25} we associate the **opposite** vertex wavefunction $\Phi_{25}^{(3)}(\vec{t}) = -\Phi_{45}^{(3)}(\vec{t})$ and the **same normalized** vertex wavefunction $\hat{\Phi}_{25}^{(3)}(\vec{t}) = \hat{\Phi}_{45}^{(3)}(\vec{t})$ for all times \vec{t} . We leave as an exercise to the reader the computation of the vacuum divisor for this example (see Figure 18).

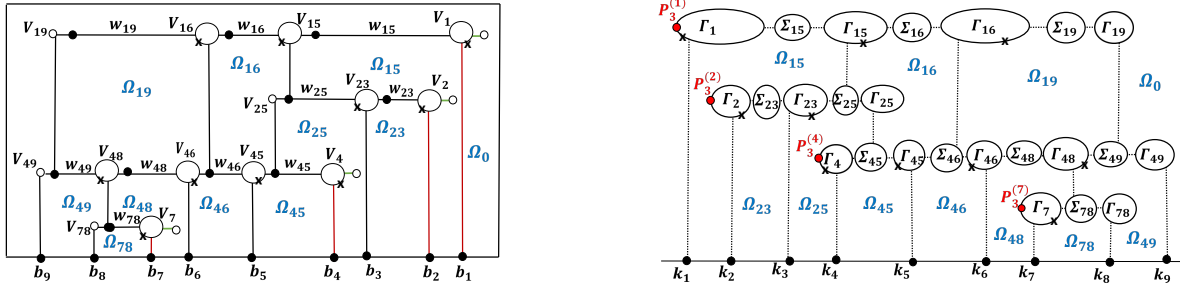


FIGURE 18. The vacuum divisor (red crosses) of the normalized v.v.w. on \mathcal{N}'_T [left] and the vacuum divisor (red crosses) on the degenerate M-curve Γ [right] for Example 2.2.

6.3. The vacuum wavefunction on $\Gamma(\mathcal{N}_T)$ and its pole divisor. In the next Theorem, we construct a normalized vacuum KP wavefunction $\hat{\phi}(P, \vec{t})$ satisfying Definition 4.4. At any given marked point on $\Gamma \setminus \{P_0\}$, we impose that $\hat{\phi}(P, \vec{t})$ coincides with the value of the normalized

vacuum vertex wavefunction defined in Definition 6.2 on the corresponding edge of \mathcal{N}'_T for all \vec{t} . On each copy of \mathbb{CP}^1 corresponding to an internal vertex we extend it using the following rules

- (1) On Γ_0 it is the normalized Sato vacuum wavefunction;
- (2) On any copy of \mathbb{CP}^1 corresponding either to an internal black vertex or to a bivalent white vertex, $\hat{\phi}(P, \vec{t})$ is a constant function;
- (3) On any copy of \mathbb{CP}^1 corresponding to a trivalent white vertex $\hat{\phi}(P, \vec{t})$ is meromorphic of degree 1.

Then, by construction, $\hat{\phi}(P, \vec{t})$ has an essential singularity at $P_0 \in \Gamma \cap \Omega_0$, and effective degree $|D|$ divisor of poles $\mathcal{D}_{\text{vac}, \Gamma} = (P_{i_r j_l}^{(0)}, r \in [k], j \in [0, N_r - 1])$ in the real part of $\Gamma \setminus \{P_0\}$, such that $\zeta(P_{i_r j_l}^{(0)}) = \gamma_{i_r j_l}^{(0)}$ as in (53) and (54), where ζ is the local coordinate on the corresponding component $\Gamma_{i_r j_l}$.

Definition 6.4. *The vacuum wavefunction $\hat{\phi}$ on $\Gamma(\mathcal{N}_T)$. Let the data be as in Remark 6.1. Let Γ and the marked points on Γ be as in Example 4.1. Let $\Phi(\vec{t})$ and $\hat{\Phi}(\vec{t})$ respectively be the v.v.w. and its normalization as in Definition 6.2 and (52), with $\vec{t}_0 = (x_0, 0, \dots)$ as in Remark 6.3. Define $\hat{\phi}(P, \vec{t})$ as follows:*

- (1) the restriction of $\hat{\phi}$ to Γ_0 is denoted $\hat{\phi}_0$ and is the normalized Sato vacuum wavefunction

$$(57) \quad \hat{\phi}_0(\zeta, \vec{t}) = e^{\theta(\vec{t} - \vec{t}_0)}, \quad \theta(\vec{t} - \vec{t}_0) = \zeta(x - x_0) + \sum_{l \geq 2} \zeta^l t_l,$$

that is $\hat{\phi}_0(\kappa_j, \vec{t}) = \hat{\Phi}_j^{(2)}(\vec{t})$, for any $j \in [n]$ and for all \vec{t} .

- (2) for any $r \in [k]$, $s \in [N_r]$ denote $\hat{\phi}'_{i_r j_s}(P, \vec{t})$ the restriction of $\hat{\phi}$ to $\Sigma_{i_r j_s}$ and assign it the value of the normalized vertex function $\hat{\Phi}_{i_r j_s}^{(3)}(\vec{t})$:

$$(58) \quad \hat{\phi}'_{i_r j_s}(P, \vec{t}) = \hat{\Phi}_{i_r j_s}^{(3)}(\vec{t}), \quad \forall \vec{t};$$

- (3) for any $r \in [k]$, denote $\hat{\phi}_{i_r}(P, \vec{t})$ the restriction of $\hat{\phi}$ to Γ_{i_r} and define it as follows:

- (a) If $N_r = 0$, then assign the value $\hat{\phi}_0(\kappa_j, \vec{t})$ to $\hat{\phi}_{i_r}(P, \vec{t})$, for all P and \vec{t} :

$$\hat{\phi}_{i_r}(P, \vec{t}) = \hat{\phi}_0(\kappa_{i_r}, \vec{t}) = e^{\theta_{i_r}(\vec{t} - \vec{t}_0)}, \quad \theta_{i_r}(\vec{t} - \vec{t}_0) = \kappa_{i_r}(x - x_0) + \sum_{l \geq 2} \kappa_{i_r}^l t_l;$$

- (b) Otherwise it is meromorphic with exactly one real pole and it is uniquely identified by the conditions

$$(59) \quad \hat{\phi}_{i_r}(P_{i_r}^{(m)}, \vec{t}) = \hat{\Phi}_{i_r}^{(m)}(\vec{t}), \quad m \in [3], \quad \forall \vec{t};$$

i.e. it takes the form

$$(60) \quad \hat{\phi}_{i_r}(\zeta, \vec{t}) = \frac{\Phi_{i_r}^{(1)}(\vec{t})(\zeta - 1) + \Phi_{i_r}^{(2)}(\vec{t})\zeta}{\Phi_{i_r}^{(3)}(\vec{t}_0) \left(\zeta - \gamma_{i_r}^{(0)} \right)},$$

with $\gamma_{i_r}^{(0)} = \frac{\Phi_{i_r}^{(1)}(\vec{t}_0)}{\Phi_{i_r}^{(3)}(\vec{t}_0)}$ as in (54).

(4) for any $r \in [k]$ and $s \in [N_r - 1]$, denote $\hat{\phi}_{i_r j_s}(P, \vec{t})$, the restriction of $\hat{\phi}$ to $\Gamma_{i_r j_s}$. $\hat{\phi}_{i_r j_s}(P, \vec{t})$ is regular in \vec{t} , meromorphic for $P \in \Gamma_{i_r j_s}$ with exactly one real pole and it is uniquely identified by the conditions

$$(61) \quad \hat{\phi}_{i_r j_s}(P_{i_r j_s}^{(m)}, \vec{t}) = \hat{\Phi}_{i_r j_s}^{(m)}(\vec{t}), \quad m \in [3], \quad \forall \vec{t};$$

i.e. in the local coordinate ζ , it takes the form

$$(62) \quad \hat{\phi}_{i_r j_s}(\zeta, \vec{t}) = \frac{\Phi_{i_r j_s}^{(1)}(\vec{t})(\zeta - 1) + \Phi_{i_r j_s}^{(2)}(\vec{t})\zeta}{\Phi_{i_r j_s}^{(3)}(\vec{t}_0) \left(\zeta - \gamma_{i_r j_s}^{(0)} \right)},$$

with $\gamma_{i_r j_s}^{(0)} = \frac{\Phi_{i_r j_s}^{(1)}(\vec{t}_0)}{\Phi_{i_r j_s}^{(3)}(\vec{t}_0)}$ as in (53).

(5) for any $r \in [k]$, denote $\hat{\phi}_{i_r j_{N_r}}(P, \vec{t})$ the restriction of $\hat{\phi}$ to $\Gamma_{i_r j_{N_r}}$ and assign it the value

$$(63) \quad \hat{\phi}_{i_r j_{N_r}}(P, \vec{t}) = \Phi_{i_r j_{N_r}}^{(2)}(\vec{t}), \quad \forall P \in \Gamma_{i_r j_{N_r}}, \vec{t}.$$

Theorem 6.1. **The vacuum divisor (Theorem 4.1 for $\Gamma(\mathcal{N}_T)$ for the lexicographically minimal base I).** $\hat{\phi}$ as in Definition 6.4 is the real and regular vacuum wavefunction on $\Gamma(\mathcal{N}_T)$ for I as in Remark 6.1, that is it satisfies all the properties of Definition 4.4 on $\Gamma \setminus \{P_0\}$. In particular, for any $r \in [k]$, $\hat{\phi}(P_{i_r}^{(3)}, \vec{t}) = f^{(r)}(\vec{t})$, for all \vec{t} , where $f^{(r)}(\vec{t})$ is heat hierarchy solution associated to the r -th row of the RREF representative matrix in $[A]$ and the vacuum divisor $\mathcal{D}_{\text{vac}, \mathcal{N}'_T}$ of $\hat{\phi}(P, \vec{t})$ satisfies:

- (1) It consists of $|D|$ simple poles and no pole belongs to Γ_0 ;
- (2) On each $\Gamma_{i_r j_l}$ there is exactly one pole, $r \in [k]$ and $l \in [N_r - 1]$;
- (3) On each Γ_{i_r} there is exactly one pole, $r \in [k]$;
- (4) For any finite oval $\Omega_{i_r j_l}$, $r \in [k], l \in [N_r]$, let $\nu_{i_r j_l} = \#\{\mathcal{D}_{\text{vac}, \Gamma(\mathcal{N}_T)} \cap \Omega_{i_r j_l}\}$ and $\mu_{i_r j_l} = \#\{P_{i_s}^{(3)} \in \Omega_{i_r j_l}, s \in [k]\}$ respectively be the number of poles and the number of Darboux source points in $\Omega_{i_r j_l}$. Then for all $r \in [k], l \in [N_r]$,

$$(64) \quad \nu_{i_r j_l} + \mu_{i_r j_l} = \text{odd number};$$

(5) Let $s_0 = \#\{\mathcal{D}_{\text{vac}, \Gamma(\mathcal{N}_T)} \cap \Omega_0\}$ and $\mu_0 = \#\{P_{i_s}^{(3)} \in \Omega_0, s \in [k]\}$, respectively be the number of poles and the number of Darboux source points in the infinite oval Ω_0 . Then

$$(65) \quad \nu_0 + \mu_0 + k = \text{even number.}$$

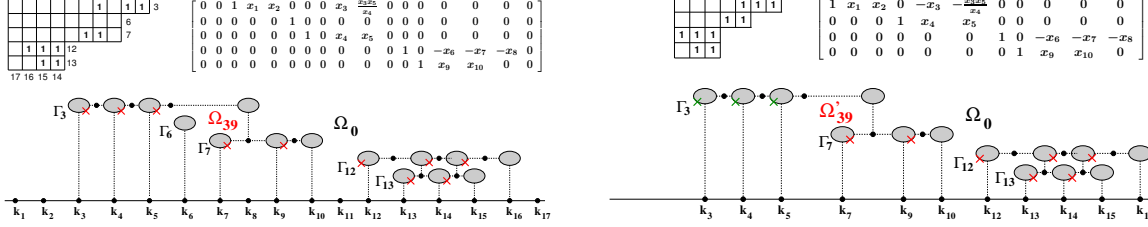


FIGURE 19. We illustrate Case b) in the proof of Theorem 6.1 for the example discussed in Remark 6.5.

Proof. The only untrivial statements are properties (4) and (5). Let us preliminarily notice that copies of \mathbb{CP}^1 corresponding to isolated boundary sources contribute to the counting only with a Darboux zero point, while those corresponding to not isolated boundary sources contribute with a pole and a Darboux zero point. Moreover, in the local coordinate all poles have positive ζ -coordinate by definition: $\zeta(P_{i_r j_l}^{(0)}) = \gamma_{i_r j_l}^{(0)}, \zeta(P_{i_r}^{(0)}) = \gamma_{i_r}^{(0)} > 0$, for any $r \in [k]$ and $l \in [N_r]$ so that:

- (1) for any fixed $r \in [k]$ and $l \in [N_r]$, the finite oval $\Omega_{i_r j_l}$ may contain only poles belonging either to $\Gamma_{i_r j_l}$ or to $\Gamma_{i_r j_{l-1}}$ or to Γ_{i_r+d} , with $d \in [k-r]$;
- (2) Ω_0 may contain only poles belonging to Γ_{i_r} , with $r \in [k]$.

Let's prove (65) first.

Case a) First of all, let us suppose that there exists a path in \mathcal{N}_T joining i_1 to j_{N_k} . Then, either $i_1 = 1$ and $N_k = n$ or all $b_j, j \in [i_1 - 1] \cup [j_{N-k} + 1, n]$ are isolated boundary sinks. In either case $\Gamma_{i_s} \cap \Omega_0 \neq \emptyset$ if and only if $s = 1$ and $\mu_0 = 1$. The pole on Γ_{i_1} has ζ -coordinate

$$\gamma_{i_1}^{(0)} = \frac{\Phi_{i_1}^{(1)}(\vec{t}_0)}{\Phi_{i_1}^{(1)}(\vec{t}_0) + e^{\theta_{i_1}(t_0)}} > 0$$

and $\text{sign}(\Phi_{i_1}^{(1)}(\vec{t}_0)) = (-1)^{k-1}$ by construction (compare Lemma 6.2 with Theorem 5.1). Then, if k is even, $\gamma_{i_1}^{(0)} > 1$, the pole $P_{i_1}^{(0)} \in \Omega_0$, $\nu_0 = 1$ and (65) holds. If k is odd, $0 < \gamma_{i_1}^{(0)} < 1$, $P_{i_1}^{(0)} \notin \Omega_0$, $\nu_0 = 0$ and (65) again holds true.

Case b) Otherwise, there exist $1 \leq s_1 < \dots < s_d \leq k$ such that $i_{s_l} \in I$, for any $l \in [d]$, and indexes $\bar{j}_l, l \in [d]$, satisfying $1 \leq i_{s_1} \leq \bar{j}_1 < i_{s_2} \leq \bar{j}_2 < \dots < i_{s_d} \leq \bar{j}_d \leq n$ such that, for any fixed

$l \in [d]$, if $i_{s_l} = \bar{j}_l$ then $b_{i_{s_l}}$ is an isolated boundary source; otherwise \bar{j}_l is the maximum non pivot index such that there exists a path from the boundary source $b_{i_{s_l}}$ to the boundary sink $b_{\bar{j}_l}$.

In this case $\Omega_0 \cap \Gamma_{i_r} \neq \emptyset$ if and only if $r \in \{s_1, \dots, s_d\}$. For any fixed $l \in [d]$, we apply the argument of Case a) to the subgraph of \mathcal{N}_T containing only boundary vertexes between $b_{i_{s_l}}$ and $b_{\bar{j}_l}$, and again (65) holds true. We refer to Figure 19 for an illustrating example.

To prove (64), it is sufficient to use an induction argument starting from the ovals associated to the last row of the Le–diagram and moving along each row from the leftmost box towards the pivot. Notice that any time we add a new oval in this way, we create a provisional infinite oval for which (65) holds true.

Let $r = k$. If b_{i_k} is an isolated boundary source, then we do not create any finite oval and we pass to next row. If $N_k \geq 1$, then all entries of the last row of the RREF representative matrix A are positive, so that $\gamma_{i_k j_l}^{(0)}, \gamma_{i_k}^{(0)} \in]0, 1[$ for any $l \in [N_k - 1]$. Then each finite oval $\Omega_{i_k j_l}$, $l \in [N_k]$ contains only the pole $P_{i_k j_{l-1}}^{(0)}$ and (64) is satisfied.

Now set the counter $r = k - 1$.

- (1) If $b_{i_{k-1}}$ is an isolated boundary source, then we do not create any finite oval and we pass to next row. Observe that the provisional infinite oval created using the last two rows of the Le–diagram, contains 2 Darboux zeros, $P_{i_{k-1}}^{(3)}, P_{i_k}^{(3)}$ and no pole.
- (2) If $N_{k-1} \geq 1$ and $j_{N_{k-1}} < i_k$, then also all matrix entries of the $(k-1)$ –th row are positive and again each finite oval $\Omega_{i_{k-1} j_l}$, $l \in [N_{k-1}]$ contains only the pole $P_{i_{k-1} j_{l-1}}^{(0)}$ and (64) is satisfied. Finally the provisional infinite oval created after adding all ovals associated to the last two rows of the Le–diagram, contains 2 Darboux zeros, $P_{i_{k-1}}^{(3)}, P_{i_k}^{(3)}$ and no pole.
- (3) If $N_{k-1} \geq 1$ and $j_{N_{k-1}} > i_k$, let $\bar{s} \in [N_{k-1}]$ be the index such that $\Omega_{i_{k-1} j_{\bar{s}}} \cap \Gamma_{i_k} \neq \emptyset$.

Then for any fixed oval $\Omega_{i_{k-1} j_s}$, with $s > \bar{s}$, $\Phi_{i_{k-1} j_{s-1}}^{(2)}(\vec{t}_0) \Phi_{i_{k-1} j_{s-1}}^{(1)}(\vec{t}_0) > 0$, $\gamma_{i_{k-1} j_{s-1}}^{(0)} \in]0, 1[$, and $P_{i_{k-1} j_{s-1}}^{(0)} \in \Omega_{i_{k-1} j_s}$. Every such oval contains exactly one pole and no Darboux zero, so that (64) is satisfied.

For $s = \bar{s}$, the oval $\Omega_{i_{k-1} j_{\bar{s}}}$ contains the Darboux zero $P_{i_k}^{(3)}$. So by construction, $\Phi_{i_{k-1} j_{\bar{s}-1}}^{(2)}(\vec{t}_0) \Phi_{i_{k-1} j_{\bar{s}-1}}^{(1)}(\vec{t}_0) < 0$, $\gamma_{i_{k-1} j_{\bar{s}-1}}^{(0)} > 1$, $P_{i_{k-1} j_{\bar{s}-1}}^{(0)} \in \Omega_{i_{k-1} j_{\bar{s}}}$. Then $\Omega_{i_{k-1} j_{\bar{s}}}$ does not contain any pole and exactly one Darboux zero point, so that (64) is satisfied.

For any fixed $s < \bar{s}$, by definition $\Phi_{i_{k-1} j_{s-1}}^{(2)}(\vec{t}_0) \Phi_{i_{k-1} j_{s-1}}^{(1)}(\vec{t}_0) < 0$, $\gamma_{i_{k-1} j_{s-1}}^{(0)} > 1$, and $P_{i_{k-1} j_{s-1}}^{(0)} \in \Omega_{i_{k-1} j_s}$. Then the oval $\Omega_{i_{k-1} j_s}$ contains exactly one pole $P_{i_{k-1} j_s}^{(0)}$ and (64) is satisfied.

By construction, the provisional infinite oval created after adding all ovals associated to the last two rows of the Le–diagram, contains the Darboux zero $P_{i_{k-1}}^{(3)}$ and the pole $P_{i_{k-1}}^{(0)}$.

Let us now suppose to have verified (64) for all ovals up to row $\bar{r} + 1$ and let's prove it for the \bar{r} -th row of the Le–diagram. We proceed as for the case $r = k - 1$, starting by adding the oval $\Omega_{i_{\bar{r}}j_{N_{\bar{r}}}}$ and proceeding adding ovals following the \bar{r} -th row of the Le–diagram from left to right.

For any $s \in [N_{\bar{r}}]$, let \bar{d}_s be the number of Darboux zero points and poles contained in the provisional infinite oval before adding $\Omega_{i_{\bar{r}}j_s}$, which fall in $\Omega_{i_{\bar{r}}j_s}$. By construction, $(-1)^{\bar{d}_s} \Phi_{i_{\bar{r}}j_{s-1}}^{(2)}(\vec{t}_0) \Phi_{i_{\bar{r}}j_{s-1}}^{(1)}(\vec{t}_0) > 0$.

If \bar{d}_s is odd, $\gamma_{i_{k-1}j_{s-1}}^{(0)} > 1$, and $P_{i_{k-1}j_{s-1}}^{(0)} \in \Omega_{i_{k-1}j_{s-1}}$. Then the oval $\Omega_{i_{k-1}j_s}$ contains exactly \bar{d}_s poles and Darboux zeros and (64) is satisfied.

If \bar{d}_s is even, $\gamma_{i_{k-1}j_{s-1}}^{(0)} < 1$, $P_{i_{k-1}j_{s-1}}^{(0)} \in \Omega_{i_{k-1}j_s}$. Then the oval $\Omega_{i_{k-1}j_s}$ contains exactly $1 + \bar{d}_s$ poles and Darboux zeros and (64) is satisfied. \square

Remark 6.5. The effect of the isolated boundary vertexes on the effective vacuum divisor. Any KP soliton solution is associated to a unique irreducible cell in $Gr^{TNN}(k', n')$ which is obtained eliminating all isolated boundary vertexes from the Le–diagram. An isolated boundary sink b_j does not affect the vacuum divisor. Instead the elimination of an isolated boundary source b_{i_s} (i.e. of a row filled by zeros in the Le–diagram) produces a change of sign in the matrix elements in all the rows $r \in [1, s - 1]$ which lie to the right of the i_s -th column. This change of sign is encoded in the basis of vectors associated to the reduced matrix, which in turn effects the sign of the vacuum vertex wavefunction and the position of the vacuum divisor in the oval where we remove Γ_{i_s} and in all the ovals to the left and above it. We show an example in Figure 19 of both the un–reduced and reduced vacuum divisors. The original Le–diagram in Fig.19[above left] has RREF matrix A depending on 10 positive parameters x_l , $l \in [10]$ and its degenerate \mathbb{M} -curve is shown in Fig.19[below left]. The red crosses are the divisor points of the KP vacuum wavefunction: here $k = 5$, $d = 2$, $s_1 = 1$, $s_2 = 4$, $i_1 = 3$, $i_4 = 12$, $j_1 = 10$ and $j_2 = 16$. The infinite oval Ω_0 intersects Γ_3 and Γ_{12} and $\mu_0 = 2$. $\Phi_{12}^{(1)}(\vec{t}_0)$ has the sign of the entry $A_{12}^4 = -x_8 < 0$, $\Phi^{(2)}(\vec{t}_0) = \exp(\theta_{12}(\vec{t}_0)) > 0$ so that $\gamma_{12}^{(0)} > 1$ and $P_{12}^{(0)} \in \Omega_0$. $\Phi_3^{(1)}(\vec{t}_0)$ has the sign of the entry $A_{10}^1 = (x_3x_5)/x_4 > 0$, $\Phi^{(2)}(\vec{t}_0) = \exp(\theta_3(\vec{t}_0)) > 0$ so that $\gamma_3^{(0)} < 1$ and $P_3^{(0)} \notin \Omega_0$. In conclusion $\nu_0 = 1$ and $k + \mu_0 + \nu_0 = 8$ is even.

The reduced Le–diagram and the reduced matrix (see Fig.19[above right]) are obtained eliminating, respectively, all isolated boundary sources and sinks. In the degenerate rational curve

(Fig.19[below right]), this transformation eliminates Γ_6 and changes the pole divisor in the oval Ω'_{39} which corresponds to Ω_{39} and in all the ovals to the left and above such oval. The red divisor points are the same as in Figure 19, the green divisor points are those effected by the transformation.

The proof of Theorem 4.1 on $\Gamma(\mathcal{N}_T)$ follows immediately from Theorem 6.1.

7. SYSTEMS OF VECTORS FOR GENERAL TRIVALENT PERFECT BIPARTITE ORIENTED NETWORKS

In this Section we generalize the construction of Sections 5 and 6 to any planar oriented bipartite trivalent perfect network \mathcal{N} in the disk (in the following we call it just network), representing a given point $[A] \in \mathcal{S}_{\mathcal{M}}^{\text{TNN}} \subset Gr^{\text{TNN}}(k, n)$.

Since the edges of \mathcal{N} correspond to the double points of $\Gamma(\mathcal{N})$, it is natural to define the vacuum wave function or, equivalently, the vectors on the edges of \mathcal{N} . Each component of the vector is equal, up to a sign, to the sum of the weights of all oriented paths connecting this edge to the corresponding boundary point.

Due to the huge gauge freedom of the problem, fixing the orientation does not single out a unique system of vectors on $(\mathcal{N}, \mathcal{O})$. For any $(\mathcal{N}, \mathcal{O})$, we reduce the problem to a finite number of solutions by imposing that each edge e at a boundary sink b_j has unit weight so that the vector E_e is the j -th element of the canonical basis up to sign. Then we show how a change of orientation \mathcal{O} of \mathcal{N} affects these vectors.

Using such vectors, in section 9 we construct a vacuum vertex wavefunction $\Phi_{\mathcal{N}, \mathcal{O}}(\vec{t})$ and a corresponding vacuum divisor $\mathcal{D}_{\text{vac}, \Gamma}$ on $\Gamma(\mathcal{N})$, and prove the invariance of the effective KP divisor of the normalized dressed wavefunction with respect to changes of orientation of \mathcal{N} .

Let us assume that the orientation \mathcal{O} is fixed. To fix a gauge we introduce an additional structure on $(\mathcal{N}, \mathcal{O})$. First of all, we deform the boundary of the network in such a way that all boundary vertexes lie at a common straight interval. Then we choose an oriented direction \mathfrak{l} with the following properties:

- (1) The ray with the direction \mathfrak{l} starting at a boundary vertex points inside the disk.
- (2) No internal edge is parallel to this direction.
- (3) All rays starting from boundary vertexes do not contain internal vertexes.

Remark 7.1. In [24], the authors introduce a gauge ray direction to compute the winding number of a path joining boundary vertexes. Here we use it also to generalize the notion of number of

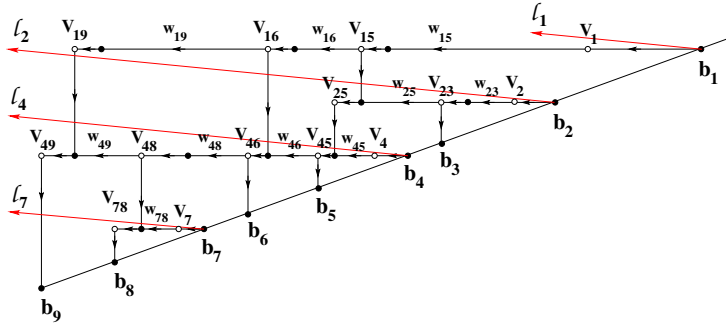


FIGURE 20. The rays starting at the boundary sources for a given orientation of the network uniquely fix the gauge.

boundary source points crossed by a path when the path starts at an internal edge e . Therefore the sign of the components of the corresponding vector E_e will be obtained from the overall contribution of the generalized winding number and the generalized intersection number with gauge rays assigned to each path starting at e .

To the system $(\mathcal{N}, \mathcal{O}, \mathfrak{l})$, we assign a unique system of vectors and we prove that we have the following invariance properties:

- (1) If the orientation \mathcal{O} is fixed and the direction \mathfrak{l} changes, then the vector assigned to each edge e may only change the sign;
- (2) If we change the orientation \mathcal{O} and keep the direction \mathfrak{l} invariant, each new vector is a linear combination of the old vector and of a basis of heat hierarchy solutions generating the Darboux transformation.

The first property ensures that we uniquely assign a vacuum divisor to each $(\mathcal{N}, \mathcal{O})$ and that such vacuum divisor does not depend on the gauge direction, while the second property ensures that the effective KP divisor associated to the normalized Darboux transformed wavefunction depends only on the network \mathcal{N} and neither on its orientation nor the gauge direction.

7.1. The system of vectors and its basic properties for fixed gauge and fixed orientation. Let b_{i_r} , $r \in [k]$, b_{j_l} , $l \in [n - k]$, respectively be the set of boundary sources and boundary sinks associated to the given orientation. Then draw the rays \mathfrak{l}_{i_r} , $r \in [k]$, associated with the pivot columns of the given orientation. In Figure 20 we choose a gauge direction for the network \mathcal{N}_T of Example 2.2 with the orientation induced by the Le-diagram.

We assign three numbers to each oriented path \mathcal{P} ^{||}, starting at a vertex (either a boundary source or internal vertex) and ending at a boundary sink:

- (1) Its weight $w(\mathcal{P})$, which is simply the product of the weights of all edges in \mathcal{P} . If we pass the same edge e of weight w_e l times, the weight is counted as w_e^l .
- (2) The generalized winding number $\text{wind}(\mathcal{P})$: we count how many times the tangent vector to the path is parallel and has the same orientation as \mathfrak{l} . We extend the tangent vector to a continuous function using the same rules as in [52].
- (3) The number $\text{int}(\mathcal{P})$ of intersections between the path and the rays \mathfrak{l}_r , $r \in [k]$.

Remark 7.2. *The local rule at the edges to compute the winding number of a path \mathcal{P}*

We remark that the generalized winding number of a given path may be computed summing the local winding numbers at each couple of its edges. For any ordered pair (e, f) of oriented vectors, define

$$s(e, f) = \begin{cases} +1 & \text{if the ordered pair is positively oriented} \\ 0 & \text{if } e \text{ and } f \text{ are parallel} \\ -1 & \text{if the ordered pair is negatively oriented} \end{cases}$$

Let $\mathcal{P} = \{e_1 \cdots - e_k - e_{k+1} - \cdots - e_m\}$ and let \mathfrak{l} be the gauge ray direction. Then the winding number of the ordered pair (e_k, e_{k+1}) is

$$\text{wind}(e_k, e_{k+1}) = \begin{cases} +1 & \text{if } s(e_k, e_{k+1}) = s(e_k, \mathfrak{l}) = s(\mathfrak{l}, e_{k+1}) = 1 \\ -1 & \text{if } s(e_k, f) = s(e_k, \mathfrak{l}) = s(\mathfrak{l}, e_{k+1}) = -1 \\ 0 & \text{otherwise.} \end{cases}$$

We illustrate the rule in Figure 21. Then the generalized winding of the path \mathcal{P} is just the sum of the local winding numbers of the ordered pairs (e_k, e_{k+1}) of its edges:

$$\text{wind}(\mathcal{P}) = \sum_{k=1}^{m-1} \text{wind}(e_k, e_{k+1}).$$

^{||}At each edge the orientation of the path coincides with the orientation of this edge in the graph

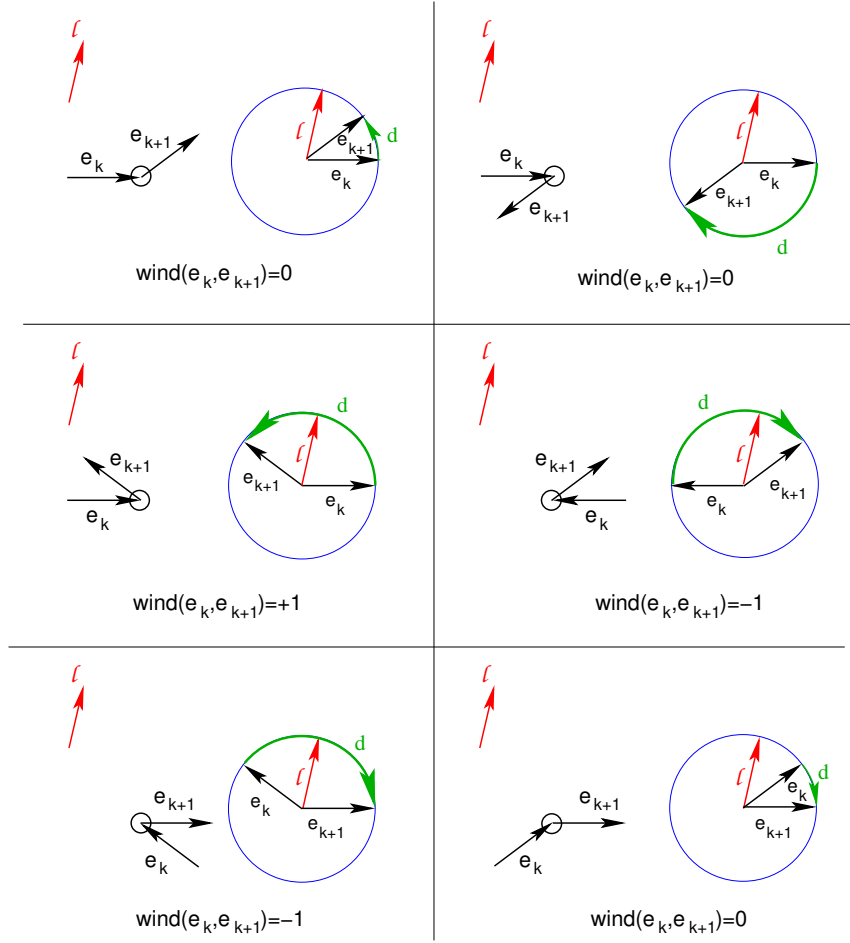


FIGURE 21. The local rule to compute the winding number.

Then we assign to each edge e the following row vector E_e : we consider all possible directed paths $\mathcal{P} : e \rightarrow b_j$, in $(\mathcal{N}, \mathcal{O})$ such that the first segment is e , and the end point is the boundary vertex b_j , $j \in [n]$. The j -th component of E_e is defined as:

$$(66) \quad (E_e)_j = \sum_{\mathcal{P}: e \rightarrow b_j} (-1)^{\text{wind}(\mathcal{P}) + \text{int}(\mathcal{P})} w(\mathcal{P}).$$

If there is no path from e to b_j , the j -th component of E_e is assigned to be zero. In particular, all components corresponding to the boundary sources for a given orientation are equal to zero. Moreover, in case e is a edge belonging to the connected component of an isolated boundary sink b_j , then E_e is proportional to the j -th vector of the canonical basis, while if e is an edge belonging to the connected component of an isolated boundary source, then E_e is the null vector.

If the number of paths starting at e and ending at b_j is infinite, we adapt the summation procedure in [52], and, following [18], see also [42], we adapt the notion of loop-erased walk to our situation, since our walks start at an edge, not a vertex.

Definition 7.1. Edge loop-erased walks. Let \mathcal{P} be a walk (directed path) given by

$$V_e \xrightarrow{e} V_1 \xrightarrow{e_1} V_2 \rightarrow \dots \rightarrow b_j,$$

where V_e is the initial vertex of the edge e . The edge loop-erased part of \mathcal{P} , denoted $LE(\mathcal{P})$, is defined recursively as follows. If \mathcal{P} does not pass any edge twice (i.e., all edges e_i are distinct), then $LE(\mathcal{P}) = \mathcal{P}$. Otherwise, set $LE(\mathcal{P}) = LE(\mathcal{P}_0)$, where \mathcal{P}_0 is obtained from \mathcal{P} , by removing the first edge loop it makes; more precisely, find $e_l = e_s$ with the smallest value of s , and remove

$$V_l \xrightarrow{e_l} V_{l+1} \xrightarrow{e_{l+1}} V_{l+2} \rightarrow \dots \xrightarrow{e_{s-1}} V_s,$$

from \mathcal{P} to obtain \mathcal{P}_0 .

Remark 7.3. An edge loop-erased walk can pass twice through the first vertex V_e , but it can not pass twice any other vertex due to the trivalency property. For example, the directed path 1, 2, 3, 4, 5, 6, 7, 8, 12 at Figure 22 is edge loop-erased but it passes twice through the starting vertex V_1 . In general, the edge loop-erased walk does not coincide with the loop-erased walk defined in [18], [42]. For instance, the directed path 1, 2, 3, 4, 5, 6, 7, 8, 9, 4, 11 has edge loop-erased walk 1, 2, 3, 4, 11 and the loop-erased walk 7, 8, 9, 4, 11.

In our text we never use loop-erased walks in the sense of [18], therefore we use the notation $LE(\mathcal{P})$, in the sense of Definition 7.1.

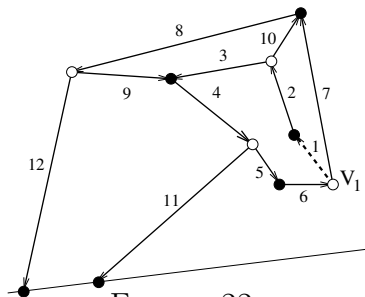


FIGURE 22.

Now we associate with each path starting at e and ending at b_j an unique edge loop-erased walk, and we formally reshuffle the summation over infinitely many paths to summation over finite number of equivalent classes $[LE(\mathcal{P}_s)]$, each one consisting of all paths sharing the same

edge loop-erased walk, $LE(\mathcal{P}_s)$, $s = 1, \dots, S$. Let us remark, that the $\text{int}(\mathcal{P}) - \text{int}(LE(\mathcal{P}_s)) = 0 \pmod{2}$ for any $\mathcal{P} \in [LE(\mathcal{P}_s)]$, and, moreover, $\text{wind}(\mathcal{P}) - \text{wind}(LE(\mathcal{P}_s))$ has the same parity as the number of simple cycles of \mathcal{P} minus the number of simple cycles of $LE(\mathcal{P}_s)$, where the latter path may have only zero or one simple cycle.

Then (66) may be expressed in the following way:

$$(67) \quad (E_e)_j = \sum_{s=1}^S (-1)^{\text{wind}(LE(\mathcal{P}_s)) + \text{int}(LE(\mathcal{P}_s))} \left[\sum_{\substack{\mathcal{P}: e \rightarrow b_j \\ \mathcal{P} \in [LE(\mathcal{P}_s)]}} (-1)^{\text{wind}(\mathcal{P}) - \text{wind}(LE(\mathcal{P}_s))} w(\mathcal{P}) \right].$$

We remark that the winding number along each simple closed loop introduces a $-$ sign in agreement with [52]. Therefore the summation over paths may be interpreted as a discretization of path integration in some spinor theory. In typical spinor theories the change of phase during the rotation of the spinor corresponds to standard measure on the group $U(1)$ and requires the use of complex numbers. The introduction of the gauge direction forces the use of δ -type measures instead of the standard measure on $U(1)$, and it permits to work with real numbers only.

A deep result of [52], see also [58], states that each infinite summation in the square bracket results in a subtraction-free rational expression $w([LE(\mathcal{P}_s)])$.

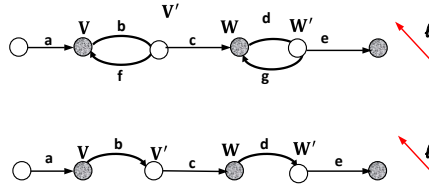


FIGURE 23. We group together all paths starting at a given edge into a finite number of equivalence classes of paths sharing the same edge loop-erased path.

For instance, in the case of Figure 23 all paths $\mathcal{P}_{m,l}$ cycling $m \geq 0$ times around the vertexes V', V and $l \geq 0$ times around the vertexes W', W are grouped together into $[LE(\mathcal{P})]$ and in (66) we substitute $w([LE(\mathcal{P})]) = \frac{abcde}{(1+bf)(1+dg)}$ to the infinite sum $\sum_{m,l} (-1)^{m+l} w(\mathcal{P}_{m,l})$.

Example 7.1. For the orientation and gauge as in Figure 20, the vectors E_e coincide with the vertex vectors of Definition 6.2 for Example 2.2.

Lemma 7.1. *The edge vectors E_e on $(\mathcal{N}, \mathcal{O}, \mathfrak{l})$ satisfy a linear equation at each white or bivalent black vertex, and two linear equations at each trivalent black vertex. For a given network these equations are defined in terms of the weights, the orientation and the gauge direction.*

Proof. Any bivalent vertex has exactly one incoming edge e and one outgoing edge f , therefore, by definition, any path starting at e passes through f . It means that the vector E_e is proportional to the vector E_f , and

$$E_e = (-1)^{\text{int}(e)+\text{wind}(e,f)} w_e E_f,$$

where $\text{int}(e)$ denotes the number of intersections of the gauge boundary rays with the edge e , while $\text{wind}(ef)$ denotes the winding number of the path containing the two edges e and f with respect to the gauge direction.

A trivalent white vertex has exactly one incoming edge e_3 and outgoing edges e_1, e_2 . Any path starting at e_3 passes at the first step either through e_1 or through e_2 . Therefore

$$E_3 = (-1)^{\text{int}(e_3)+\text{wind}(e_3,e_1)} w_3 E_1 + (-1)^{\text{int}(e_3)+\text{wind}(e_3,e_2)} w_3 E_2,$$

where E_k denotes the vector associated to the edge e_k .

A trivalent black vertex has exactly two incoming edges e_2, e_3 and one outgoing edge e_1 . Any path starting at e_2 or e_3 passes at the first step through e_1 . Therefore

$$E_2 = (-1)^{\text{int}(e_2)+\text{wind}(e_2,e_1)} w_2 E_1,$$

$$E_3 = (-1)^{\text{int}(e_3)+\text{wind}(e_3,e_1)} w_3 E_1.$$

where E_k denotes the vector associated to the edge e_k . □

In Figure 24 we illustrate these relations at trivalent vertexes assuming that the incoming edges do not intersect the gauge boundary rays.

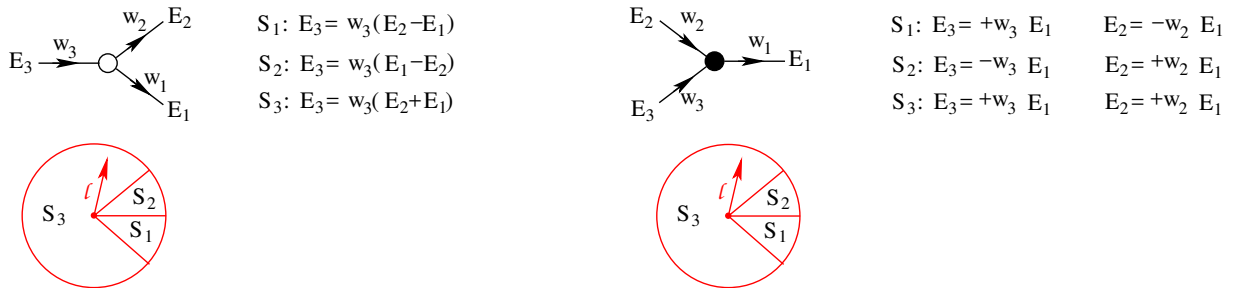


FIGURE 24. *The linear system at black and white vertexes.*

For instance, if \mathfrak{l} belongs to the sector S_1 , at the white vertex $E_3 = w_3(E_2 - E_1)$, where E_j denotes the vector associated to the edge e_j , $j \in [3]$, while at the black vertex $E_3 = w_3E_1$ and $E_2 = -w_2E_1$.

According to our definition all components of vectors associated either to a boundary source or to an isolated boundary sink are zero for any edge $e \in \mathcal{N}$.

7.2. Rational representation of the components of E_e and null vectors. In this section we first show that the components of E_e are rational expression in the weights with subtraction-free denominator. As a consequence, the j -th component of E_e may be null even if there exist paths starting at e and ending at b_j .

Proposition 7.1. Rational representation for the components of vectors E_e Given $(\mathcal{N}, \mathcal{O}, \mathfrak{l})$, let $e \in \mathcal{N}$ such that there is a path starting at e and ending at the boundary sink b_j . Then $(E_e)_j$ is a rational expression in term of the weights on the graph with subtraction-free denominator.

Proof. The proof of this statement is a straightforward adaptation of the proof of Lemma 4.4 in [52]. Let us fix an edge e in the graph and a boundary sink b_j such that there exists at least one directed path from e to b_j . Following [52], we prove the statement by induction on the number of internal edges.

If e is directly connected to b_j , nothing has to be proven. Otherwise, let V be the internal vertex connected to b_j , and, following [52], pick an internal edge e_V at V , and construct a new network $\tilde{\mathcal{N}}$ by erasing e_V , and adding a boundary sink b' and a boundary source b'' respectively, connected to the initial and the final vertex of e_V by unit edges. Let us denote by $\tilde{E}(a, b)$ the b -th component of the vector associated to the edge a in $\tilde{\mathcal{N}}$.

To obtain from $\tilde{\mathcal{N}}$ a network equivalent to \mathcal{N} , it is sufficient to add an additional edge from b' to b'' with the weight q , which was the weight of e_V .

We have 3 possible configurations:

- (1) The vertex V is white and it is the initial vertex of e_V (see Figure 25). In this case $\tilde{E}(b'', b')$ and $\tilde{E}(b'', b_j)$ are positive while $\tilde{E}(e, b_j)$ and $E(e, b_j)$ have opposite sign. Moreover, for any edge a $\tilde{E}(a, b_j) = p\tilde{E}(a, b')$. We assume here that b' and b_j are sufficiently close to

each other. Therefore

$$\begin{aligned} E(e, b_j) &= -\tilde{E}(e, b_j) + \tilde{E}(e, b')q\tilde{E}(b'', b_j) - \tilde{E}(e, b')q\tilde{E}(b'', b')q\tilde{E}(b'', b_j) + \cdots \\ &= -\tilde{E}(e, b_j) + \frac{\tilde{E}(e, b')q\tilde{E}(b'', b_j)}{1 + q\tilde{E}(b'', b')} = \frac{-\tilde{E}(e, b_j)}{1 + q\tilde{E}(b'', b')} \end{aligned}$$

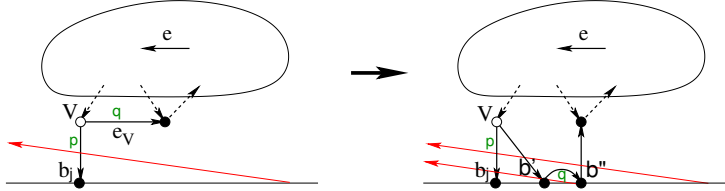


FIGURE 25.

- (2) The vertex V is white and it is the final vertex of e_V (see Figure 26). In this case $\tilde{E}(e, b_j) = 0$, $\tilde{E}(b'', b')$ is positive and $\tilde{E}(e, b')$ has the same sign as $E(e, b_j)$, and $\tilde{E}(b'', b_j) = p$.

$$E(e, b_j) = \tilde{E}(e, b')q\tilde{E}(b'', b_j) - \tilde{E}(e, b')q\tilde{E}(b'', b')q\tilde{E}(b'', b_j) + \cdots = \frac{qp\tilde{E}(e, b')}{1 + q\tilde{E}(b'', b')}$$

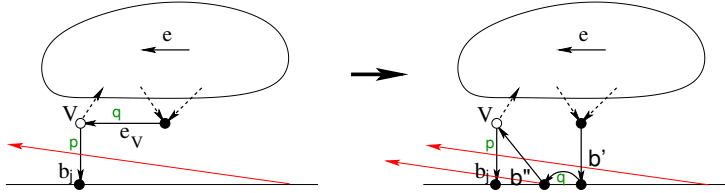


FIGURE 26.

- (3) The vertex V is black and it is the final vertex of e_V (see Figure 27). In this case $\tilde{E}(b'', b') = 0$. All paths connecting e to b_j form two groups: the paths reaching b_j either through f_v or through e_V respectively. After the transformation to $\tilde{\mathcal{N}}$ the paths from the first group ends at b_j , but they change the sign. The paths from the second group ends at b' and keep the original sign. Therefore,

$$E(e, b_j) = -\tilde{E}(e, b_j) + \tilde{E}(e, b')qp.$$

The sum is finite, therefore we can write it as a fraction with subtraction-free denominator.

□

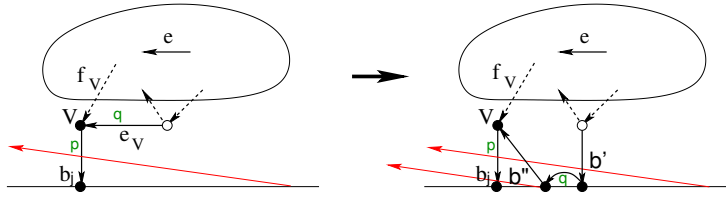


FIGURE 27.

In contrast with the vectors associated to the boundary edges, a component of a vector associated to an internal edge can be equal to zero even if the corresponding boundary sink can be reached from that edge. In Figure 28 we present such an example. All weights are equal to 1 except the edges with the weights p and q marked green. In blue we write the j -th component of the corresponding vector.

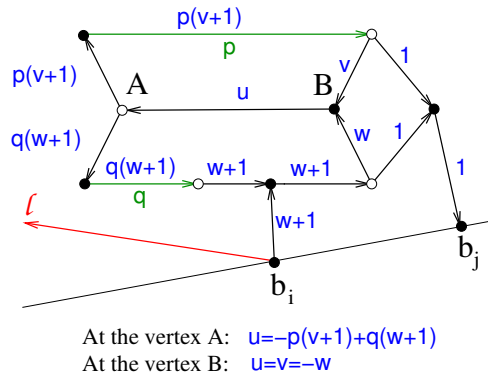


FIGURE 28. *The appearance of null components.*

Solving the system of equation at the vertexes A and B we get:

$$u = \frac{q - p}{1 + p + q}.$$

If $p = q$, then $u = v = w = 0$. We remark, that

$$w + 1 = \frac{1 + 2p}{1 + p + q} > 0,$$

for any choice of $p, q > 0$.

Let e be an edge ending at the black vertex V_b and at the white vertex V_w . If $E_e = 0$, then all other edges at V_b carry null vectors; the same occurs if V_w is bivalent. If V_w is trivalent, then the other edges at V_w carry proportional vectors.

7.3. The dependence of E_e on the gauge ray direction \mathfrak{l} . We now discuss the effect of a change of direction in the gauge ray \mathfrak{l} on the vectors E_e .

Proposition 7.2. *The dependence of the system of vectors on the ray direction \mathfrak{l}* Let $(\mathcal{N}, \mathcal{O})$ be an oriented network and consider two gauge directions \mathfrak{l} and \mathfrak{l}' .

- (1) *For any boundary source edge e_{i_r} the vector $E_{e_{i_r}}$ does not depend on the gauge direction \mathfrak{l} and it coincides with the r -th row of the generalized RREF of $[A]$, associated to the pivot set I , minus the i_r -th vector of the canonical basis, which we denote E_{i_r} ,*

$$(68) \quad E_{e_{i_r}} = A[r] - E_{i_r}.$$

- (2) *For any other internal edge e we have $E'_e = \pm E_e$, where E_e and E'_e respectively denote the vectors associated the edge e and gauge directions \mathfrak{l} and \mathfrak{l}' .*

Proof. It is sufficient to prove both statements for edge loop-erased paths only, because adding loops result in change of signs independent on the gauge direction.

Let us prove the first statement. Let \mathcal{P} be an edge loop-erased path starting at the boundary source \bar{i} and ending at the boundary sink j . Let us denote $\mathfrak{n}(\mathcal{P})$ (resp. $\mathfrak{n}'(\mathcal{P})$) be the sum of the generalized winding and intersection numbers of \mathcal{P} w.r.t. the gauge direction \mathfrak{l} (resp. w.r.t. \mathfrak{l}'). Then the following property holds true:

$$(69) \quad \mathfrak{n}(\mathcal{P}) - \mathfrak{n}'(\mathcal{P}) = 0 \pmod{2};$$

Indeed \mathcal{P} is an acyclic path from the boundary source \bar{i} , to some boundary sink j . Without loss of generality we may assume that $\bar{i} < j$. All pivot rays $\mathfrak{l}_{i_r}, i_r \in [\bar{i} - 1] \cup [j, n]$ intersect \mathcal{P} an even number of times, all pivot rays $\mathfrak{l}_{i_r}, i_r \in [\bar{i} + 1, j]$ intersect \mathcal{P} an odd number of times, while $\mathfrak{l}_{\bar{i}}$ intersects \mathcal{P} either an even or an odd number of times. In the first case the winding number of the path is even, while in the second case it is odd (see Figure 29 [left]) and we get (69). A consequence of (69) is that the components of $E_{\bar{i}}$ are invariant with respect to changes of the gauge direction.

To prove the second statement, consider a continuous change of the gauge direction from \mathfrak{l} to \mathfrak{l}' . Let us point out, that every time the gauge direction is parallel and co-directional to an internal edge, the winding number changes $0 \pmod{2}$. It changes $1 \pmod{2}$ only if the gauge direction is parallel and co-directional to the first edge (it can never be parallel and co-directional to the last edge).

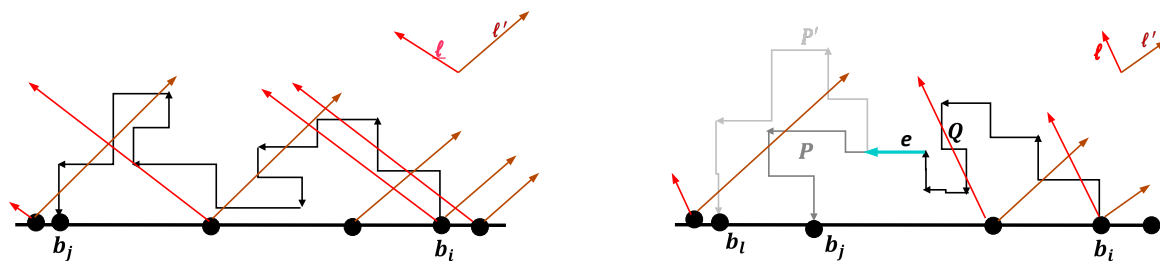


FIGURE 29. We illustrate the statement of Proposition 7.2.

Similarly, if a gauge line passes through an internal vertex, then the intersection number $0 \pmod{2}$. It changes $1 \pmod{2}$ only if one of the gauge lines passes through the first vertex of the path (again it can never pass through the final vertex).

Since the first edge e and its initial vertex are common to all paths starting at e , all components of the vector E_e either remain invariant, or are simultaneously multiplied by -1 (see also Figure 29 [right]).

Finally, (68) follows directly from [52]. \square

7.4. The dependence of E_e on the orientation of the graph. We now explain how the system of vectors change when we change the orientation of the graph.

Proposition 7.3. *The dependence of the system of vectors on the orientation of the network.* Let \mathcal{N} be a network representing a given point $[A] \in Gr^{TNN}(k, n)$ and let $\mathcal{O}, \hat{\mathcal{O}}$ be two perfect orientations of \mathcal{N} and \mathfrak{l} be a gauge ray direction. Let E_e and \hat{E}_e respectively be the system of vectors associated to $(\mathcal{N}, \mathcal{O}, \mathfrak{l})$ and to $(\mathcal{N}, \hat{\mathcal{O}}, \mathfrak{l})$. Let $A[r]$, $r \in [k]$, denote the r -th row of a representative matrix of $[A]$. Then for any $e \in \mathcal{N}$, there exist real constants α_e, c_e^r , $r \in [k]$ such that

$$(70) \quad \hat{E}_e = \alpha_e E_e + \sum_{r=1}^k c_e^r A[r].$$

The proof of the Proposition follows from Lemmas 7.2 and 7.3, since any admissible change of orientation can be represented as a composition of elementary changes of orientation (see [52]), namely:

- (1) A change of orientation along a simple cycle;
- (2) A change of orientation along a non-self-intersecting oriented path from a boundary source to a boundary sink.

Here we use the standard rule, that if an edge does not change orientation, we do not change its weight, otherwise, we replace the original weight by its reciprocal.

At this aim we first describe a transformation from a system of vectors \tilde{E}_e on $(\mathcal{N}, \mathcal{O}, \mathfrak{l})$ to a system of vectors \hat{E}_e on $(\mathcal{N}, \hat{\mathcal{O}}, \mathfrak{l})$, where we change the orientation along a non-self-intersecting oriented path \mathcal{P}_0 from a boundary source i_0 to a boundary sink j_0 .

Let us divide the interior of the disk into a finite number of regions bounded by the gauge ray \mathfrak{l}_{i_0} oriented upwards, by the gauge ray \mathfrak{l}_{j_0} oriented downwards, by the path \mathcal{P}_0 oriented as in $(\mathcal{N}, \mathcal{O}, \mathfrak{l})$ and by the boundary of the disk divided into two arcs, each oriented from j_0 to i_0 . We obtain two types of regions: we mark a region with a $+$ if all intervals of its boundary have the same orientation, otherwise we mark it with $-$ (see Figure 30).

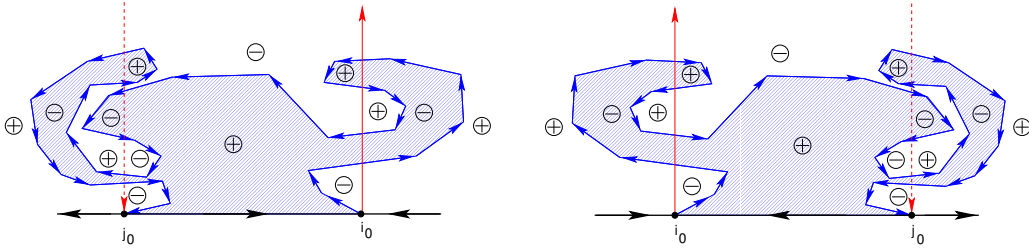


FIGURE 30. We illustrate the marking of the regions.

Let us first define the sign rule for all edges not belonging to \mathcal{P}_0 :

$$(71) \quad \hat{E}_e = \begin{cases} \tilde{E}_e & \text{if the starting vertex of } e \text{ belongs to a } + \text{ region,} \\ -\tilde{E}_e & \text{if the starting vertex of } e \text{ belongs to a } - \text{ region,} \end{cases}$$

where, in case the initial vertex of e belongs to \mathcal{P}_0 , we make an infinitely small shift of the starting point in the direction of the vector before assigning it to a region.

Let us now define the sign rule for all edges belonging to \mathcal{P}_0 . To any edge $e \in \mathcal{P}_0$ in the original orientation \mathcal{O} , we assign the index $\epsilon(e) = \epsilon_1(e) + \epsilon_2(e) + \epsilon_3(e)$ in the following way:

- (1) We look at the region to the left and near to the ending point of e and assign index

$$\epsilon_1(e) = \begin{cases} 0 & \text{if the region is marked with } +, \\ 1 & \text{if the region is marked with } -; \end{cases}$$

- (2) We consider the ordered pair (e, \mathfrak{l}) and assign index

$$\epsilon_2(e) = \begin{cases} 0 & \text{if the pair is positively oriented,} \\ 1 & \text{if the pair is negatively oriented;} \end{cases}$$

(3) We count the number of intersections with the gauge lines \mathfrak{l}_{i_r} , $r \in [k]$ and we define

$$\epsilon_3(e) = \#\{\text{intersections with gauge lines } \mathfrak{l}_{i_r}, r \in [k]\}.$$

Then we define the vector \hat{E}_e assigned to $e \in \mathcal{P}_0$ in the new orientation, $(\mathcal{N}, \hat{\mathcal{O}}, \mathfrak{l})$, as

$$(72) \quad \hat{E}_e = \frac{(-1)^{\epsilon(e)}}{w_e} \tilde{E}_e.$$

Let us now prove that the system \hat{E}_e defined in (71) and (72) is the solution of the linear relations on $(\mathcal{N}, \hat{\mathcal{O}}, \mathfrak{l})$ with the required boundary conditions with a proper choice of the system \tilde{E}_e .

Lemma 7.2. *The effect of a change of orientation along a non self-intersecting path from a boundary source to a boundary sink. Let $I = \{1 \leq i_1 < i_2 < \dots < i_k\}$ and $\bar{I} = \{1 \leq j_1 < j_2 < \dots < j_{n-k}\}$ respectively be the pivot and non-pivot indexes in the representative matrix A associated to $(\mathcal{N}, \mathcal{O}, \mathfrak{l})$. Assume that we change the orientation along a non-self-intersecting oriented path \mathcal{P}_0 from a boundary source i_0 to a boundary sink j_0 . Let \tilde{E}_e be the system of vectors on $(\mathcal{N}, \mathcal{O}, \mathfrak{l})$ corresponding to the following choice of boundary conditions at edges e_j ending at boundary sinks b_j , $j \in \bar{I}$:*

$$(73) \quad \tilde{E}_{e_j} = \begin{cases} E_{e_j} & \text{if } j \neq j_0; \\ E_{b_{j_0}} - \frac{(E_{b_{j_0}})_{j_0}}{(A[r_0])_{j_0}} A[r_0], & \text{if } j = j_0, \end{cases}$$

where $A[r_0]$ is the row of the matrix A associated to the source i_0 .

Then the system \hat{E}_e defined in (71) and (72) is the system of vectors on the network $(\mathcal{N}, \hat{\mathcal{O}}, \mathfrak{l})$ with boundary conditions

$$(74) \quad \hat{E}_{e_j} = \begin{cases} (-1)^{\text{int}(e_j)'} E_j & \text{if } j \in \bar{I} \setminus \{j_0\} \\ (-1)^{\text{int}(e_0)'} E_{i_0}, & \text{if } j = i_0, \end{cases}$$

where $E_k(l) = \delta_{k,l}$, and

$$\text{int}(e)' = \#\{\text{intersections of } e \text{ with the gauge rays } \mathfrak{l}_{j_0}, \mathfrak{l}_{i_r}, r \in [k], i_r \neq i_0\}.$$

Proof. The new system of vectors \tilde{E} on $(\mathcal{N}, \mathcal{O}, \mathfrak{l})$ satisfies the linear relations at all internal vertexes of $(\mathcal{N}, \mathcal{O}, \mathfrak{l})$ and the difference of $\tilde{E}_e - E_e$ is again a solution of the same linear system with the following boundary conditions: at each edge ending at a boundary sink except b_j the vector is equal to 0, and:

$$\tilde{E}_{e_j} - E_{e_j} = -\frac{(E_{e_j})_j}{(A[r])_j} A[r],$$

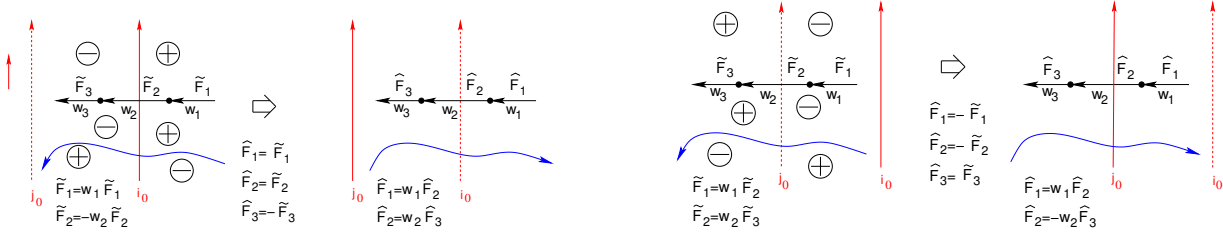


FIGURE 31. The consistency of the linear system in both orientations when an edge not belonging to \mathcal{P}_0 crosses either l_{i_0} or l_{j_0} .

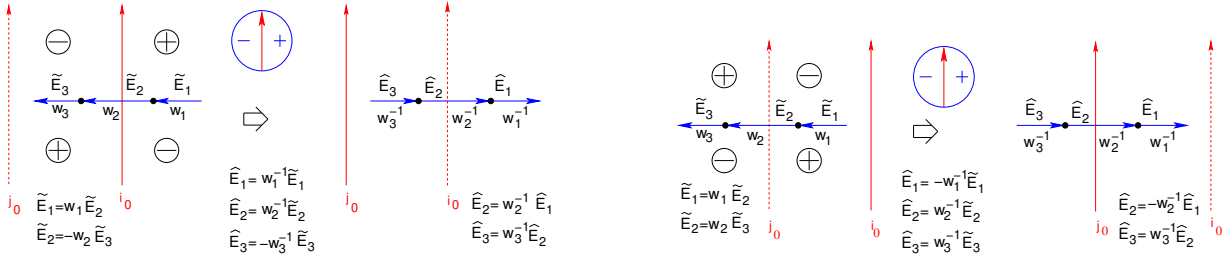


FIGURE 32. The consistency of the linear system in both orientations when an edge of \mathcal{P}_0 crosses either l_{i_0} or l_{j_0} .

therefore at all edges the difference is proportional to $A[r]$. In particular $\tilde{E}_{e_{i_0}} = -E_{i_0}$ (recall that by construction $E_{e_{i_0}} = A[r] - E_{i_0}$). So each vector \hat{E}_e is a linear combination of the vector E_e and $A[r_0]$.

Let us now prove that the system \hat{E}_e solves the linear system on $(\mathcal{N}, \hat{\mathcal{O}}, \mathfrak{l})$ with boundary conditions (74). To explain the role of the sign changes, we assume without loss of generality that all edges crossing a gauge line including l_{j_0} join bivalent vertexes; indeed we may add internal vertexes of degree two without changing the boundary measurement map.

The check of the consistency of the linear system at vertexes including edges either crossing regions or belonging to \mathcal{P}_0 is direct and we illustrate it in Figures 31, 32, 33 and 34. We remark that if we change the direction of one of the vectors in the Figures, the rules remain consistent.

Finally let us check that the boundary condition is (74). First of all, any given boundary edge e_j , $j \neq j_0, i_0$, has its ending vertex of a in a + region and its initial vertex may fall in a - region only if it intersects exactly one of the two gauge rays l_{i_0} or l_{j_0} . The latter is exactly the unique case in which $\langle E_{e_j}, \hat{E}_{e_j} \rangle = \langle \tilde{E}_{e_j}, \hat{E}_{e_j} \rangle = -1$.

The edge e_{i_0} belongs to the path \mathcal{P}_0 and, without loss of generality, we assume that it does not intersect any gauge ray in both orientations of the network. Then, by construction, $\tilde{E}_{e_{i_0}} = -E_{i_0}$,

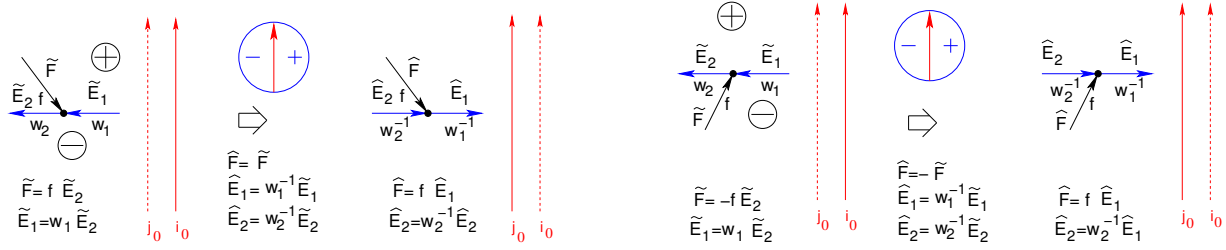


FIGURE 33. The consistency of the linear system in both orientations at trivalent black edges.

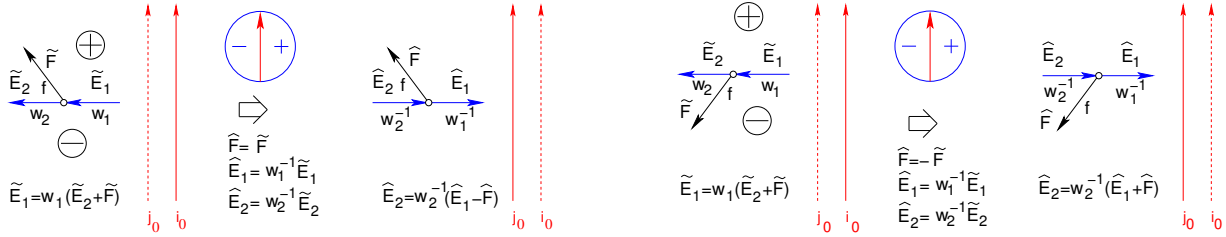
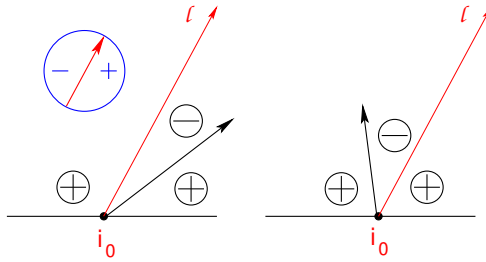


FIGURE 34. The consistency of the linear system in both orientations at trivalent white edges.

since $E_{e_{i_0}} = A[i_r] - E_{i_0}$, $\hat{E}_{e_{i_0}} = E_{i_0}$ and

$$\epsilon(e_{i_0}) = \epsilon_1(e_{i_0}) + \epsilon_2(e_{i_0}) = 1,$$

since, either e_{i_0} has a + region to the left and the pair (e, ℓ) is negatively oriented or it has a - region to the left and the pair (e, ℓ) is positively oriented (see Figure 35). \square

FIGURE 35. The rule of the sign at e_{i_0} .

Let us now describe the change of signs if we change the orientation in $(\mathcal{N}, \mathcal{O}, \ell)$ along a closed simple path \mathcal{Q}_0 . \mathcal{Q}_0 divides the interior of the disk into two regions: we mark the external region to \mathcal{Q}_0 with a + and the internal region with -.

If $e \notin \mathcal{Q}_0$, then the edge lies in one such region and we

$$(75) \quad \hat{E}_e = \begin{cases} E_e & \text{if } e \text{ belongs to the } + \text{ region,} \\ -E_e & \text{if } e \text{ belongs to the } - \text{ region.} \end{cases}$$

If $e \in \mathcal{Q}_0$, we consider the original orientation \mathcal{O} , and we assign the index $\epsilon(e) = \epsilon_1(e) + \epsilon_2(e) + \epsilon_3(e)$ in the following way:

(1) We look at the region to the left of e and assign index

$$\epsilon_1(e) = \begin{cases} 0 & \text{if the region is marked with +,} \\ 1 & \text{if the region is marked with -;} \end{cases}$$

(2) We consider the ordered pair (e, \mathfrak{l}) and assign index

$$\epsilon_2(e) = \begin{cases} 0 & \text{if the pair is positively oriented,} \\ 1 & \text{if the pair is negatively oriented;} \end{cases}$$

(3) We count the number of intersections with the gauge lines \mathfrak{l}_{i_r} , $r \in [k]$ and we define

$$\epsilon_3(e) = \#\{\text{intersections with gauge lines } \mathfrak{l}_{i_r}, r \in [k]\}.$$

Then we define the vector \hat{E}_e assigned to $e \in \mathcal{P}_0$ in the new orientation, $(\mathcal{N}, \hat{\mathcal{O}}, \mathfrak{l})$, as

$$(76) \quad \hat{E}_e = \frac{(-1)^{\epsilon(e)}}{w_e} E_e.$$

Then the system \hat{E}_e defined in (75) and (76) satisfies the linear relations on $(\mathcal{N}, \hat{\mathcal{O}}, \mathfrak{l})$ by construction. We have thus proven the following Lemma

Lemma 7.3. *The effect of a change of orientation along a simple closed cycle. Let $I = \{1 \leq i_1 < i_2 < \dots < i_k \leq n\}$ be the pivot indexes for $(\mathcal{N}, \mathcal{O}, \mathfrak{l})$. Assume that we change the orientation along a simple closed cycle \mathcal{Q}_0 and let $(\mathcal{N}, \hat{\mathcal{O}}, \mathfrak{l})$ be the newly oriented network. Let E_e be the system of vectors on $(\mathcal{N}, \mathcal{O}, \mathfrak{l})$ and \hat{E}_e be the system of vectors defined in (75) and (76).*

Then the system \hat{E}_e is the system of vectors on the network $(\mathcal{N}, \hat{\mathcal{O}}, \mathfrak{l})$ with boundary conditions

$$(77) \quad \hat{E}_{e_j} = E_j, \quad j \in \bar{I}.$$

8. THE EFFECT OF MOVES AND REDUCTIONS ON THE SYSTEM OF VECTORS

Postnikov [52] introduces a set of local transformations on plabic networks which leaves invariant the boundary measurement map. Below we restrict ourselves to plabic networks in which the degree of each internal vertex is less than or equal to three and we explain the effect of such moves on the system of vectors introduced in Section 7 for a given choice of orientation and of gauge ray direction. Indeed the edge vectors for different choices of orientation and gauge directions change according to Propositions 7.2 and 7.3, and to Lemmas 7.2 and 7.3. There are three moves:

- (M1) The square move (see Figure 36);
- (M2) The unicolored edge contraction/uncontraction (see Figure 37);
- (M3) The middle vertex insertion/removal (see Figure 40);

and three reductions:

- (R1) The parallel edge reduction (see Figure 41);
- (R2) The dipole reduction (see Figure 41);
- (R3) The leaf reduction (see Figure 42).

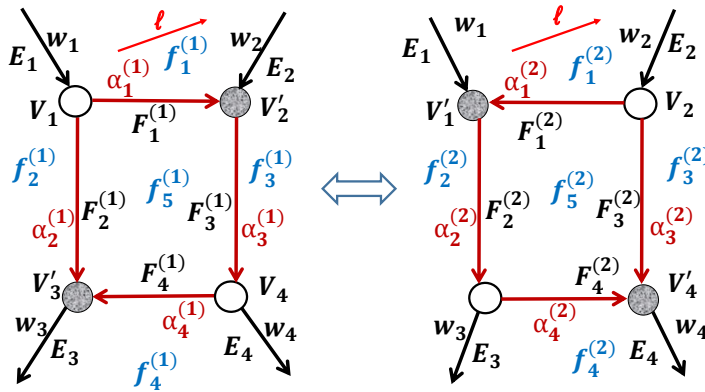


FIGURE 36. *The square move*

8.1. **(M1) The square move.** Let us explain the effect of the square move [52] on the system of vectors. The relation between the face weights before and after the square move is

$$f_5^{(2)} = (f_5^{(1)})^{-1}, \quad f_1^{(2)} = \frac{f_1^{(1)}}{1 + 1/f_5^{(1)}}, \quad f_2^{(2)} = f_2^{(1)}(1 + f_5^{(1)}), \quad f_3^{(2)} = f_3^{(1)}(1 + f_5^{(1)}), \quad f_4^{(2)} = \frac{f_4^{(1)}}{1 + 1/f_5^{(1)}},$$

so that the relation between the edge weights with the orientation and gauge ray direction as in Figure 36 is

$$\alpha_1^{(2)} = \frac{\alpha_3^{(1)} \alpha_4^{(1)}}{\alpha_2^{(2)}}, \quad \alpha_2^{(2)} = \alpha_2^{(1)} + \alpha_1^{(1)} \alpha_3^{(1)} \alpha_4^{(1)}, \quad \alpha_3^{(2)} = \frac{\alpha_2^{(1)} \alpha_3^{(1)}}{\alpha_2^{(2)}}, \quad \alpha_4^{(2)} = \frac{\alpha_1^{(1)} \alpha_3^{(1)}}{\alpha_2^{(2)}}.$$

We see that the system of equations on the edges outside the square is the same before and after the move. The boundary conditions also remain unchanged. From the uniqueness of the solution we see that the all vectors outside the square including E_1, E_2, E_3, E_4 remain the same. The relations between the system of vectors $F_j^{(2)}$ and $F_j^{(1)}$, $j \in [4]$, for the given orientation are

$$(78) \quad F_2^{(2)} = F_2^{(1)} + \alpha_1^{(1)} F_3^{(1)}, \quad F_3^{(2)} = -\alpha_1^{(2)} F_2^{(1)} + \frac{\alpha_3^{(2)}}{\alpha_3^{(1)}} F_3^{(1)},$$

and

$$(79) \quad F_1^{(1)} = \alpha_1^{(1)} F_3^{(1)}, \quad F_4^{(1)} = \frac{\alpha_4^{(1)}}{\alpha_2^{(1)}} F_3^{(1)}, \quad F_1^{(2)} = \alpha_1^{(2)} F_2^{(2)}, \quad F_4^{(2)} = \frac{\alpha_4^{(2)}}{\alpha_3^{(2)}} F_3^{(2)},$$

where we have used

$$(80) \quad \begin{aligned} E_1 &= w_1(F_1^{(1)} + F_2^{(1)}) = w_1 F_2^{(2)}, & E_2 &= w_2 F_3^{(1)} = w_2(F_1^{(2)} + F_3^{(2)}), \\ E_3 &= \frac{F_2^{(1)}}{\alpha_2^{(1)}} = \frac{F_4^{(1)}}{\alpha_4^{(1)}} = \frac{F_2^{(2)}}{\alpha_2^{(2)}} - F_4^{(2)}, & E_4 &= \frac{F_3^{(2)}}{\alpha_3^{(2)}} = \frac{F_4^{(2)}}{\alpha_4^{(2)}} = \frac{F_3^{(1)}}{\alpha_3^{(1)}} - F_4^{(1)}. \end{aligned}$$

8.2. (M2) The unicolored edge contraction/uncontraction. The unicolored edge contraction/uncontraction consists of the elimination/addition of an internal vertex of equal color and of a unit edge, it leaves invariant the face weights and the boundary measurement map. In Figure 37 we show an example of possible configurations equivalent w.r.t to such move.

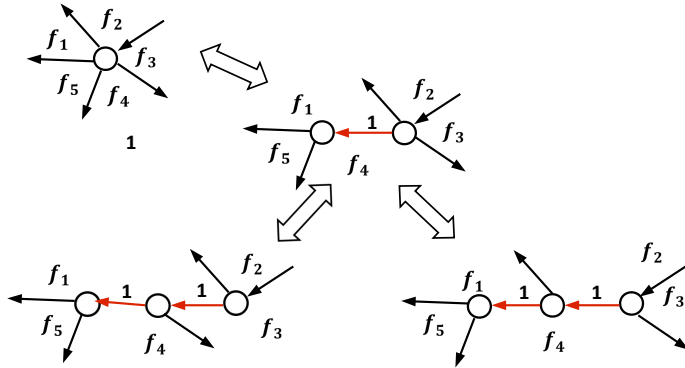


FIGURE 37. The unicolored edge contraction/uncontraction

Since we work with trivalent graphs, there are two cases of interest to us: the insertion/removal of a Darboux vertex next to a boundary vertex (see Figure 38) and the flip move (see Figure 39).

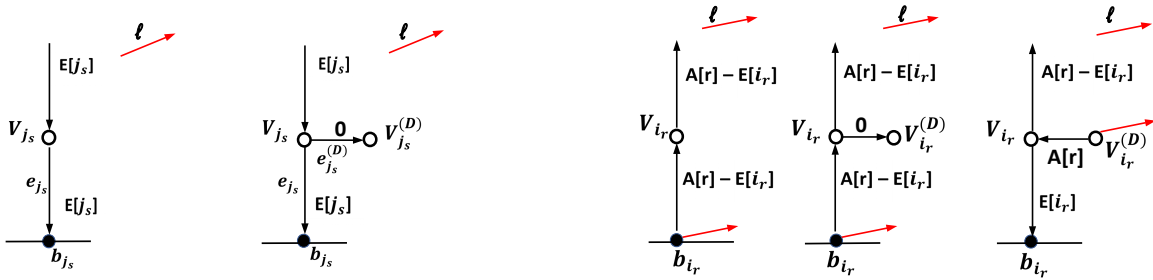


FIGURE 38. The insertion/removal of a Darboux vertex next to a boundary sink [left] and to a boundary source [right].

The insertion/removal of a Darboux vertex leaves invariant the system of vectors except for the edges $e_l = [b_l, V_l]$, $e_l^{(D)} = V_l, V_l^{(D)}$, more precisely

- (1) The insertion of a univalent white Darboux vertex $V_{j_s}^{(D)}$ at the vertex V_{j_s} next to the boundary sink b_{j_s} , $s \in [n - k]$, produces a null vector on the edge $e_{j_s}^{(D)}$ joining $V_{j_s}^{(D)}$ to V_{j_s} and keeps invariant the vectors of the other edges at V_{j_s} ;
- (2) At a boundary source b_{i_r} , we combine the insertion of the Darboux vertex $V_{i_r}^{(D)}$, the change of orientation of the edges $e_{i_r} = [b_{i_r}, V_{i_r}]$ and $e_{i_r}^{(D)} = [V_{i_r}, V_{i_r}^{(D)}]$ and the translation of the boundary ray from b_{i_r} to $V_{i_r}^{(D)}$, $r \in [k]$. It is not restrictive to assume that the vertexes b_{i_r} , V_{i_r} and $V_{i_r}^{(D)}$ are so near to each other that moving the r -th boundary ray does not effect its intersections with the rest of the graph and that there is no intersection of boundary rays with $e_{i_r}^{(D)}$. Then the effect of the composition of these three transformations on vectors associated to e_{i_r} and $e_{i_r}^{(D)}$ is the following: $E_{e_{i_r}}$ changes from $A[r] - E[i_r]$ to $E[i_r]$, while $E_{e_{i_r}^{(D)}}$ changes from 0 to $A[r]$.

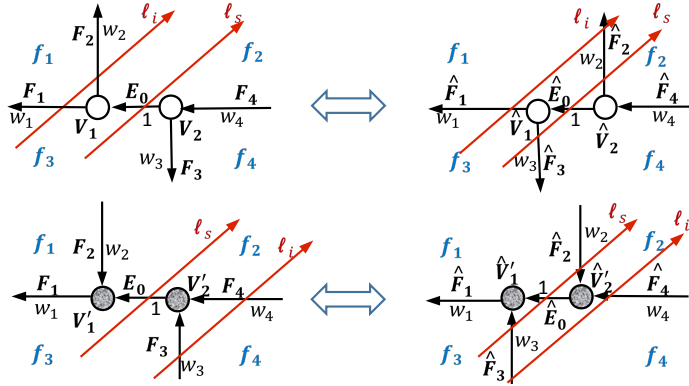


FIGURE 39. The insertion/removal of an unicolored internal vertex is equivalent to a flip move of the unicolored vertexes.

The contraction/uncontraction of an unicolored internal edge combined with the trivalency condition is equivalent to a flip of the unicolored vertexes involved in the move. It is possible to express such transformation as a combination of elementary flip moves each involving a pair of white vertexes (see Figure 39 for an example). At any edge e_l , $l \in [4]$, ending at just one of the flipping vertexes, the number of intersections with a gauge ray l_i is invariant except for the gauge rays l_s crossing the unit edge e_0 joining the flipping vertexes. The flip moves acts on the edge vectors as follows:

- (1) The flip move of two white vertexes leaves invariant the edge vectors at e_1, e_4 ; it changes the sign of the edge vectors at e_2 and e_3 if a gauge ray crosses e_0 and acts untrivially on the flipping edge e_0 . For instance, in the case illustrated in Figure 39 we have:

(81)

$$\hat{F}_1 = F_1, \quad \hat{F}_2 = -F_2, \quad \hat{F}_3 = -F_3, \quad \hat{F}_4 = F_4, \quad E_0 = -F_1 - F_2, \quad \hat{E}_0 = -\hat{F}_1 - \hat{F}_3;$$

- (2) The flip move of two black vertexes leaves invariant all edge vectors at $e_l, l \in [0, 5]$. For instance, in the case illustrated in Figure 39 we have:

$$(82) \quad \hat{H}_1 = H_1, \quad \hat{H}_2 = H_2, \quad \hat{H}_3 = H_3, \quad \hat{H}_4 = H_4, \quad \hat{E}_0 = E_0 = -E_1.$$

8.3. (M3) The middle edge insertion/removal. The middle edge insertion/removal concerns bivalent vertexes (see Figure 40). The relation between the vectors E_1, E_2 and E_{12} is simply, $E_{12} = E_2$.

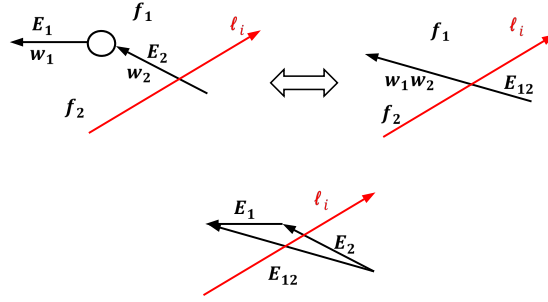


FIGURE 40. The middle edge insertion/removal.

8.4. (R1) The parallel edge reduction and (R2) the dipole reduction. The parallel edge reduction consists of the removal of two trivalent vertexes of different color connected by a pair of parallel edges (see Figure 41[top part]). If the parallel edge separates two distinct faces the relation of the face weights before and after the reduction is

$$f'_1 = \frac{f_1}{1 + f_0^{-1}}, \quad f'_2 = f_2(1 + f_0),$$

otherwise, if $f_1 = f_2$ correspond to the same face $f'_1 = f'_2 = f_1 f_0$. For the configuration shown in the Figure the relations between the edge weights and the edge vectors respectively are

$$w'_1 = w_1(w_2 + w_3)w_4, \quad E'_1 = E_1.$$

The dipole reduction consists of the elimination of an isolated component consisting of two vertexes joined by an edge e (see Figure 41[bottom part]). The transformation leaves invariant the weight of the face containing such component. Since the edge vector at e is $E_e = 0$, this transformation acts trivially on the vector system.

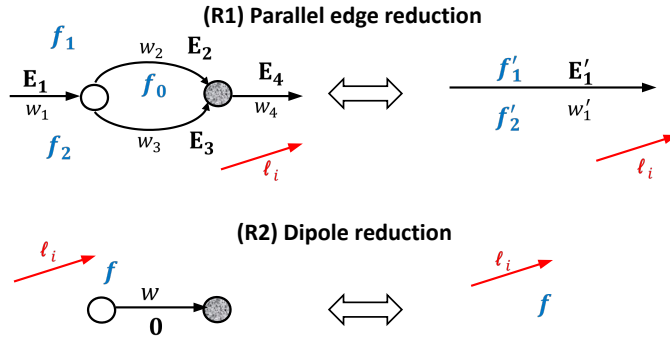


FIGURE 41. The parallel edge and the dipole reductions.

8.5. **(R3) The leaf reduction.** The leaf reduction occurs when a network contains a vertex u incident to a single edge e_1 ending at a trivalent vertex (see Figure 42): in this case it is possible to remove u and e_1 , disconnect e_2 and e_3 , assign the color of u at all newly created vertexes of the edges e_{12} and e_{13} . If we had two faces of weights f_1 and f_2 in the initial configuration, then we merge them into a single face of weight $f_{12} = f_1 f_2$; otherwise $f_{12} = f_1$ and the effect of the transformation is to create new isolated components. In any case

$$E_{12} = w_1 E_2, \quad E_{13} = w_3 E_3.$$

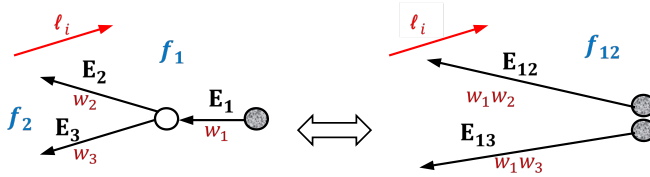


FIGURE 42. The leaf reduction.

Remark 8.1. Null vectors Null vectors are associated by definition to the edges of isolated components inside the graph and to those belonging to paths connected to an isolated boundary source. We may have a null vector at the edge e , only if the white vertex incident with e has the other edge vectors which are linearly dependent. Using Postnikov moves and reductions we may obtain a null vector at some edge starting from an initial configuration without null vectors only in the following cases:

- (1) With (M1), only if E_3 and E_4 are linearly dependent (see Figure 36);
- (2) Using (M2) to create a Darboux vertex at a boundary sink (see Figure 38);
- (3) Using the flip move in (M2) at two internal white vertexes when F_1, F_3 are linearly dependent (see Figure 39);
- (4) Unreducing a leaf using (R3) if E_{13} and E_{12} are proportional (see Figure 42).

If we change the orientation of the graph, either a null edge vector remains null or it coincides with a heat hierarchy solution for all times. The latter situation occurs at the Darboux vertices if we change the base in the matroid and induces a transformation in the position of **vacuum** divisor points, leaving invariant the position of the **KP** divisor points.

9. THE CONSTRUCTION OF THE KP DIVISOR ON $\Gamma(\mathcal{N})$

Let us fix the soliton data $(\mathcal{K}, [A])$, $\mathcal{K} = \{\kappa_1 < \dots < \kappa_n\}$ and $[A] \in \mathcal{S}_{\mathcal{M}}^{\text{TNN}} \subset Gr^{\text{TNN}}(k, n)$ and a planar oriented bipartite perfect trivalent network in the disk $(\mathcal{N}, \mathcal{O}, \mathfrak{l})$, associated to $[A]$.

In this section, for any given soliton data $(\mathcal{K}, [A])$ and for any \mathcal{N} satisfying Assumption 9.1**, we construct a degree g effective KP divisor $\mathcal{D}_{\text{KP}, \Gamma}$ contained in the union of all the $g + 1$ ovals of $\Gamma(\mathcal{N})$. In particular $\mathcal{D}_{\text{KP}, \Gamma}$ does not depend neither on the gauge ray direction nor on the orientation chosen in the construction, but only on the soliton data and the graph used to construct the reducible rational curve (Theorem 4.2). In the next section, we complete the proof of Theorem 4.1 on $\Gamma(\mathcal{N})$ using the combinatorics of the network to count the number of divisor points in each oval.

Both the vacuum and the KP wavefunctions are defined using systems of vectors characterized in Section 7. Therefore the construction of $\mathcal{D}_{\text{KP}, \Gamma}$ may be carried out both in the case in which $[A]$ belongs to an irreducible or to a reducible positroid cell.

However, since, by definition, both the vacuum and the KP wavefunctions are constant with respect to the spectral parameter on the components of $\Gamma(\mathcal{N})$ corresponding to the subgraph of \mathcal{N} containing either an isolated boundary source or an isolated boundary sink, we explain the detailed construction of the KP wavefunction and characterize the vacuum and KP divisors only in the case of soliton data in **irreducible positroid cells** to avoid unnecessary technicalities.

Similarly, the system of vectors $E_e = (0, \dots, 0)$ on all edges of disconnected components in the graph. Therefore by construction both the vacuum and the KP wavefunctions are trivial on

**this Assumption is fulfilled for any soliton data on \mathcal{N}_T and for generic data in general.

the corresponding isolated components of the reducible curve. Again, in the rest of the paper, we assume that \mathcal{N} is a **connected graph** to avoid unnecessary technicalities.

Assumption 9.1. The network \mathcal{N} Let $[A]$ be a point in the irreducible positroid cell $\mathcal{S}_{\mathcal{M}}^{TNN} \subset Gr^{TNN}(k, n)$ We assume that \mathcal{N} is a planar bipartite perfectly oriented connected network in the disk with the following properties:

- (1) It has $g + 1$ faces with $g \geq |D|$, where $|D|$ is equal to the dimension of the given positroid cell;
- (2) It does not possess internal sources or sinks;
- (3) All vertexes are at most trivalent;
- (4) It is move–reduction equivalent to the Le–network \mathcal{N}_T (that is it belongs to the family of networks representing $[A]$);
- (5) The system of edge vectors does not possess null vectors in any orientation of \mathcal{N} .

We remark that moves and reductions generically transform/create/eliminate non zero vectors into non zero ones for generic points in any given positroid cell, so that, for generic choice of the initial edge weights, we may move-reduce \mathcal{N} to \mathcal{N}_T respecting (5) at any step.

Plan of the section

- (1) **The modified network \mathcal{N}' .** We insert a Darboux vertex next to each boundary sink or source vertex using move (M2) (see Figure 38) and call the transformed network \mathcal{N}' . Each Darboux sink/source edge corresponds to a Darboux sink/source marked point in $\Gamma(\mathcal{N})$ (Γ is not changed! we are simply adding a set of marked points). This transformation is motivated by the following technical reasons:
 - (a) Any marked point on Γ corresponds to an edge in the graph. The addition of Darboux sink and sources edges allows to control **changes in the divisors due to changes of the base in the matroid for $[A]$** ;
 - (b) With our choice of orientation in \mathcal{N}' **Sato boundary conditions for the vacuum wavefunction** are automatically satisfied on \mathcal{N}' ;
 - (c) The **Darboux transformed vertex wavefunction** takes the same value at **all** edges common to \mathcal{N} and \mathcal{N}' .
- (2) **The vacuum and dressed vertex wavefunctions** At the edges $e \in \mathcal{N}'$ we define a non normalized vacuum vertex wavefunction $\Phi_e(\vec{t})$ and its dressing $\Psi_e(\vec{t})$ using the system of vectors introduced in section 7. Using the linear relations at the white vertexes we assign

a degree $g + n - k$ vacuum divisor $\mathcal{D}_{\text{vac}, \mathcal{N}'}$ and a degree $g + n - k$ dressed divisor $\mathcal{D}_{\text{dr}, \mathcal{N}'}$ to \mathcal{N}' and characterize its properties w.r.t. changes of gauge ray direction and orientation in the graph;

- (3) **The vacuum divisor and the vacuum wavefunction on Γ** The vacuum divisor $\mathcal{D}_{\text{vac}, \Gamma}$ on Γ is obtained from $\mathcal{D}_{\text{vac}, \mathcal{N}'}$ eliminating the $n - k$ Darboux sink points. By construction $\mathcal{D}_{\text{vac}, \Gamma}$ depends on the base in the matroid \mathcal{M} . The normalized vacuum wavefunction $\hat{\phi}$ on Γ is obtained imposing that it coincides for all times at each marked point with the value of the normalized vacuum vertex wavefunction at the corresponding edge in \mathcal{N}' . By construction it is meromorphic of degree $\mathfrak{d} \leq g$ and its effective pole divisor is $\mathcal{D}_{\text{vac}, \Gamma}$;
- (4) **The KP divisor and the KP wavefunction on Γ** By construction the KP divisor $\mathcal{D}_{\text{KP}, \Gamma} = \mathcal{D}_{\text{KP}, \Gamma}(\mathcal{K}, [A])$ is contained in the union of the ovals of Γ and it is obtained from $\mathcal{D}_{\text{dr}, \mathcal{N}'}$ eliminating the n Darboux sink and source divisor points and adding the degree k Sato divisor;
- (5) **The invariance of the KP divisor with respect to changes of base in \mathcal{M} .** On each component $\Gamma_l = \mathbb{CP}^1$ of $\Gamma(\mathcal{N})$ corresponding to a trivalent white vertex V_l of \mathcal{N} , we have four real ordered marked points corresponding to the edges at V_l and to the dressed point divisor. A change of orientation of \mathcal{N} induces a change in the local coordinate used on Γ_l , that is it leaves invariant the order and the position of the four points on Γ_l .

9.1. The modified network \mathcal{N}' . To obtain a consistent system of linear equations on the whole network $(\mathcal{N}, \mathcal{O}, \mathfrak{l})$, such that at each edge ending at a boundary vertex b_s , $s \in [n]$, the vector E_{b_s} is the s -th vector of the canonical basis, we generalize the construction in Section 6 and consider the network $(\mathcal{N}', \mathcal{O}, \mathfrak{l})$ where:

- (1) \mathcal{N}' is the network obtained from \mathcal{N} adding an edge with unit weight and a white vertex $V_s^{(D)}$ at each bivalent white vertex V_s associated to the boundary vertex b_s , $s \in [n]$ (see Figure 38);
- (2) \mathcal{O} is the orientation of \mathcal{N}' such that
 - (a) For any $s \in [n]$, the edge joining $V_s^{(D)}$ and V_s points towards $V_s^{(D)}$ if b_s is a boundary sink, otherwise it points towards V_s ;
 - (b) The edge joining V_{i_r} to the boundary source b_{i_r} points towards b_{i_r} for any $r \in [k]$;
 - (c) All other edges are oriented as in $(\mathcal{N}, \mathcal{O})$;
- (3) The gauge direction is the same, but the line \mathfrak{l}_{i_r} starts at $V_{i_r}^{(D)}$, for any $r \in [k]$.

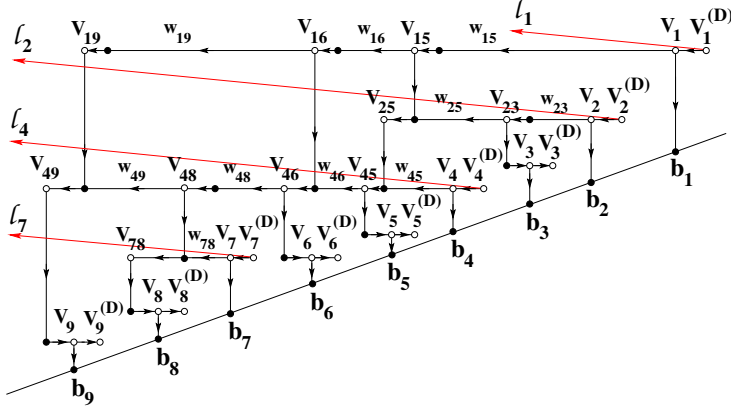


FIGURE 43. The modified network $(\mathcal{N}', \mathcal{O}, \mathfrak{l})$ for the example of Figure 20.

In Figure 43, we illustrate such modified network in the case of Example 2.2.

We assume that the vertex $V_s^{(D)}$ is sufficiently near to b_s for any $s \in [n]$, so that on $(\mathcal{N}', \mathcal{O}, \mathfrak{l})$ we do not modify the set of intersections of \mathfrak{l}_{i_r} when we move it from b_{i_r} in \mathcal{N} to $V_{i_r}^{(D)}$ in \mathcal{N}' . We then extend the system of vectors E_e to \mathcal{N}' as explained in Section 8.2.

Remark 9.1. *The effect of a change in the orientation or in the gauge ray direction on the system of vectors on \mathcal{N}' . The system of vectors on \mathcal{N}' changes in agreement with Propositions 7.2 and 7.3 when we change either the gauge ray direction or the orientation.*

Remark 9.2. *The relation between trivalent white vertexes and faces in \mathcal{N} and \mathcal{N}' . Let us suppose that \mathcal{N} is an oriented planar bipartite trivalent perfect network with $g + 1$ faces associated to a given point in $[A]$ in an irreducible component in $Gr^{TNN}(k, n)$. Let us suppose that \mathcal{N} does not possess internal vertexes of degree one. Let t_W, t_B, d_W and d_B respectively be the number of trivalent white, of trivalent black, of bivalent white, and of bivalent black internal vertexes of \mathcal{N} . Let n_I be the number of internal edges (i.e. edges not connected to a boundary vertex) of \mathcal{N} . Then by Euler formula we have*

$$g = n_I + n - (t_W + t_B + d_W + d_B).$$

The number of edges and the number of vertexes, moreover satisfies the following identity

$$3(t_W + t_B) + 2(d_W + d_B) = 2n_I + n.$$

The total number of linear conditions at the vertexes is $2t_B + t_W + d_W + d_B$, and the consistency of the linear system guarantees that such number is equal to $n_I + k$. From the above three identities,

we easily obtain for \mathcal{N}

$$(83) \quad t_W = g - k, \quad t_B = g - n + k, \quad n_I = 3g - 2n + d_W + d_B.$$

\mathcal{N}' has by construction the same number of faces and $t_W + n$ trivalent white vertexes.

Remark 9.3. Relation with the construction in [2]. For data $[A] \in Gr^{TP}(k, n)$, there is an interpretation in term of positions of Darboux points in \mathcal{N}' of the algebraic construction in [2] of a system of vectors and coefficients associated to the representative matrix in banded form. Let \mathcal{N}'_T be the modified Le-network for $[A]$ with the standard orientation and use move (M2) to add a white vertex with unit edge and null vector at each bivalent white vertex $V_{i_r j_{n-k+r}}$, $r \in [k]$, (see Figure 44[left] for an example in $Gr^{TP}(3, 5)$): the augmented system of vectors preserves its compatibility. Then invert the direction of each horizontal path from $V_{i_r j_{n-k+r}}$ to V_{i_r} , taking the reciprocal of the weights on each edge which changes of direction, we move the gauge lines to the new Darboux point. The transformed system of vectors is compatible since it satisfies the linear system at each vertex; it is straightforward to show that it coincides with the one used in [2] for the choice of gauge ray direction of Figure 44[right]. In particular, at the new Darboux points the edge vector coincides with the r -th row of the representative matrix in banded form.

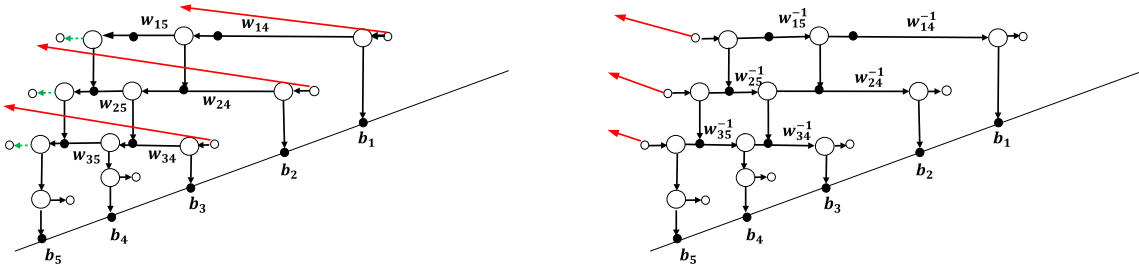


FIGURE 44. The graphical interpretation of the algebraic construction in [2] in the case of $[A] \in Gr^{TP}(3, 5)$.

9.2. The vacuum and the KP vertex wavefunctions. In this section we define the vacuum vertex wavefunction and the KP vertex wavefunction on $(\mathcal{N}', \mathcal{O}, \mathfrak{l})$ and introduce an effective vacuum divisor and an effective dressed divisor.

Definition 9.1. The vacuum vertex wavefunction (vacuum v.w.) and the dressed vertex wavefunction (dressed v.w.) on $(\mathcal{N}', \mathcal{O}, \mathfrak{l})$. Let $(\mathcal{N}', \mathcal{O}, \mathfrak{l})$ be the extended oriented

network associated to the soliton data $(\mathcal{K}, [A])$ and E_e the system of vectors on \mathcal{N}' . We define the vacuum vertex wavefunction (vacuum v.w.) on $(\mathcal{N}', \mathcal{O}, \mathfrak{l})$ as follows

$$(84) \quad \Phi_{e, \mathcal{O}, \mathfrak{l}}(\vec{t}) \equiv \langle E_e, \mathfrak{E}_\theta(\vec{t}) \rangle, \quad e \in \mathcal{N}'$$

where $\mathfrak{E}_\theta(\vec{t}) = (e^{\theta_1(\vec{t})}, \dots, e^{\theta_n(\vec{t})})$, $\theta_j(\vec{t}) = \sum_{l \geq 1} \kappa_j^l t_l$ and $\vec{t} = (t_1 = x, t_2 = y, t_3 = t, t_4, \dots)$ are the KP times, and $\langle \cdot, \cdot \rangle$ denotes the usual scalar product, as in Remark 6.1.

Let $\mathfrak{D}^{(k)}$ be the Darboux transformation for $(\mathcal{K}, [A])$. We define the dressed vertex wavefunction (dressed v.w.) on $(\mathcal{N}', \mathcal{O}, \mathfrak{l})$ as follows

$$(85) \quad \Psi_{e, \mathcal{O}, \mathfrak{l}}(\vec{t}) \equiv \mathfrak{D}^{(k)} \Phi_{e, \mathcal{O}, \mathfrak{l}}(\vec{t}).$$

Remark 9.4. *The set of edges on which the vacuum v.w. $\Phi_e(\vec{t}) \equiv 0$ or the dressed v.w. $\Psi_e(\vec{t}) \equiv 0$ for all \vec{t} . By our Assumption 9.1 on \mathcal{N} , the only edges e on which $E_e = (0, \dots, 0)$ is a null vector correspond to the Darboux edges for the boundary sinks and such set depends only on the base I inducing the chosen orientation of \mathcal{N}' (see Figure 38). In the following we call such edges Darboux sink edges and we denote $\mathcal{E}(I)$ the complementary set to the Darboux sink edges for the base I .*

We remark that both the vacuum v.w. and the dressed v.w. are identically zero for all times at the Darboux sink edges e : $\Phi_{e, \mathcal{O}, \mathfrak{l}}(\vec{t}) \equiv 0$, $\Psi_{e, \mathcal{O}, \mathfrak{l}}(\vec{t}) \equiv 0$.

Moreover $\Psi_{e, \mathcal{O}, \mathfrak{l}}(\vec{t}) \equiv 0$ for all \vec{t} also at all edges such that E_e is a linear combination of the row vectors of a representative matrix of $[A]$, that is if $\Phi_{e, \mathcal{O}, \mathfrak{l}}(\vec{t})$ is a linear combination of the heat hierarchy solutions generating the Darboux transformation $\mathfrak{D}^{(k)}$. By Assumption 9.1 on the network, this case may occur only when $e \in \mathcal{N}'$ is the Darboux edge for a boundary source. In the following we call the latter edges Darboux source edges for the base I .

Therefore the set of edges $\Psi_{e, \mathcal{O}, \mathfrak{l}}(\vec{t}) \neq 0$ does not depend on the base and we denote \mathcal{E} the complement in the set of edges of \mathcal{N}' of the set of Darboux source and sink edges.

Remark 9.5. *The initial time \vec{t}_0 . Let $(\mathcal{N}', \mathcal{O}, \mathfrak{l})$, the vacuum and the dressed v.w. be given and let $\mathcal{E}(I)$ and \mathcal{E} be as in Remark 9.4. Proceeding as in the case of the Le network \mathcal{N}'_T , we take $\vec{t}_0 = (x_0, 0, \dots)$ such that*

- (1) *For any $e \in \mathcal{E}(I)$, the sign of the vacuum v.w. $\Phi_{e, \mathcal{O}, \mathfrak{l}}(\vec{t}_0)$ is the same of the coefficient of the highest phase appearing in it;*
- (2) *For any $e \in \mathcal{E}$, the dressed v.w. $\Psi_{e, \mathcal{O}, \mathfrak{l}}(\vec{t}_0) \neq 0$.*

The following lemma follows from Lemma 7.1 and justifies the assignment of a vacuum divisor point and a dressed divisor point to each trivalent white vertex.

Lemma 9.1. *The linear system* *Let $(\mathcal{N}', \mathcal{O}, \mathfrak{l})$ be the oriented network associated to the soliton data $(\mathcal{K}, [A])$, with $[A] \in \mathcal{S}_{\mathcal{M}}^{TNN} \subset Gr^{TNN}(k, n)$. Let E_e , $\Phi_{e, \mathcal{O}, \mathfrak{l}}(\vec{t})$ and $\Psi_{e, \mathcal{O}, \mathfrak{l}}(\vec{t})$ respectively be the system of vectors, the vacuum v.w. and the dressed v.w. on \mathcal{N}' and let $\mathfrak{D}^{(k)}$ be the Darboux transformation for $(\mathcal{K}, [A])$.*

Then both the vacuum v.w. $\Phi_{e, \mathcal{O}, \mathfrak{l}}(\vec{t})$ and the dressed v.w. $\Psi_{e, \mathcal{O}, \mathfrak{l}}(\vec{t})$ satisfy the same linear system as E_e at each $e \in \mathcal{N}'$ for all \vec{t} . More precisely,

- (1) *At any bivalent vertex incident with the incoming edge e and the outgoing edge f ,*

$$\begin{aligned}\Phi_{e, \mathcal{O}, \mathfrak{l}}(\vec{t}) &= (-1)^{int(e) + wind(e, f)} w_e \Phi_{f, \mathcal{O}, \mathfrak{l}}(\vec{t}), \\ \Psi_{e, \mathcal{O}, \mathfrak{l}}(\vec{t}) &= (-1)^{int(e) + wind(e, f)} w_e \Psi_{f, \mathcal{O}, \mathfrak{l}}(\vec{t}),\end{aligned}$$

where $int(e)$ denotes the number of intersections of the gauge boundary rays with the edge e , while $wind(e, f)$ denotes the winding number of the path containing the two edges e and f with respect to the gauge direction;

- (2) *At any trivalent white vertex incident with the incoming edge e_3 and the outgoing edges e_1, e_2 ,*

$$(86) \quad \begin{aligned}\Phi_{e_3, \mathcal{O}, \mathfrak{l}}(\vec{t}) &= (-1)^{int(e_3)} w_3 \left((-1)^{wind(e_3, e_1)} \Phi_{e_1, \mathcal{O}, \mathfrak{l}}(\vec{t}) + (-1)^{wind(e_3, e_2)} \Phi_{e_2, \mathcal{O}, \mathfrak{l}}(\vec{t}) \right), \\ \Psi_{e_3, \mathcal{O}, \mathfrak{l}}(\vec{t}) &= (-1)^{int(e_3)} w_3 \left((-1)^{wind(e_3, e_1)} \Psi_{e_1, \mathcal{O}, \mathfrak{l}}(\vec{t}) + (-1)^{wind(e_3, e_2)} \Psi_{e_2, \mathcal{O}, \mathfrak{l}}(\vec{t}) \right);\end{aligned}$$

- (3) *At any trivalent black vertex incident with the incoming edges e_2, e_3 and the outgoing edge e_1 ,*

$$\begin{aligned}\Phi_{e_m, \mathcal{O}, \mathfrak{l}}(\vec{t}) &= (-1)^{int(e_m) + wind(e_m, e_1)} w_m \Phi_{e_1, \mathcal{O}, \mathfrak{l}}(\vec{t}), & m = 2, 3, \\ \Psi_{e_m, \mathcal{O}, \mathfrak{l}}(\vec{t}) &= (-1)^{int(e_m) + wind(e_m, e_1)} w_m \Psi_{e_1, \mathcal{O}, \mathfrak{l}}(\vec{t}), & m = 2, 3.\end{aligned}$$

In view of the above we associate a vacuum network divisor and dressed network divisor to $(\mathcal{N}', \mathcal{O}, \mathfrak{l})$ as follows.

Definition 9.2. *The vacuum network divisor $\mathcal{D}_{\text{vac}, \mathcal{N}'}$ and the dressed network divisor $\mathcal{D}_{\text{dr}, \mathcal{N}'}$.* *At each trivalent white vertex V of $(\mathcal{N}', \mathcal{O}, \mathfrak{l})$, let $\Phi_{e_m, \mathcal{O}, \mathfrak{l}}(\vec{t})$ be the vacuum v.w. on the edge e_m , $m \in [3]$, defined above. Then we assign the following vacuum network divisor number*

$\gamma_{\text{vac},V}$ to V :

$$(87) \quad \gamma_{\text{vac},V} = \frac{(-1)^{\text{wind}(e_3, e_1)} \Phi_{e_1, \mathcal{O}, \mathfrak{l}}(\vec{t}_0)}{(-1)^{\text{wind}(e_3, e_1)} \Phi_{e_1, \mathcal{O}, \mathfrak{l}}(\vec{t}_0) + (-1)^{\text{wind}(e_3, e_2)} \Phi_{e_2, \mathcal{O}, \mathfrak{l}}(\vec{t}_0)},$$

where $\text{wind}(e_3, e_i)$ is the winding number of the directed path $[e_3, e_i]$, $i = 1, 2$.

We call $\mathcal{D}_{\text{vac}, \mathcal{N}'} = \{\gamma_{\text{vac}, V_l}, l \in [g + n - k]\}$ the vacuum network divisor on \mathcal{N}' , where V_l , $l \in [g + n - k]$, are the trivalent white vertices of the network.

At each trivalent white vertex V of $(\mathcal{N}', \mathcal{O}, \mathfrak{l})$, let $\Psi_{e_m, \mathcal{O}, \mathfrak{l}}(\vec{t})$ be the dressed v.w. on the edge e_m , $m \in [3]$, defined above. Then, to V we assign the dressed network divisor number

$$(88) \quad \gamma_{\text{dr},V} = \frac{(-1)^{\text{wind}(e_3, e_1)} \Psi_{e_1, \mathcal{O}, \mathfrak{l}}(\vec{t}_0)}{(-1)^{\text{wind}(e_3, e_1)} \Psi_{e_1, \mathcal{O}, \mathfrak{l}}(\vec{t}_0) + (-1)^{\text{wind}(e_3, e_2)} \Psi_{e_2, \mathcal{O}, \mathfrak{l}}(\vec{t}_0)},$$

with $\text{wind}(e_3, e_i)$ as above. If V is a trivalent vertex, associated to a Darboux source, the denominator in (88) is zero, and we set $\gamma_{\text{dr},V} = \infty$.

We call $\mathcal{D}_{\text{dr}, \mathcal{N}'} = \{\gamma_{\text{dr}, V_l}, l \in [g + n - k]\}$ the dressed network divisor on \mathcal{N}' , where V_l , $l \in [g + n - k]$, are the trivalent white vertices of the network.

By definition, both the vacuum and the dressed network divisor numbers at each trivalent white vertex are real and represent the local coordinate of a point on the corresponding copy of \mathbb{CP}^1 in Γ . In general, on $(\mathcal{N}', \mathcal{O}, \mathfrak{l})$, the value of the vacuum or dressed network divisor number at a given trivalent white vertex V depends on the choice of \vec{t}_0 . If this is not the case we call the corresponding **network divisor number trivial**. If $\mathcal{N}' = \mathcal{N}'_T$, by construction the only trivial network divisor numbers may occur at Darboux edges. In the case of a general network, such trivial network divisor numbers occur also at all vertexes where the linear system in Lemma 9.1 involves linearly dependent vectors.

Lemma 9.2. Trivial network divisor numbers Let E_{e_m} , $m \in [3]$, be the edge vectors at a trivalent white vertex V of $(\mathcal{N}', \mathcal{O}, \mathfrak{l})$ and $\gamma_{\text{vac},V}$, $\gamma_{\text{dr},V}$ respectively be the vacuum and dressed network divisor numbers at V . If there exists a non zero constant c_V such that either $E_{e_2} = c_V E_{e_1}$ or $E_{e_3} = c_V E_{e_1}$ or $E_{e_3} = c_V E_{e_2}$, then at V the vacuum and dressed network divisor numbers coincide

$$\gamma_{\text{dr},V} = \gamma_{\text{vac},V}$$

and the corresponding network divisor numbers are trivial.

Proof. Indeed in the first case for all \vec{t} , $\Phi_{e_2, \mathcal{O}, l}(\vec{t}) = c_V \Phi_{e_1, \mathcal{O}, l}(\vec{t})$, $\Psi_{e_2, \mathcal{O}, l}(\vec{t}) = c_V \Psi_{e_1, \mathcal{O}, l}(\vec{t})$, and

$$\Phi_{e_3, \mathcal{O}, l}(\vec{t}) = (-1)^{\text{int}(e_3)} w_3 \left((-1)^{\text{wind}(e_3, e_1)} + c_V (-1)^{\text{wind}(e_3, e_2)} \right) \Phi_{e_1, \mathcal{O}, l}(\vec{t}),$$

$$\Psi_{e_3, \mathcal{O}, l}(\vec{t}) = (-1)^{\text{int}(e_3)} w_3 \left((-1)^{\text{wind}(e_3, e_1)} + c_V (-1)^{\text{wind}(e_3, e_2)} \right) \Psi_{e_1, \mathcal{O}, l}(\vec{t}),$$

and

$$\gamma_{\text{dr}, V} = \gamma_{\text{vac}, V} = \frac{1}{1 + c_V (-1)^{\text{wind}(e_3, e_1) + \text{wind}(e_3, e_2)}}.$$

The other cases may be treated in a similar way. \square

Below we characterize the dependence of both the vacuum and dressed network divisor numbers on the gauge ray direction, the base in the matroid and the orientation of the network, using Propositions 7.2–7.3, and Lemmas 7.2–7.3.

A change of gauge ray direction may effect the signs of the vacuum and of the dressed vertex wavefunctions at the given vertex V (Proposition 9.1), but not the vacuum and the dressed network divisor numbers thanks to the linear relations at V (Corollary 9.1).

Every change of orientation in \mathcal{N}' (either induced by a change of base in the matroid or due to a change of orientation in closed cycles) corresponds to a well defined change of the local coordinate of each copy of \mathbb{CP}^1 , and the dressed network divisor numbers change according to such coordinate transformation (Corollary 9.2). Therefore, all the positions of the corresponding divisor points on Γ remain invariant (Theorem 4.2).

The dependence of the vacuum network divisor numbers on changes of orientation in \mathcal{N}' is more complicated: any change of orientation just due to changes of orientation in closed cycles corresponds to a well defined change of the of the vacuum network divisor number in agreement with the corresponding change of coordinate in the component of the curve (Lemma 7.3). On the contrary, a change of base in the matroid untrivially changes the vacuum network divisor numbers and the position of the corresponding vacuum divisor points in Γ .

Proposition 9.1. *The dependence of the vacuum v.w. and of the dressed v.w. on the gauge ray directions and on the orientation of the network* Let \mathcal{N}' be a network representing $[A] \in \text{Gr}^{\text{TNN}}(k, n)$ and let $\mathcal{O}_s, \mathfrak{I}_s$, $s = 1, 2$, respectively be two perfect orientations and two gauge ray directions of \mathcal{N}' . Let \mathcal{K} be a system of phases. Let $f^{(\tau)}(\vec{t})$ be a system of heat hierarchy solutions generating the Darboux transformation $\mathfrak{D}^{(k)}$ for the soliton data $(\mathcal{K}, [A])$. Then, for any fixed \vec{t} and $e \in \mathcal{N}'$,

(1) the vacuum v.w. Φ and the dressed v.w. Ψ may only change of sign if we change the gauge ray direction:

$$(89) \quad \Phi_{e,\mathcal{O},l_2}(\vec{t}) = \pm \Phi_{e,\mathcal{O},l_1}(\vec{t}), \quad \Psi_{e,\mathcal{O},l_2}(\vec{t}) = \pm \Psi_{e,\mathcal{O},l_1}(\vec{t});$$

(2) if we change the perfect orientation in \mathcal{N}' from \mathcal{O}_1 to \mathcal{O}_2 , then, for any edge $e \in \mathcal{N}'$ there exist real constants α_e , c_e^r , $r \in [k]$, such that the vacuum v.w. Φ and the dressed v.w. Ψ satisfy

$$(90) \quad \Phi_{e,\mathcal{O}_2,l}(\vec{t}) = \alpha_e \Phi_{e,\mathcal{O}_1,l}(\vec{t}) + \sum_{r=1}^k c_e^r f^{(r)}(\vec{t}), \quad \Psi_{e,\mathcal{O}_2,l}(\vec{t}) = \alpha_e \Psi_{e,\mathcal{O}_1,l}(\vec{t}).$$

If the two orientations are associated to the same positions of the Darboux sinks and the Darboux sources (in the case of \mathcal{N}' it means that both orientations are associated to the same base I), then for any edge $e \in \mathcal{N}'$ there exists a real constant α_e such that the vacuum v.w. satisfies

$$(91) \quad \Phi_{e,\mathcal{O}_2(I),l}(\vec{t}) = \alpha_e \Phi_{e,\mathcal{O}_1(I),l}(\vec{t})$$

Corollary 9.1. *The independence of vacuum and dressed network divisors on the gauge ray direction.* Let l_1 and l_2 be two gauge directions for the oriented network $(\mathcal{N}', \mathcal{O})$. Then for any trivalent white vertex $V \in (\mathcal{N}', \mathcal{O})$, both the vacuum network divisor numbers and the dressed network divisor numbers computed using either l_1 or l_2 are the same:

$$(92) \quad \gamma_{\text{vac},V,l_2} = \gamma_{\text{vac},V,l_1}, \quad \gamma_{\text{dr},V,l_2} = \gamma_{\text{dr},V,l_1}.$$

The proof immediately follows by direct computation of the network divisor numbers by inserting (89) in the linear system of Lemma 9.1 at each white vertex.

Corollary 9.2. *The dependence of the dressed network divisor on the orientation.* Let \mathcal{O}_1 and \mathcal{O}_2 be two perfect orientations for network \mathcal{N} . Then for any trivalent white vertex V , such that all edges at V have the same versus in both orientations, the dressed network divisor number is the same in both orientations

$$(93) \quad \gamma_{\text{dr},V,\mathcal{O}_2} = \gamma_{\text{dr},V,\mathcal{O}_1}.$$

If at the vertex V we change orientation of edges from $(e_1^{(1)}, e_2^{(1)}, e_3^{(1)})$ to $(e_2^{(2)}, e_3^{(2)}, e_1^{(2)})$ (see Figure 45[left]), then the relation between the dressed network divisor numbers at V in the two

orientations is

$$(94) \quad \gamma_{\text{dr},V,\mathcal{O}_2} = \frac{1}{1 - \gamma_{\text{dr},V,\mathcal{O}_1}}.$$

If at the vertex V we change orientation of edges from $(e_1^{(1)}, e_2^{(1)}, e_3^{(1)})$ to $(e_3^{(2)}, e_1^{(2)}, e_2^{(2)})$ (see Figure 45[right]), then the relation between the dressed network divisor numbers at V in the two orientations is

$$(95) \quad \gamma_{\text{dr},V,\mathcal{O}_2} = \frac{\gamma_{\text{dr},V,\mathcal{O}_1}}{\gamma_{\text{dr},V,\mathcal{O}_1} - 1}.$$

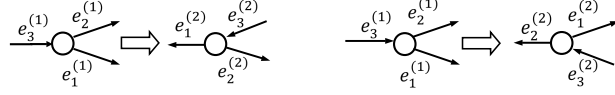


FIGURE 45. The change of orientation at a vertex V .

Proof The proof follows by direct computation of the dressed network divisor numbers using (90) and the linear system (86) at V for both orientations. For instance, (94) follows observing that

$$\Psi_{e_m^{(2)}, \mathcal{O}_2, \mathfrak{l}}(\vec{t}) = \alpha_{m-1} \Psi_{e_{m-1}^{(1)}, \mathcal{O}_1, \mathfrak{l}}(\vec{t}), \quad m = 1, 2, 3 \pmod{3}$$

and that the linear system w.r.t. both orientations imposes the constraint

$$\frac{\alpha_1}{\alpha_3 w_3} (-1)^{\text{int}_{\mathcal{O}_1}(e_3^{(1)}) + \text{wind}_{\mathcal{O}_1}(e_3^{(1)}, e_1^{(1)}) + \text{wind}_{\mathcal{O}_2}(e_3^{(2)}, e_2^{(2)}) + \text{wind}_{\mathcal{O}_2}(e_3^{(2)}, e_1^{(2)})} = -1,$$

so that

$$\begin{aligned} \gamma_{\text{dr},V,\mathcal{O}_2} &= \left(1 + \frac{(-1)^{\text{wind}(e_3^{(2)}, e_2^{(2)})} \Psi_{e_2^{(2)}, \mathcal{O}_2, \mathfrak{l}}}{(-1)^{\text{wind}(e_3^{(2)}, e_1^{(2)})} \Psi_{e_1^{(2)}, \mathcal{O}_2, \mathfrak{l}}} \right)^{-1} = \left(1 + \frac{(-1)^{\text{wind}(e_3^{(2)}, e_2^{(2)})} \alpha_1 \Psi_{e_1^{(1)}, \mathcal{O}_1, \mathfrak{l}}}{(-1)^{\text{wind}(e_3^{(2)}, e_1^{(2)})} \alpha_3 \Psi_{e_3^{(1)}, \mathcal{O}_1, \mathfrak{l}}} \right)^{-1} \\ &= \left(1 + \frac{\alpha_1 (-1)^{\text{wind}(e_3^{(2)}, e_2^{(2)}) + \text{int}_{\mathcal{O}_1}(e_3^{(1)})}}{\alpha_3 w_3 (-1)^{\text{wind}(e_3^{(2)}, e_1^{(2)})}} (-1)^{\text{wind}_{\mathcal{O}_1}(e_3^{(1)}, e_1^{(1)})} \gamma_{\text{dr},V,\mathcal{O}_1} \right)^{-1} \\ &= (1 - \gamma_{\text{dr},V,\mathcal{O}_1})^{-1}. \quad \square \end{aligned}$$

Remark 9.6. In next Section we show that the transformation of the network divisor numbers of Corollary 9.2 is due to the change of coordinates on the copy of \mathbb{CP}^1 associated with this white vertex.

Corollary 9.3. *The dependence of the vacuum network divisor numbers on the change of orientation* Let $\mathcal{O}_1 = \mathcal{O}_1(I)$ and $\mathcal{O}_2 = \mathcal{O}_2(I)$ be two perfect orientations for network \mathcal{N}' associated to the same base I . Then at any trivalent white vertex V (93)–(95) hold true with $\gamma_{\text{vac},V,\mathcal{O}_s}$, $s = 1, 2$ instead of $\gamma_{\text{dr},V,\mathcal{O}_s}$.

The proof follows using Lemma 7.3 and (76).

Remark 9.7. *Vacuum network divisor numbers and changes of base* If the change of orientation is induced by a change in the base of \mathcal{M} , then the rule for the transformation of the vacuum network divisor numbers is more complicated and we do not write it explicitly since we shall not use it in the following.

Remark 9.8. *Relation with the construction in [2].* Let $[A] \in \text{Gr}^{TP}(k, n)$. In [2] we construct a vacuum and a dressed divisor in $\Gamma(\xi)$ which may be obtained from $\Gamma(\mathcal{N}_T)$ with a convenient desingularization at certain pair of double points (see Remark 4.2). It is possible to verify that the dressed divisor points in $\Gamma(\xi)$ at **leading order in ξ** may be obtained from the dressed network divisor numbers of Definition 9.2 using the change of coordinates associated to the orientations of the networks introduced in Proposition 9.1 and Corollary 9.2, see also Figure 44.

The relation between the leading order in ξ of the vacuum divisor points constructed in [2] and the vacuum network divisor numbers on the network is more complicated because the vacuum vertex wavefunction changes according to (90).

We now normalize both the vacuum and the dressed vertex wavefunctions.

Definition 9.3. *The normalized vacuum vertex wavefunction $\hat{\Phi}$ and the KP vertex wavefunction $\hat{\Psi}$.* Let \mathcal{E} and $\mathcal{E}(I)$ be as in Remark 9.4, where $I = \{1 \leq i_1 < \dots < i_k \leq n\}$ is the base in \mathcal{M} for the gauge-oriented network $(\mathcal{N}', \mathcal{O}, \mathfrak{l})$. Let \vec{t}_0 be as in the Remark 9.5. Then

(1) *The normalized vacuum vertex wavefunction for (\mathcal{N}', I) is*

$$(96) \quad \hat{\Phi}_{e,I}(\vec{t}) = \begin{cases} \frac{\Phi_{e,\mathcal{O},\mathfrak{l}}(\vec{t})}{\Phi_{e,\mathcal{O},\mathfrak{l}}(\vec{t}_0)}, & \text{for all } e \in \mathcal{E}(I), \quad \forall \vec{t}, \\ e^{\theta_{j_s}(\vec{t}-\vec{t}_0)}, & \text{if } e \text{ is the Darboux sink edge } e_{j_s}, \quad s \in [n-k], \end{cases}$$

see also Figure 46.

(2) The KP vertex wavefunction on (\mathcal{N}', I) is

$$(97) \quad \hat{\Psi}_e(\vec{t}) = \begin{cases} \frac{\Psi_{e, \mathcal{O}, \mathbf{l}}(\vec{t})}{\Psi_{e, \mathcal{O}, \mathbf{l}}(\vec{t}_0)}, & \text{for all } e \in \mathcal{E}, \quad \forall \vec{t}, \\ \frac{\mathfrak{D}^{(k)} e^{i\theta_{i_r}(\vec{t})}}{\mathfrak{D}^{(k)} e^{i\theta_{i_r}(\vec{t}_0)}}, & \text{if } e \text{ is the Darboux source or sink edge } e_{i_r}, \quad r \in [n], \end{cases}$$

see also Figure 47.

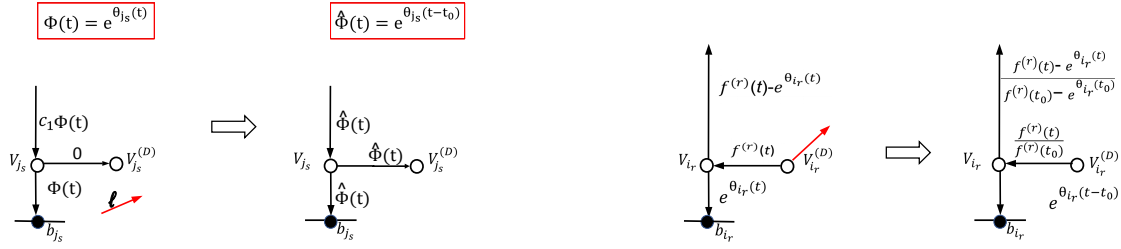


FIGURE 46. Left: At the trivalent white vertex V next to a boundary sink the normalized vacuum v.w. is constant on all edges at V ; at the trivalent white vertex V next to a boundary source [right] the normalized vacuum w.f. takes three distinct values at the edges at V .

We remark that, by construction, both the normalized vacuum vertex wavefunction $\hat{\Phi}(\vec{t})$ and the KP vertex wavefunction $\hat{\Psi}(\vec{t})$ neither depend on the gauge ray direction \mathbf{l} nor on changes of orientation of closed cycles of \mathcal{N}' . The value of the $\hat{\Phi}(\vec{t})$ at a given edge depends on the base I , while the value of the KP vertex wavefunction $\hat{\Psi}(\vec{t})$ does not depend on the base I . In particular, $\hat{\Psi}(\vec{t})$ takes the same value $\frac{\mathfrak{D}^{(k)} e^{i\theta_{\mathbf{l}}(\vec{t})}}{\mathfrak{D}^{(k)} e^{i\theta_{\mathbf{l}}(\vec{t}_0)}}$ at all edges incident either a boundary sink or a boundary source independently of the orientation of \mathcal{N}' (see Figure 47).

Moreover $\hat{\Phi}_e(\vec{t})$ (respectively $\hat{\Psi}_e(\vec{t})$) coincides at both edges at any given bivalent white vertex or at any given (bivalent or trivalent) black vertex, for all times. Finally at any trivalent white vertex $\hat{\Phi}(\vec{t})$ (respectively $\hat{\Psi}(\vec{t})$) takes either the same value at all three edges for all times or distinct values at some $\vec{t} \neq \vec{t}_0$.

9.3. The vacuum wavefunction $\hat{\phi}$ on $\Gamma(\mathcal{N})$. In this section we define the vacuum wavefunction $\hat{\phi}$ on the curve $\Gamma(\mathcal{N}) \equiv \Gamma(\mathcal{N}')$. Let the soliton data $(\mathcal{K}, [A])$ be given, with $\mathcal{K} = \{\kappa_1 < \dots < \kappa_n\}$ and $[A] \in \mathcal{S}_{\mathcal{M}}^{\text{TNN}} \subset Gr^{\text{TNN}}(k, n)$. $(\mathcal{N}, \mathcal{O}, \mathbf{l})$ is a planar bipartite oriented trivalent network for $[A]$ with $g + 1$ faces satisfying Assumption 9.1 and \mathcal{N}' is the modified network defined in

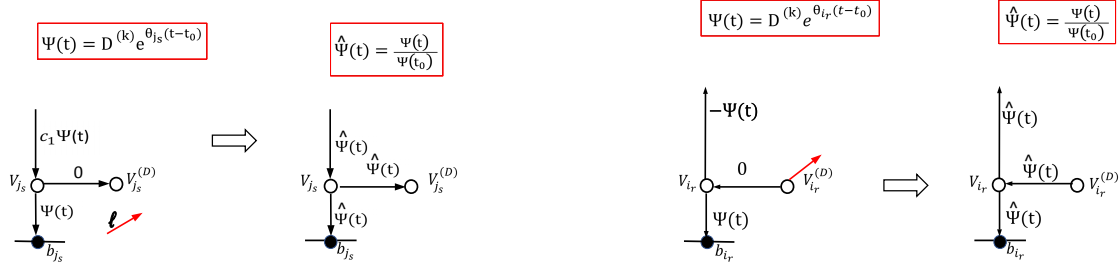


FIGURE 47. The normalized KP wavefunction at the trivalent white vertex V next to a boundary sink [left] or next to a boundary source [right] is constant on all edges at V .

Section 9.1. I is the base in \mathcal{M} associated to \mathcal{O} . Let $\mathcal{D}_{\text{vac}, \mathcal{N}'}$ be the vacuum network divisor of \mathcal{N}' defined in the previous section.

$\Gamma(\mathcal{N}) \equiv \Gamma(\mathcal{N}')$ is the reducible rational curve of Definition 4.1. We remark that there is a bijection between the set of perfect orientations of the network and the set of local coordinates ζ on each component of $\Gamma(\mathcal{N})$ (see Definition 4.2 and Figure 13). For any fixed \mathcal{O} , on the copy Γ_l , $l \in [g + n - k]$, corresponding to the trivalent white vertex V_l , we have four real ordered marked points: $P_m^{(l)}$, $m \in [3]$ corresponding to the edges at V_l , and a vacuum divisor point $P_{\text{vac}}^{(l)}$ such that $\zeta(P_{\text{vac}}^{(l)}) = \gamma_{\text{vac}, V_l}$.

A change in the orientation, induces a change in the local coordinates on the components of $\Gamma(\mathcal{N})$.

Using Corollary 9.3, it is easy to verify that changes of orientation associated to the same base I induce changes of the local coordinates of the four marked points and leave invariant their relative positions, that is each vacuum divisor point belongs to a given oval in both orientations.

On the contrary, Proposition 9.1 and Remark 9.7 imply that a change of orientation associated to a change of base may change the order of the four points since it may move $P_{\text{vac}}^{(l)}$ from the boundary of one oval to the boundary of another oval.

In view of the above remark, we suppose for the rest of the section to have fixed an orientation \mathcal{O} of \mathcal{N}' consistent with the base I and to use local coordinates ζ consistent with \mathcal{O} on each copy of \mathbb{CP}^1 in $\Gamma(\mathcal{N})$ using Definition 4.2. Since we do not discuss the effects of changes of orientation or of base we drop such dependence from the notations of the vacuum wavefunction and the vacuum divisor points.

Using the normalized vacuum v.w. on \mathcal{N}' (see Definition 9.3), we construct a vacuum wavefunction $\hat{\phi}$ on $\Gamma(\mathcal{N})$ generalizing the construction in Definition 6.4 of a vacuum wavefunction on $\Gamma(\mathcal{N}_T)$.

Since, for any fixed \vec{t} , the normalized vacuum vertex wavefunction takes the same value on all the edges at any given bivalent white vertex or bivalent or trivalent black vertex, on the copies of \mathbb{CP}^1 corresponding to such vertices we assign a vacuum wavefunction constant w.r.t. the local coordinate ζ .

If the normalized vacuum vertex wavefunction takes distinct values on the edges at a given trivalent white vertex V_l for some \vec{t} , we construct a unique meromorphic extension $\hat{\phi}$ on the corresponding copy $\Gamma_l = \mathbb{CP}^1$ assigning to $\hat{\phi}(P_m, \vec{t})$ the value of the normalized vacuum vertex wavefunction $\hat{\Phi}_{e_m, I}(\vec{t})$, $m \in [3]$. By construction the local coordinate of the pole of $\hat{\phi}$ on Γ_l is γ_{vac, V_l} .

Therefore, by construction, $\hat{\phi}$ is meromorphic of degree $\mathfrak{d} \leq g$, and the poles belong to the copies $\Gamma_l = \mathbb{CP}^1$ corresponding to trivalent white vertexes V_l carrying non trivial vacuum network divisor numbers on \mathcal{N}' .

We have defined the vacuum network divisor $\mathcal{D}_{\text{vac}, \mathcal{N}'}$. The vacuum wave function $\hat{\phi}(P, \vec{t})$ is regular at all Darboux sinks, therefore in is natural to subtract them from the divisor. Therefore we come to the following Defintuion:

Definition 9.4. *The vacuum divisor $\mathcal{D}_{\text{vac}, \Gamma(\mathcal{N})}$. We denote by $\mathcal{D}_{\text{vac}, \Gamma(\mathcal{N})}$ the following effective divisor: it is the sum of the g simple poles located at the points $P_{\text{vac}}^{(l)}$ different from the Darboux sinks.*

By construction, the vacuum divisor depends on the positions of the Darboux points and on the base I .

Definition 9.5. *The vacuum wavefunction $\hat{\phi}$ on $\Gamma(\mathcal{N})$. We define $\hat{\phi}(P, \vec{t})$ on $\Gamma(\mathcal{N}) \setminus \{P_0\}$ as follows:*

(1) *The restriction of $\hat{\phi}$ to Γ_0 is denoted $\hat{\phi}_0$ and is the normalized Sato vacuum wavefunction*

$$\hat{\phi}_0(\zeta, \vec{t}) = e^{\theta(\vec{t} - \vec{t}_0)}, \quad \theta(\vec{t}) = \sum_{l \geq 1} \zeta^l t_l.$$

(2) *Let Σ_l be the component of Γ corresponding to a given internal black vertex V_l' and let us denote $\hat{\phi}'_l(P, \vec{t})$ the restriction of $\hat{\phi}$ to Σ_l . Then, for any $P \in \Sigma_l$, $\hat{\phi}'_l(P, \vec{t})$ takes the value*

of the normalized vertex function $\hat{\Phi}_{e,I}(\vec{t})$, where e is one of the edges at V_l' :

$$\hat{\phi}'_l(\zeta(P), \vec{t}) = \hat{\Phi}_{e,I}(\vec{t}), \quad \forall \vec{t};$$

(3) Let Γ_l be the component of Γ corresponding to V_l , which is either a bivalent white vertex or a trivalent white vertex with normalized vacuum v.w. coinciding on all edges at V_l (in the latter case $\gamma_{\text{vac},V_l} \in \mathcal{D}_{\text{vac},\mathcal{N}',I}$ is a trivial vacuum network divisor number). Let us denote $\hat{\phi}_l(P, \vec{t})$ the restriction of $\hat{\phi}$ to Γ_l . Then, for any $P \in \Gamma_l$, $\hat{\phi}_l(P, \vec{t})$ takes the value of the normalized vertex function $\hat{\Phi}_{e,I}(\vec{t})$, where e is one of the edges at V_l :

$$\hat{\phi}'_l(\zeta(P), \vec{t}) = \hat{\Phi}_{e,I}(\vec{t}), \quad \forall \vec{t};$$

(4) Let Γ_l be the component of Γ corresponding to a trivalent white vertex with normalized vacuum v.w. taking distinct values on the edges at V_l for some $\vec{t} \neq \vec{t}_0$ (i.e. $\gamma_{\text{vac},V_l} \in \mathcal{D}_{\text{vac},\mathcal{N}',I}$ is a non trivial vacuum network divisor numbers). Let us denote $\hat{\phi}_l(P, \vec{t})$ the restriction of $\hat{\phi}$ to Γ_l . Then $\hat{\phi}_l$ is meromorphic of degree one in $P \in \Gamma_l$ and is uniquely identified by the conditions

$$\hat{\phi}_l(\zeta(P_l^{(m)}), \vec{t}) = \hat{\Phi}_{e_m,I}(\vec{t}), \quad m \in [3], \quad \forall \vec{t},$$

where e_m , $m \in [3]$ are the edges at V_l :

$$(98) \quad \hat{\phi}_l(\zeta(P), \vec{t}) = \frac{\hat{\Phi}_{e_3,I}(\vec{t})\zeta - \gamma_{\text{vac},V_l}\hat{\Phi}_{e_1,I}(\vec{t})}{\zeta - \gamma_{\text{vac},V_l}},$$

with γ_{vac,V_l} as in (87).

By construction, for any \vec{t} , $(\phi_{\text{vac}}(P, \vec{t})) + \mathcal{D}_{\text{vac},\Gamma(\mathcal{N})} \geq 0$ since the $n - k$ divisor points $\mathcal{D}_{\text{vac},\mathcal{N}'}$ at the Darboux sink points are trivial. Moreover by construction $\mathcal{D}_{\text{vac},\Gamma(\mathcal{N})}$ is contained in the union of all ovals. In the following Theorem we summarize the properties of the vacuum wavefunction directly following from its definition and provide the first step of the proof of Theorem 4.1 on $\Gamma(\mathcal{N})$.

Theorem 9.1. Characterization of the vacuum divisor of $\hat{\phi}$ on $\Gamma(\mathcal{N})$. Let $\hat{\phi}$, $\mathcal{D}_{\text{vac},\mathcal{N}'}$, $\mathcal{D}_{\text{vac},\Gamma(\mathcal{N})}$ on $\Gamma(\mathcal{N})$ be as in Definition 9.5. Then on each Γ_l , $l \in [g + n - k]$ corresponding to a trivalent white vertex the vacuum wavefunction satisfies

$$\hat{\phi}_l(\zeta(P), \vec{t}) = \frac{(-1)^{\text{wind}(e_3,e_1)}\Phi_{e_1}(\vec{t})(\zeta - 1) + (-1)^{\text{wind}(e_3,e_2)}\Phi_{e_2}(\vec{t})\zeta}{((-1)^{\text{wind}(e_3,e_1)}\Phi_{e_1}(\vec{t}_0) + (-1)^{\text{wind}(e_3,e_2)}\Phi_{e_2}(\vec{t}_0))(\zeta - \gamma_{\text{vac},V_l})}, \quad \forall P \in \Gamma_l, \quad \forall \vec{t}.$$

Moreover $\hat{\phi}$ satisfies the following properties of Definition 4.4 on $\Gamma \setminus \{P_0\}$.

- (1) At $\vec{t} = \vec{t}_0$ $\hat{\phi}(P, \vec{t}_0) = 1$ at all points $P \in \Gamma \setminus \{P_0\}$;
- (2) The restriction of $\hat{\phi}$ to $\Gamma_0 \setminus \{P_0\}$ coincides with the following normalization of Sato's wavefunction, $\hat{\phi}(\zeta(P), \vec{t}) = e^{\theta(\zeta, \vec{t} - \vec{t}_0)}$, where $\theta(\zeta, \vec{t}) = \sum_{l \geq 1} t_l \zeta^l$;
- (3) $\hat{\phi}(\zeta(P), \vec{t})$ is real for real values of the local coordinate ζ and for all real \vec{t} on each component of Γ ;
- (4) $\hat{\phi}$ takes compatible values at pairs of glued points $P, Q \in \Gamma$, for all \vec{t} : $\hat{\phi}(P, \vec{t}) = \hat{\phi}(Q, \vec{t})$;
- (5) $\hat{\phi}(P_{i_r}^{(3)}, \vec{t}) \equiv f^{(r)}(\vec{t})$ at each Darboux source point $P_{i_r}^{(3)}$, $r \in [k]$, for all \vec{t} , where $f^{(r)}(\vec{t}) = \sum_{j=1}^N A_j^i e^{\theta_j(\vec{t} - \vec{t}_0)}$ is r -th heat hierarchy solution associated to the I-RREF representative matrix in $[A]$;
- (6) $\hat{\phi}(\zeta, \vec{t})$ is either constant or meromorphic of degree one w.r.t. to the spectral parameter on each copy of \mathbb{CP}^1 corresponding to a trivalent white vertex of \mathcal{N} or to a boundary source or sink vertex V_l , $l \in [n]$;
- (7) $\hat{\phi}(\zeta, \vec{t})$ is constant w.r.t. to the spectral parameter on each other copy of \mathbb{CP}^1 ;
- (8) For any \vec{t} , $(\hat{\phi}(P, \vec{t})) + \mathcal{D}_{\text{vac}, \Gamma(\mathcal{N})} \geq 0$.
- (9) In the special case of the Le-network $\mathcal{N} = \mathcal{N}_T$ the divisor of poles of $\hat{\phi}(\zeta, \vec{t})$ for generic \vec{t} coincides with $\mathcal{D}_{\text{vac}, \Gamma(\mathcal{N}_T)}$;
- (10) The vacuum divisor $\mathcal{D}_{\text{vac}, \Gamma(\mathcal{N})}$ is contained in the union of the boundaries of all ovals.

The proof of the assertions is straightforward and is omitted. To complete the proof of Theorem 4.1 we must count the number of divisor points at each oval. We do this in Section 10.

9.4. The KP wavefunction $\hat{\psi}$ on $\Gamma(\mathcal{N})$ and the proof of Theorem 4.2. In this section we define the KP wavefunction $\hat{\psi}$ on the curve $\Gamma(\mathcal{N})$. $(\mathcal{K}, [A])$, $(\mathcal{N}, \mathcal{O}, \mathfrak{t})$, \mathcal{N}' , I are as in the previous section. $\mathcal{D}_{\text{dr}, \mathcal{N}'}$ is the dressed divisor of \mathcal{N}' of Definition 9.2.

In this case, for any fixed \mathcal{O} , on the copy Γ_l , $l \in [g + n - k]$, corresponding to the trivalent white vertex V_l , we have four real ordered marked points: $P_m^{(l)}$, $m \in [3]$ corresponding to the ordered edges at V_l , and the dressed divisor point $P_{\text{dr}}^{(l)}$ with local coordinate γ_{dr, V_l} .

A change in the orientation, induces a change in the local coordinates on the components of $\Gamma(\mathcal{N})$. By Corollary 9.2, it is easy to verify that **any** change of orientation in \mathcal{N}' induces changes of the local coordinates of the four marked points and leaves invariant their relative positions, that is each dressed divisor point belongs to a given oval in all orientations of \mathcal{N}' .

In view of the above remark, we suppose for the rest of the section to have fixed an orientation \mathcal{O} of \mathcal{N}' and to use local coordinates ζ consistent with \mathcal{O} on each copy of \mathbb{CP}^1 in $\Gamma(\mathcal{N})$ using Definition 4.2.

Definition 9.6. *The KP divisors on $\Gamma(\mathcal{N})$. The effective KP divisor $\mathcal{D}_{\text{KP},\Gamma}$ is a sum of g simple poles, namely*

- (1) k poles on Γ_0 coinciding with the Sato divisor at $\vec{t} = \vec{t}_0$.
- (2) $g-k$ poles $P_{\text{dr}}^{(l)}$ on the copies of \mathbb{CP}^1 , associated with trivalent white vertexes V_l containing neither Darboux source nor Darboux sink edges. The point $P_{\text{dr}}^{(l)} \in \Gamma_l$ in the local coordinate ζ induced by orientation \mathcal{O} satisfies: $\zeta(P_{\text{dr}}^{(l)}) = \gamma_{\text{dr},V_l}$.

Using the KP vertex wavefunction on \mathcal{N}' (see Definition 9.3), we construct a KP wavefunction $\hat{\psi}$ on $\Gamma(\mathcal{N})$.

Since, for any fixed \vec{t} , the KP vertex wavefunction takes the same value on all the edges at any given bivalent white vertex or bivalent or trivalent black vertex, on the copies of \mathbb{CP}^1 corresponding to such vertices we assign a KP wavefunction constant w.r.t. the local coordinate ζ .

If the KP vertex wavefunction takes distinct values on the edges at a given trivalent white vertex V_l for some \vec{t} , we construct a unique meromorphic extension $\hat{\psi}$ on the corresponding copy $\Gamma_l = \mathbb{CP}^1$ assigning to $\hat{\psi}(P_m, \vec{t})$ the value of the KP vertex wavefunction $\hat{\Psi}_{e_m, I}(\vec{t})$, $m \in [3]$. By construction the local coordinate of the pole of $\hat{\psi}$ on Γ_l is γ_{dr,V_l} .

If the KP vertex wave function takes the same value on all edges at a given trivalent white vertex V_l for all \vec{t} , we assign to $\hat{\psi}(P, \vec{t}) \equiv \hat{\psi}(P_m, \vec{t})$. In particular, this occurs at the n copies of \mathbb{CP}^1 associated to the Darboux sink and source edges.

By construction, at each double point corresponding to an edge ending either at a boundary source or a boundary sink the KP wavefunction satisfy the compatibility condition and coincides for all times with the normalized Sato wavefunction, computed for the corresponding phase.

Therefore, by construction, $\hat{\phi}$ is meromorphic of degree $\mathfrak{d}_{\text{KP}} \leq g$, and the poles belong to $\mathcal{D}_{\text{KP},\Gamma}$.

Definition 9.7. *The KP wavefunction ψ on $\Gamma(\mathcal{N}')$. We define the KP wavefunction $\hat{\psi}(P, \vec{t})$ on $\Gamma(\mathcal{N}) \setminus \{P_0\}$ as follows:*

(1) The restriction of $\hat{\psi}$ to Γ_0 is denoted $\hat{\psi}_0$ and is the normalized dressed Sato wavefunction

$$\hat{\psi}_0(\zeta, \vec{t}) = \frac{\mathfrak{D}^{(k)} \hat{\phi}_0(\zeta, \vec{t})}{\mathfrak{D}^{(k)} \hat{\phi}_0(\zeta, \vec{t}_0)}.$$

(2) Let Σ_l be the component of Γ corresponding to a given internal black vertex V_l' and let us denote $\hat{\psi}'_l(P, \vec{t})$ the restriction of $\hat{\psi}$ to Σ_l . Then, for any $P \in \Sigma_l$, $\hat{\psi}'_l(P, \vec{t})$ takes the value of the KP vertex wavefunction $\hat{\Psi}_{e,I}(\vec{t})$, where e is one of the edges at V_l' :

$$\hat{\psi}'_l(\zeta(P), \vec{t}) = \hat{\Psi}_{e,I}(\vec{t}), \quad \forall \vec{t};$$

(3) Let Γ_l be the component of Γ corresponding to V_l , which is either a bivalent white vertex or a trivalent white vertex with KP v.w. coinciding on all edges at V_l . Let us denote $\hat{\psi}_l(P, \vec{t})$ the restriction of $\hat{\psi}$ to Γ_l . Then, for any $P \in \Gamma_l$, $\hat{\psi}_l(P, \vec{t})$ takes the value $\hat{\Phi}_{e,I}(\vec{t})$, where e is one of the edges at V_l :

$$\hat{\psi}_l(\zeta(P), \vec{t}) = \hat{\Phi}_{e,I}(\vec{t}), \quad \forall \vec{t};$$

(4) Let Γ_l be the component of Γ corresponding to a trivalent white vertex with KP v.w. taking distinct values on the edges at V_l for some $\vec{t} \neq \vec{t}_0$. Let us denote $\hat{\psi}_l(P, \vec{t})$ the restriction of $\hat{\psi}$ to Γ_l . Then $\hat{\psi}_l$ is meromorphic in $P \in \Gamma_l$ and is uniquely identified by the conditions

$$\hat{\psi}_l(\zeta(P_l^{(m)}), \vec{t}) = \hat{\Psi}_{e_m, \circ}(\vec{t}), \quad m \in [3], \quad \forall \vec{t},$$

where e_m , $m \in [3]$ are the edges at V_l :

$$(99) \quad \hat{\psi}_l(\zeta(P), \vec{t}) = \frac{\hat{\Psi}_{e_3, I}(\vec{t}) \zeta - \gamma_{\text{dr}, V_l} \hat{\Psi}_{e_1, I}(\vec{t})}{\zeta - \gamma_{\text{dr}, V_l}},$$

with γ_{dr, V_l} as in (88).

By construction, $\mathcal{D}_{\text{KP}, \Gamma}$ is contained in the union of all ovals. Moreover

$$\hat{\psi}(P, \vec{t}) = \frac{\mathfrak{D}^{(k)} \hat{\phi}(P, \vec{t})}{\mathfrak{D}^{(k)} \hat{\phi}(P, \vec{t}_0)}, \quad \forall P \in \Gamma \setminus \{P_0\}, \quad \forall \vec{t},$$

so that $\hat{\psi}$ is the KP wavefunction for the soliton data $(\mathcal{K}, [A])$ on $\Gamma = \Gamma(\mathcal{N})$ provided that Theorem 4.1 holds true.

Theorem 9.2. Characterization of divisor of $\hat{\psi}$ on $\Gamma(\mathcal{N})$. Let $\hat{\psi}$, $\mathcal{D}_{\text{dr}, \mathcal{N}'}$, $\mathcal{D}_{\text{KP}, \Gamma}$ on $\Gamma(\mathcal{N})$ be as in Definition 9.7. Then on each Γ_l , $l \in [g+n-k]$ corresponding to a trivalent white vertex the KP wavefunction satisfies

$$\hat{\psi}_l(\zeta(P), \vec{t}) = \frac{(-1)^{\text{wind}(e_3, e_1)} \Psi_{e_1}(\vec{t})(\zeta - 1) + (-1)^{\text{wind}(e_3, e_2)} \Psi_{e_2}(\vec{t}) \zeta}{((-1)^{\text{wind}(e_3, e_1)} \Psi_{e_1}(\vec{t}_0) + (-1)^{\text{wind}(e_3, e_2)} \Psi_{e_2}(\vec{t}_0))(\zeta - \gamma_{\text{dr}, V_l})}, \quad \forall P \in \Gamma_l, \quad \forall \vec{t}.$$

Moreover $\hat{\psi}$ satisfies the following properties of Definition 3.3 on $\Gamma \setminus \{P_0\}$.

- (1) At $\vec{t} = \vec{t}_0$ $\hat{\psi}(P, \vec{t}_0) = 1$ at all points $P \in \Gamma \setminus \{P_0\}$;
- (2) $\hat{\psi}(\zeta(P), \vec{t})$ is real for real values of the local coordinate ζ and for all real \vec{t} on each component of Γ ;
- (3) $\hat{\psi}$ takes compatible values at pairs of glued points $P, Q \in \Gamma$, for all \vec{t} : $\hat{\psi}(P, \vec{t}) = \hat{\psi}(Q, \vec{t})$;
- (4) $\hat{\psi}(\zeta, \vec{t})$ is constant w.r.t. to the spectral parameter on each copy of \mathbb{CP}^1 corresponding to a boundary source or sink vertex V_l , $l \in [n]$;
- (5) $\hat{\psi}(\zeta, \vec{t})$ is either constant or meromorphic of degree one w.r.t. to the spectral parameter on each copy of \mathbb{CP}^1 corresponding to any other trivalent white vertex of \mathcal{N} . $\hat{\phi}(\zeta, \vec{t})$ is constant w.r.t. to the spectral parameter on each other copy of \mathbb{CP}^1 ;
- (6) $\mathcal{D}_{\text{KP}, \Gamma} + (\hat{\psi}(P, \vec{t})) \geq 0$ for all \vec{t} .
- (7) In the special case of the Le-network $\mathcal{N} = \mathcal{N}_T$ the divisor of poles of $\hat{\psi}(P, \vec{t})$ coincides with $\mathcal{D}_{\text{KP}, \Gamma}$ for almost all \vec{t} ;
- (8) The $\mathcal{D}_{\text{KP}, \Gamma}$ divisor is contained in the union of the boundaries of all ovals.

The proof of the assertions is straightforward and is omitted. We now prove Theorem 4.2

Theorem 9.3. (Theorem 4.2). *Let us denote ζ_s , $s = 1, 2$, the local coordinates on the components of $\Gamma(\mathcal{N})$ respectively for orientations \mathcal{O}_1 and \mathcal{O}_2 of \mathcal{N}' . For any given trivalent white vertex, V_l , let $e_m^{(s)}$, $m \in [3]$, $s = 1, 2$ the edges at V_l , where $e_3^{(s)}$ is the unique edge pointing inwards at V_l in orientation \mathcal{O}_s . Let $P_m^{(s)}$ be the marked point on Γ_l corresponding to $e_m^{(s)}$.*

Then the following holds:

- (1) *If all edges at V_l have the same versus in both orientations, then $P_m^{(2)} = P_m^{(1)}$, $m \in [3]$, the local coordinates on Γ_l are the same $\zeta_1 = \zeta_2$ and (93) implies that the divisor point on Γ_l is the same and has the same coordinate*

$$\zeta_2(P_{\text{dr}}^{(l)}) = \zeta_1(P_{\text{dr}}^{(l)});$$

- (2) *If at V_l we change orientation of edges from $(e_1^{(1)}, e_2^{(1)}, e_3^{(1)})$ to $(e_2^{(2)}, e_3^{(2)}, e_1^{(2)})$ (see Figure 45[left]), then $P_m^{(2)} = P_{m-1}^{(1)}$ induces the change of coordinate $\zeta_2 = (1 - \zeta_1)^{-1}$ on Γ_l . Therefore (94) implies that the divisor point on Γ_l is the same and its local coordinates changes as*

$$\zeta_2(P_{\text{dr}}^{(l)}) = (1 - \zeta_1(P_{\text{dr}}^{(l)}))^{-1};$$

(3) If at V_l we change orientation of edges from $(e_1^{(1)}, e_2^{(1)}, e_3^{(1)})$ to $(e_3^{(2)}, e_1^{(2)}, e_2^{(2)})$ (see Figure 45[right]), then $P_m^{(2)} = P_{m+1}^{(1)}$ induces the change of coordinate $\zeta_2 = \zeta_1/(\zeta_1 - 1)$ on Γ_l . Therefore (95) implies that the divisor point on Γ_l is the same and its local coordinate changes as

$$\zeta_2(P_{\text{dr}}^{(l)}) = \frac{\zeta_1(P_{\text{dr}}^{(l)})}{\zeta_1(P_{\text{dr}}^{(l)}) - 1}.$$

The proof follows directly from the definition of the KP wavefunction on $\Gamma(\mathcal{N})$ and Corollary 9.2.

Remark 9.9. Relation with the construction in [2]. In the case $[A] \in Gr^{TP}(k, n)$, Theorem 4.2 applies also for the KP divisor points in $\Gamma(\xi)$ at **leading order in ξ** since they may be obtained from the dressed divisor points of Definition 9.2 using the change of coordinates associated to the orientations of the networks introduced in Remark 9.8, in agreement with Corollary 9.2.

10. THE COMBINATORIAL CHARACTERIZATION OF THE REALITY AND REGULARITY CONDITIONS FOR BOTH THE VACUUM AND THE KP DIVISORS.

In this section we show that the position of each divisor (vacuum or KP) point in the intersection of Γ_l with the ovals is determined by an index of each pair of the edges at the corresponding trivalent white vertex V_l and we use such index to complete the proof of Theorem 4.1.

Using the indexes it is also possible to directly compute the position of the KP divisor in each oval and prove that we have one divisor point at each finite oval. Indeed we have introduced the vacuum wavefunction to obtain the KP divisor using the dressing.

In the following a, b, c denote either the edge at V_l or the corresponding marked point on Γ_l , w_a is the weight of a , f_{ab} is the face of \mathcal{N} bounded by the edges a, b and Ω_{ab} is the corresponding oval in $\Gamma(\mathcal{N})$ (see also Figure 48).

In this section we use the network divisor numbers defined on \mathcal{N}' . Let us recall the definition of the (vacuum or dressed) network divisor number associated to V_l . Let $\Psi_s = \Psi_{s, \mathcal{N}, \mathcal{O}, \Gamma}(\vec{t}_0)$, be either the vacuum or the dressed vertex wavefunction at the edges $s = a, b, c$ of a given trivalent white vertex V_l as in Definition 9.1.

Then the linear relation at V_l is

$$\Psi_c = (-1)^{\text{int}(c)} w_c \left((-1)^{\text{wind}(a,c)} \Psi_a + (-1)^{\text{wind}(b,c)} \Psi_b \right),$$

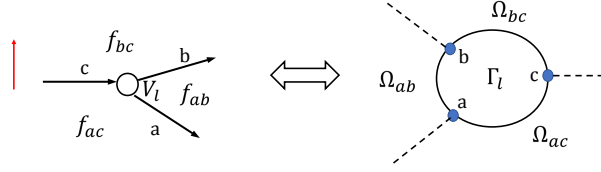


FIGURE 48. The correspondence between faces at V_l and ovals bounded by Γ_l . The red line is the line orthogonal to the line containing boundary source and sink vertexes, w.r.t. which we reflect the graph to construct the curve.

and the (vacuum or KP) divisor point in the local coordinates induced by the orientation of \mathcal{N}' is

$$(100) \quad \begin{aligned} \gamma &= \frac{(-1)^{\text{wind}(a,c)} \Psi_a}{(-1)^{\text{wind}(a,c)} \Psi_a + (-1)^{\text{wind}(b,c)} \Psi_b} = w_c (-1)^{\text{int}(c) + \text{wind}(a,c)} \frac{\Psi_a}{\Psi_c} \\ &= \left(1 + (-1)^{\text{wind}(a,c) + \text{wind}(b,c)} \frac{\Psi_b}{\Psi_a} \right)^{-1} = 1 - w_c (-1)^{\text{int}(c) + \text{wind}(b,c)} \frac{\Psi_b}{\Psi_c} \end{aligned}$$

To each pair of edges f, g at a white or black vertex V_l we assign the following indexes:

- (1) **Index of change of direction** $\epsilon_{cd}(f, g)$: it marks the fact that both edges at the vertex V_l are pointing outwards or inwards:

$$\epsilon_{cd}(f, g) = \begin{cases} 1 & \text{if both } f, g \text{ point outwards at the white vertex } V_l, \\ 1 & \text{if both } f, g \text{ point inwards at the black vertex } V_l, \\ 0 & \text{otherwise.} \end{cases}$$

- (2) **Index of change of sign** $\epsilon_{cs}(f, g)$: it marks the sign of the product of the (vacuum or dressed) wavefunction $\Psi_f \Psi_g$ at the corresponding marked points $f, g \in \Gamma_l$:

$$\epsilon_{cs}(f, g) = \begin{cases} 1 & \text{if } \Psi_f \Psi_g < 0, \\ 1 & \text{if } \Psi_f \Psi_g = 0 \text{ and } \Psi_f + \Psi_g < 0, \\ 0 & \text{otherwise.} \end{cases}$$

- (3) **Index of intersection** $\epsilon_{int}(f, g)$: it marks the number of intersections with gauge rays with edges pointing inward at V_l :

$$\epsilon_{int}(f, g) = \begin{cases} \text{int}(f) & \text{if } f \text{ points inwards at } V_l, \\ \text{int}(g) & \text{if } g \text{ points inwards at } V_l, \\ \text{int}(f) + \text{int}(g) & \text{if both } f, g \text{ point inwards at } V_l, \\ 0 & \text{otherwise.} \end{cases}$$

- (4) **Index of winding** $\epsilon_{wind}(f, g)$: it is the winding of the pair (f, g) if one of the edges points inwards and the other outwards at V_l , otherwise it is the sum of the winding indexes at V_l :

$$\epsilon_{wind}(f, g) = \begin{cases} \text{wind}(f, g) & \text{if one edge points inwards and the other outwards,} \\ \text{wind}(f, h) + \text{wind}(g, h) & \text{if } \epsilon_{cd}(f, g) = 1 \text{ and } h \text{ is the third edge at } V_l. \end{cases}$$

The following Lemma explains the relations among such indexes at each vertex.

Lemma 10.1. *Relations among the indexes of a pair of edges at a vertex. Let (f, g) be a pair of edges at the vertex V_l and let $\epsilon_{cd}(f, g)$, $\epsilon_{wind}(f, g)$, $\epsilon_{int}(f, g)$, $\epsilon_{cs}(f, g)$ as above and let us define the total index at (f, g) , $\epsilon_{tot}(f, g)$ as*

$$(101) \quad \epsilon_{tot}(f, g) = \epsilon_{cd}(f, g) + \epsilon_{cs}(f, g) + \epsilon_{int}(f, g) + \epsilon_{wind}(f, g).$$

Then the following holds true:

- (1) *If V_l is a bivalent vertex then*

$$(102) \quad \epsilon_{cs}(f, g) = \epsilon_{wind}(f, g) + \epsilon_{int}(f, g) \pmod{2}, \quad \epsilon_{tot}(f, g) = 0 \pmod{2};$$

- (2) *If V_l is a trivalent black vertex then*

$$(103) \quad \epsilon_{cs}(f, g) = \epsilon_{wind}(f, g) + \epsilon_{int}(f, g) \pmod{2}, \quad \epsilon_{tot}(f, g) = \epsilon_{cd}(f, g) \pmod{2};$$

The proof of the lemma follows directly from the definitions of the indexes and the linear relations at the vertexes. We illustrate it in Figures 49 and 50.

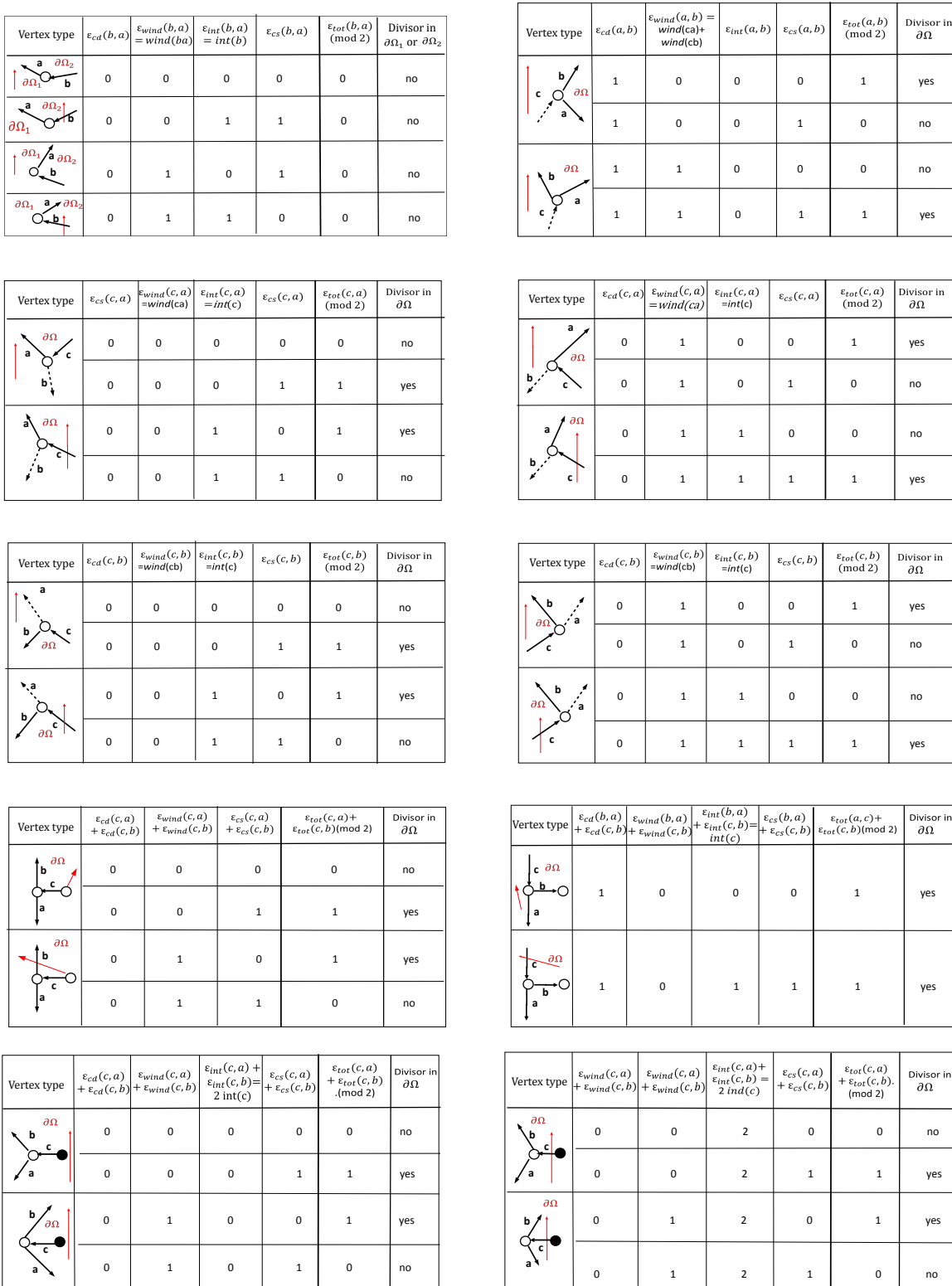


FIGURE 49. We associate an index ϵ_{tot} to each pair of edges at a white vertex. For simplicity we denote with the same symbol $\partial\Omega$ both the boundary of the face in \mathcal{N}' and the corresponding boundary of the oval in Γ . The divisor point associated to the vertex V_i belongs to $\partial\Omega \cap \Gamma_i$ if the corresponding face is bounded by a pair of edges at V_i with odd index.

Vertex type	$\epsilon_{cd}(b, c)$	$\epsilon_{wind}(b, c)$ = $wind(b, c)$	$\epsilon_{int}(b, c)$ = $int(b)$	$\epsilon_{cs}(b, c)$	$\epsilon_{tot}(b, c) \pmod 2$
	0	1	0	1	0
	0	1	1	0	0
	0	0	0	0	0
	0	0	1	1	0

Vertex type	$\epsilon_{cd}(a, b)$	$\epsilon_{wind}(a, b) = w(a, c) + w(b, c)$	$\epsilon_{int}(a, b) = int(a) + int(b)$	$\epsilon_{cs}(a, b)$	$\epsilon_{tot}(a, b) \pmod 2$
	1	0	0	0	1
	1	1	0	1	1
	1	0	1	1	1
	1	1	1	0	1

FIGURE 50. We associate an index ϵ_{tot} to each pair of edges at a black vertex. For simplicity we denote with the same symbol $\partial\Omega$ both the boundary of the face in \mathcal{N}' and the corresponding boundary of the oval in Γ .

We now discuss the position of vacuum or dressed divisor points in the ovals of Γ . We recall that \vec{t}_0 has been fixed so that the vacuum (resp. dressed) vertex wavefunction is equal to zero only at the edges corresponding to Darboux sink points (resp. all Darboux points) on Γ .

Any trivalent white vertex bounds either two or three faces by construction (see Figure 49). Using the definition of divisor point (see formula (100)) and Figure 49, it is evident that the intersection of an oval $\partial\Omega_s$ with a component Γ_l contains a vacuum or dressed divisor point if and only if the total index of the corresponding pair of edges at V_l bounding the face F_s in \mathcal{N}' is odd.

Vertex type	$\epsilon_{cd}(e_j, e_{j+1})$	$\epsilon_{wind}(e_j, e_{j+1})$	$\epsilon_{int}(e_j, e_{j+1})$	$\epsilon_{cs}(e_j, e_{j+1})$	$\epsilon_{tot}(e_j, e_{j+1})$	Divisor in $\partial\Omega \cap \Gamma_0$
	0	0	0	0	0	no
	0	0	0	1	1	yes

FIGURE 51. We associate an index ϵ_{tot} to each pair of consecutive edges at the boundary of the disk. For simplicity we use the same symbols $\partial\Omega$ (resp. Γ_0) to denote both the boundary of the face in \mathcal{N}' and the corresponding boundary of the oval in Γ (resp. the boundary of the disk in \mathcal{N}' and the corresponding Sato component in Γ). In Corollary ... we prove that a Sato divisor point belongs to $\partial\Omega \cap \Gamma_0$ if and only if Ω is a finite oval and the wavefunction changes of sign at the corresponding edges in \mathcal{N}' .

To complete the characterization of the positions of KP divisor points, we must include the Sato divisor. Let F_s be the face in \mathcal{N}' corresponding to the oval Ω_s . If the boundary of the face F_s contains portions of the boundary of the disk we need to add the contribution coming from the boundary (see Figure 51). In our counting rule, the boundary of the disk is oriented clockwise.

For simplicity, we suppose that all edges ending at a boundary vertex are parallel. Finally by construction the intersection index at each such edge is zero. Each portion of the boundary of the disk bounding the given face is marked by two consecutive boundary vertexes b_j, b_{j+1} and we assign an index to each such pair. In the case of the vacuum divisor, $\epsilon_{cs}(b_j, b_{j+1}) = 0$ by definition and there is no divisor point on $\Gamma_0 \cap \Omega_s$. In the case of the dressed vertex wavefunction, let $e(b_j), e(b_{j+1})$ respectively be the edges at b_j, b_{j+1} . Then $\Psi_{e(b_j)}(\vec{t}_0)\Psi_{e(b_{j+1})}(\vec{t}_0) < 0$ implies that there is an odd number of Sato divisor point in $\Gamma_0 \cap \Omega_s$, while $\Psi_{e(b_j)}(\vec{t}_0)\Psi_{e(b_{j+1})}(\vec{t}_0) > 0$ implies that there is an even number of Sato divisor points belonging to the interval $] \kappa_j, \kappa_{j+1}[$. We show below that the number of Sato divisor points at each finite edge b_j, b_{j+1} is, indeed, zero or one.

We summarize the above discussion in the following statement.

Theorem 10.1. *Characterization of position of vacuum or dressed divisor points in the ovals* Let (e_1, e_2) be the pair of edges at the trivalent white vertex V_l bounding the face F_s in \mathcal{N}' and let P_1, P_2 be the corresponding marked points in the component Γ_l bounding the oval Ω_s in $\Gamma(\mathcal{N})$. Let ζ be the local coordinate on Γ_l induced by the orientation of \mathcal{N}' and, to fix notations, suppose that $\zeta(P_1) < \zeta(P_2)$. Let γ_l be the (vacuum or dressed) network divisor number for V_l . Then the correspondent divisor point $\bar{P}^{(l)}$ belongs to $\Omega_s \cap \Gamma_l$, that is $\zeta(\bar{P}^{(l)}) = \gamma_l \in [\zeta(P_1), \zeta(P_2)]$, if and only if $\epsilon_{tot}(e_1, e_2)$ is odd:

$$\epsilon_{tot}(e_1, e_2) = 1 \pmod{2} \iff P^{(l)} \in \partial\Omega_s \cap \Gamma_l.$$

Remark 10.1. Here we use the cyclic order on real part of \mathbb{CP}^1 , therefore $\zeta(P_1) = \infty$, and $\zeta(P_2) = 0$, then $\zeta(P_1) < \zeta(P_2)$ in our notations.

In the following Lemma we give relations among the indexes inside a given oval which will be used to complete the proof of Theorem 4.1 in the general case.

Lemma 10.2. Let $\Omega_s, s \in [0, g]$ be an oval and let F_s be the corresponding face of \mathcal{N}' . Let n_s be the total number of pair of edges at internal vertexes bounding F_s and denote $(V_l; f_l, g_l), l \in [n_s]$, the triples of vertexes V_l and pair of edges (f_l, g_l) at V_l bounding F_s . Let m_s be the number of pair of edges $(e_{b_{j_r}}, e_{b_{j_r+1}}), r \in [m_s]$, ending at the boundary of the disk and bounding F_s . Let $\mu_{s,sou}, \mu_{s,si}$ respectively be the number of univalent white vertexes corresponding to Darboux boundary sources or sinks and belonging to F_s , and let us denote $\rho_s \leq m_s$ the total number of changes of signs of the wavefunction occurring at the edges of F_s ending at the boundary of the disk. Then

(1) For any $s \in [g]$ (finite oval)

$$\begin{aligned}
 (104) \quad & \mu_{s,si} + \sum_{l=1}^{n_s} \epsilon_{wind}(f_l, g_l) + \sum_{\substack{l=1 \\ v_l \text{ white}}}^{n_s} \epsilon_{cd}(f_l, g_l) = 1 \pmod{2}, \\
 & \mu_{s,sou} + \sum_{l=1}^{n_s} \epsilon_{int}(f_l, g_l) = 0 \pmod{2}, \\
 & \rho_s + \sum_{l=1}^{n_s} \epsilon_{cs}(f_l, g_l) = 0 \pmod{2}.
 \end{aligned}$$

(2) If $s = 0$ (infinite oval)

$$\begin{aligned}
 (105) \quad & \mu_{0,si} + \sum_{l=1}^{n_0} \epsilon_{wind}(f_l, g_l) + \sum_{\substack{l=1 \\ v_l \text{ white}}}^{n_0} \epsilon_{cd}(f_l, g_l) = 0 \pmod{2}, \\
 & \mu_{0,sou} + k + \sum_{l=1}^{n_0} \epsilon_{int}(f_l, g_l) = 0 \pmod{2}, \\
 & \rho_0 + \sum_{l=1}^{n_0} \epsilon_{cs}(f_l, g_l) = 0 \pmod{2}.
 \end{aligned}$$

Proof. The only untrivial statement is the first one in both (104) and (105). We prove the statement by induction in the number of trivalent white vertexes changing direction.

First of all let F_s be an internal face of the network \mathcal{N}' , i.e. a face whose boundary does not contain portions of the boundary of the disk. If there are no internal sources or sinks in F_s and no changes of directions at the vertexes bounding F_s then the statement holds true since the total winding number of the face is an odd number

$$\sum_{l=1}^{n_s} \epsilon_{wind}(f_l, g_l) = 1 \pmod{2}.$$

Now suppose to insert a change of direction in F_s along the path $\pi = (e_i, e_{i+1}, \dots, e_{j-1}, e_j)$ changing all directions of the edges e_r , $r \in [i+1, j-1]$ (see Figure 52[left]). Then the winding of F_s will change by one:

$$\sum_{r=i}^{j-1} (\epsilon_{wind}(e_r, e_{r+1}) - \epsilon_{wind}(e'_r, e'_{r+1})) = 1 \pmod{2}.$$

If the oval F_s intersects the boundary of the disk, then each boundary sink edge in F_s increases by one the counter of the trivalent white vertexes changing of direction and keeps the winding of F_s invariant. If we move a boundary source edge from F_s to the other face, then the overall contribution from the edges at such vertex due to winding and changes of direction is the same at each face before and after such move (see Figure 52[middle]). Finally it is straightforward to check that internal black sources behave like boundary Darboux sources (see Figure 52[right]).

The proof in the case $s = 0$ (infinite oval) goes along the same lines with the only difference that in the simplest case where there are neither internal sources nor sinks in F_0 nor changes of directions at the internal vertexes bounding F_0 then

$$\sum_{l=1}^{n_0} \epsilon_{wind}(f_l, g_l) = 0 \pmod{2}.$$

□

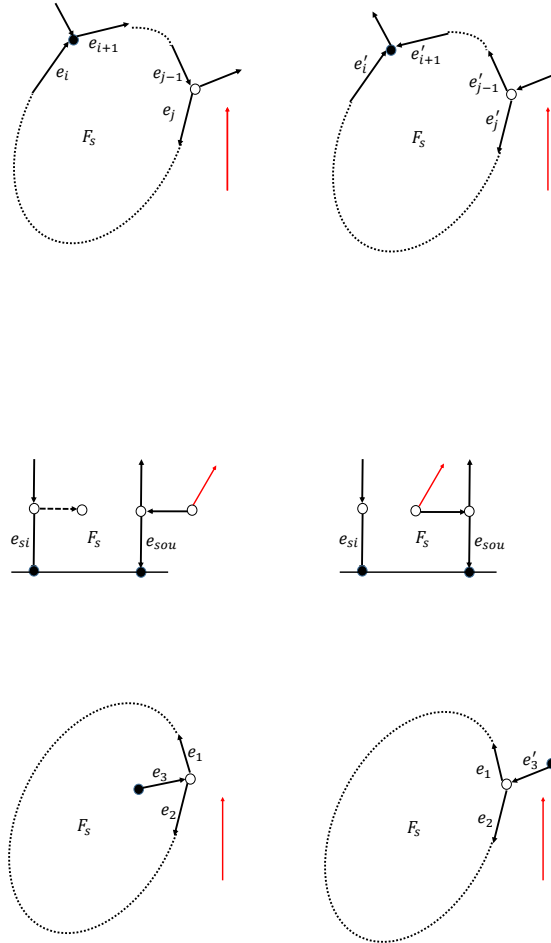


FIGURE 52. The relation between winding and changes of direction.

We are now ready to complete the proof of Theorem 4.1 using the Lemmas above.

Remark 10.2. Notations used in the next Theorem In the following Theorem $\mathcal{D} = \{\gamma_l, l \in [g + n - k]\}$ denotes either the vacuum network divisor $\mathcal{D}_{\text{vac}, \mathcal{N}', I}$ or the dressed network divisor $\mathcal{D}_{\text{dr}, \mathcal{N}'}$, where \mathcal{N}' is a given oriented network with $g + 1$ faces for $[A]$.

$\Gamma = \Gamma(\mathcal{N}) = \Gamma(\mathcal{N}')$ is the reducible rational curve for \mathcal{N} and Ω_s , $s \in [0, g]$, is the oval in Γ corresponding to the face F_s in the network. As usual, we denote F_0 the face corresponding to the infinite oval Ω_0 which contains the essential singularity.

For simplicity, we use the same symbol $\mathcal{D} \subset \Gamma(\mathcal{N})$ to denote the set of divisor points $P_l \in \Gamma_l$, $l \in [g+n-k]$, such that $\zeta(P_l) = \gamma_l$, with ζ the coordinate on Γ_l associated to the given orientation of the network.

In every oval Ω_s , $s \in [0, g]$, of $\Gamma(\mathcal{N})$, ν_s denotes the number of divisor points of \mathcal{D} belonging to the oval:

$$\nu_s = \#(\mathcal{D} \cap \partial\Omega_s),$$

μ_s , $\mu_{s,sou}$ and $\mu_{s,si}$ respectively denote the total number of Darboux univalent vertexes, of Darboux source univalent vertexes and of Darboux sink univalent vertexes belonging to F_s .

To count the number of divisor points on $\Gamma_0 \cap \Omega_s$, where Γ_0 is the $\mathbb{C}\mathbb{P}^1$ component corresponding to the boundary of the disk, we use the index ρ_s , $s \in [g]$. ρ_s is simply the total number of changes of signs of the vertex wavefunction on the edges at the boundary vertexes belonging to the intersection of F_s with the boundary of the disk. We remark that, by construction, $\rho_s = 0$ for all $s \in [0, g]$, if \mathcal{D} is the vacuum network divisor.

Theorem 10.2. *The number of divisor points in each oval (Theorem 4.1, items (1b)-(1c)). Let \mathcal{N}' , Γ , \mathcal{D} , ν_s , μ_s , $\mu_{s,sou}$, $\mu_{s,si}$ and ρ_s , $s \in [g]$ be as above. Then*

$$(106) \quad \nu_s + \mu_s + \rho_s = \begin{cases} 1 \pmod{2} & \text{if } s \in [g], \\ k \pmod{2} & \text{if } s = 0. \end{cases}$$

Proof. The proof follows applying Theorem 10.1 and Lemmas 10.1–10.2. For any fixed $s \in [g]$ let $(V_r; f_r, g_r^{(s)})$, $r \in [n_s]$, be the set of pair of edges f_r, g_r at internal vertexes V_r bounding F_s , where $[n_s]$ is the total number of pair of edges bounding F_s . We remark that a given vertex V may appear twice if two pairs of edges at V belong to the boundary of F_s (see Figure 49).

By construction, a divisor point $P_l \in \mathcal{D}$ belongs to $\Gamma_l \cap \Omega_s$ if and only if Γ_l corresponds to a white trivalent vertex V_l carrying an odd index at the edges $(V_l^{(s)}, f_l^{(s)}, g_l^{(s)})$ bounding F_s (see Theorem 10.1). Therefore the number ν_s of divisor points in $\mathcal{D} \cap \Omega_s$ satisfies

$$(107) \quad \nu_s = \sum_{\substack{r=1 \\ V_r \text{ tr.w.}}}^{n_s} \epsilon_{tot}(f_r, g_r) = \sum_{\substack{r=1 \\ V_r \text{ tr.w.}}}^{n_s} \epsilon_{cd}(f_r, g_r) + \sum_{\substack{r=1 \\ V_r \text{ tr.w.}}}^{n_s} \left(\epsilon_{cs}(f_r, g_r) + \epsilon_{wind}(f_r, g_r) + \epsilon_{int}(f_r, g_r) \right),$$

where the sums above run on all pair of edges at trivalent white vertexes belonging to the boundary of F_s . Using (102) and (103), the second sum in the r.h.s. of (107) has the same parity if we substitute it with the total contribution to the winding, change of sign and intersection indexes due to **all** pair of edges at internal vertexes bounding F_s , that is

$$(108) \quad \sum_{\substack{r=1 \\ V_r \text{ tr.w.}}}^{n_s} (\epsilon_{cs}(f_r, g_r) + \epsilon_{wind}(f_r, g_r) + \epsilon_{int}(f_r, g_r)) = \sum_{r=1}^{n_s} (\epsilon_{cs}(f_r, g_r) + \epsilon_{wind}(f_r, g_r) + \epsilon_{int}(f_r, g_r)) \pmod{2}.$$

Therefore, inserting (104), (107) and (108) in the r.h.s. of (106), for any $s \in [g]$, we easily get

$$(109) \quad \begin{aligned} \nu_s + \mu_s + \rho_s &\equiv \sum_{\substack{r=1 \\ V_r \text{ tr.w.}}}^{n_s} \epsilon_{tot}(f_r, g_r) + \mu_s + \rho_s = \sum_{\substack{r=1 \\ V_r \text{ tr.w.}}}^{n_s} \epsilon_{cd}(f_r, g_r) + \sum_{r=1}^{n_s} (\epsilon_{cs}(f_r, g_r) + \epsilon_{wind}(f_r, g_r) + \\ &+ \epsilon_{int}(f_r, g_r)) + \mu_{s,so} + \mu_{s,si} + \rho_s = 1 \pmod{2}. \end{aligned}$$

The proof of (106) at the infinite oval follows using (105) instead of (104):

$$(110) \quad \begin{aligned} \nu_0 + \mu_0 + \rho_0 + k &= \sum_{l, V_l \text{ tr.w.}} \epsilon_{tot}(f_l, g_l) + \mu_0 + \rho_0 + k = \\ &= \sum_{l, V_l \text{ tr.w.}} \epsilon_{cd}(f_l, g_l) + \sum_{l, V_l \text{ tr.w.}} (\epsilon_{cs}(f_l, g_l) + \epsilon_{wind}(f_l, g_l) + \epsilon_{int}(f_l, g_l)) + \mu_0 + \rho_0 + k = \\ &= \sum_{l, V_l \text{ tr.w.}} \epsilon_{cd}(f_l, g_l) + \sum_{l=1}^{n_s} (\epsilon_{cs}(f_l, g_l) + \epsilon_{wind}(f_l, g_l) + \epsilon_{int}(f_l, g_l)) + \mu_0 + \rho_0 + k = 0 \pmod{2}. \end{aligned}$$

□

The vacuum divisor on $\Gamma(\mathcal{N})$ is obtained from the vacuum network divisor $\mathcal{D} \equiv \mathcal{D}_{\text{vac}, \mathcal{N}', I}$ by eliminating the Darboux sink divisor points P_{j_s} , $s \in [n-k]$: $\mathcal{D}_{\text{vac}, \Gamma(\mathcal{N})} = \mathcal{D} \setminus \{P_{j_s}, s \in [n-k]\}$. In this case, we denote $\nu'_s = \nu_s - \mu_{s,si}$ the number of divisor points in $\mathcal{D}_{\text{vac}, \Gamma(\mathcal{N})} \cap \Omega_s$ for $s \in [0, g]$, and (106) becomes

$$(111) \quad \nu'_s + \mu_{s,so} = \begin{cases} 1 \pmod{2} & \text{if } s \in [g], \\ k \pmod{2} & \text{if } s = 0, \end{cases}$$

since $\rho_s = 0$ for any $s \in [0, g]$. So we completed the proof of Theorem 4.1 for curves associated to general networks.

If $\mathcal{D} \equiv \mathcal{D}_{\text{dr}, \mathcal{N}'}$ is the dressed network divisor, then $\mathcal{D}_{\text{KP}, \Gamma}$ is obtained from \mathcal{D} by eliminating the Darboux sink and source divisor points P_{j_s} , $s \in [n]$ and by adding the Sato divisor \mathcal{D}_S :

$\mathcal{D}_{\text{KP},\Gamma} = (\mathcal{D} \cup \mathcal{D}_S) \setminus \{P_{j_s}, s \in [n]\}$. In this case we denote $\nu_s'' = \nu_s - \mu_s$ the number of divisor points in $\mathcal{D}_{\text{KP},\Gamma} \cap (\Omega_s \setminus \Gamma_0)$. Therefore, (106) becomes

$$(112) \quad \nu_s'' + \rho_s = \begin{cases} 1 \pmod{2} & \text{if } s \in [g], \\ k \pmod{2} & \text{if } s = 0. \end{cases}$$

Since $\mathcal{D}_{\text{KP},\Gamma}$ an effective divisor of degree g , and each finite oval $\Omega_s, s \in [g]$ contains odd number of divisor points, then each $\Omega_s, s \in [g]$ contains **exactly one pole of $\mathcal{D}_{\text{KP},\Gamma}$** , and Ω_0 contains **no divisor points of $\mathcal{D}_{\text{KP},\Gamma}$** . As a corollary we see, that each $\Omega_s, s \in [g]$ contains either 0 or 1 Sato divisor point, and either 0 or 1 non-Sato divisor point. We summarize this as:

Corollary 10.1. *Let Ω_s be a finite oval of $\Gamma(\mathcal{N})$, then*

- (1) Ω_s contains exactly one divisor point of $\mathcal{D}_{\text{KP},\Gamma}$;
- (2) $\nu_s'' = 0, \rho_s = 1$ iff Ω_s contains one Sato divisor point;
- (3) $\nu_s'' = 1, \rho_s = 0$ iff Ω_s contains no Sato divisor point.

11. THE EFFECT OF POSTNIKOV MOVES AND REDUCTIONS ON THE KP DIVISOR

In this section we explain the role of Postnikov moves and reductions on the effective vacuum or dressed divisor. We label with the same indexes the vertexes, edges, faces in the network corresponding to components, double points, ovals in the curve. Let $(\mathcal{N}'_1, \mathcal{O}_1, \mathfrak{l})$ be an oriented network. Let $(\mathcal{N}'_2, \mathcal{O}_2, \mathfrak{l})$ be the oriented network obtained from it by applying one move (M1)–(M3) or one reduction (R1)–(R3), and assume that the orientation \mathcal{O}_2 coincides with \mathcal{O}_1 at all edges except at those involved in the move or reduction where we use Postnikov rules to assign the orientation. Let $\mathcal{D}_{\text{vac},\mathcal{N}'_l,I}, \mathcal{D}_{\text{dr},\mathcal{N}'_l}, \mathcal{D}_{\text{KP},\Gamma(\mathcal{N}'_l)}, \mathcal{D}_{\text{vac},\Gamma(\mathcal{N}'_l)}, l = 1, 2$, respectively be the vacuum and dressed network divisors and the vacuum and KP divisors before ($l = 1$) and after ($l = 2$) the transformation. Finally let $g(l) + 1$ and $\Omega_s^{(l)}, s \in [0, g(l)], l = 1, 2$, respectively be the number of ovals and their labeling in the two configurations.

To simplify notations, we use the same symbol $\gamma_l^{(s)}$ for the divisor number and the divisor point.

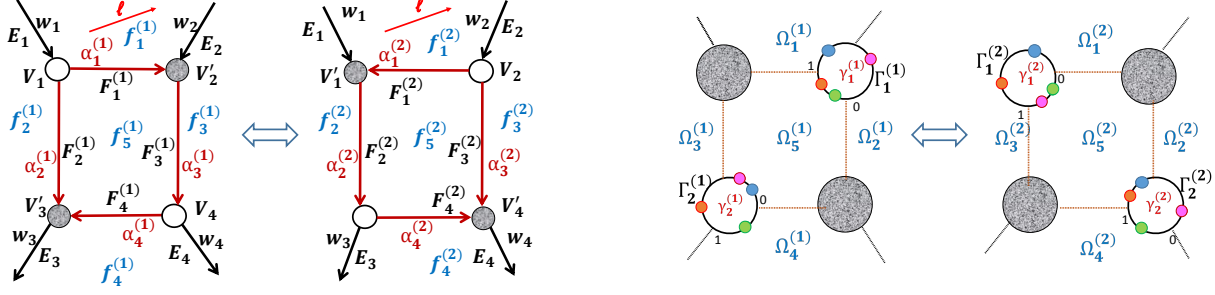


FIGURE 53. The effect of the square move [left] on the possible configurations of effective vacuum or dressed poles [right].

Lemma 11.1. *The effect of the square move (M1) on the divisor* Let \mathcal{N}'_2 be obtained from \mathcal{N}'_1 via move (M1). Let $\mathcal{D}(\mathcal{N}'_l)$ either be the vacuum or dressed network divisor for $l = 1, 2$. Then

- (1) the number of ovals is invariant: $g(2) = g(1)$;
- (2) the number of effective (vacuum or) dressed divisor points is invariant in every oval: $\nu_l^{(2)} = \nu_l^{(1)}$, $l \in [0, g(1)]$;
- (3) $\mathcal{D}(\mathcal{N}'_2) = \left(\mathcal{D}(\mathcal{N}'_1) \setminus \{\gamma_1^{(1)}, \gamma_2^{(1)}\}\right) \cup \{\gamma_1^{(2)}, \gamma_2^{(2)}\}$, where $\gamma_l^{(s)}$, $l = 1, 2$, is the pole on $\Gamma_l^{(s)}$, the copy of \mathbb{CP}^1 associated to each white vertex involved in the square move on \mathcal{N}'_s , $s = 1, 2$;
- (4) Either $\gamma_l^{(s)}$, $s = 1, 2$, $l = 1, 2$ are all untrivial divisor poles or all trivial divisor points.

The proof is omitted. In Figure 53 we show the position of the poles before and after the square move using the formulas of the example in Section 8.1. In such case

$$\gamma_1^{(1)} = \frac{\alpha_2^{(1)}}{1 + \alpha_4^{(2)} c(\vec{t}_0)}, \quad \gamma_2^{(1)} = \frac{\alpha_1^{(1)}}{\alpha_4^{(1)} + c(\vec{t}_0)}, \quad \gamma_1^{(2)} = \frac{\alpha_4^{(1)} (1 + \alpha_4^{(2)} c(\vec{t}_0))}{\alpha_4^{(1)} + c(\vec{t}_0)}, \quad \gamma_2^{(2)} = \frac{1}{1 + \alpha_4^{(2)} c(\vec{t}_0)},$$

where $c(\vec{t}_0) = \Phi_{U_4}(\vec{t}_0) / \Phi_{U_3}(\vec{t}_0)$ is the ratio of the dressed wavefunction at the edges corresponding to vectors U_3 and U_4 . The colors of poles correspond to the following conditions on $c(\vec{t}_0)$:

TABLE 2. The square move and the effective vacuum or dressed divisor

Position of poles in $\Gamma^{(1)}$	Position of poles in $\Gamma^{(2)}$	Color used	Range of parameter
$\gamma_1^{(1)} \in \Omega_5^{(1)}, \gamma_2^{(1)} \in \Omega_4^{(1)}$	$\gamma_1^{(2)} \in \Omega_5^{(2)}, \gamma_2^{(2)} \in \Omega_4^{(2)}$	Green	$c(\vec{t}_0) > 0$
$\gamma_1^{(1)} \in \Omega_5^{(1)}, \gamma_2^{(1)} \in \Omega_2^{(1)}$	$\gamma_1^{(2)} \in \Omega_2^{(2)}, \gamma_2^{(2)} \in \Omega_5^{(2)}$	Red	$-\alpha_4^{(1)} < c(\vec{t}_0) < 0$
$\gamma_1^{(1)} \in \Omega_1^{(1)}, \gamma_2^{(1)} \in \Omega_5^{(1)}$	$\gamma_1^{(2)} \in \Omega_1^{(2)}, \gamma_2^{(2)} \in \Omega_5^{(2)}$	Blue	$-(\alpha_4^{(2)})^{-1} < c(\vec{t}_0) < -\alpha_4^{(1)}$
$\gamma_1^{(1)} \in \Omega_3^{(1)}, \gamma_2^{(1)} \in \Omega_5^{(1)}$	$\gamma_1^{(2)} \in \Omega_5^{(2)}, \gamma_2^{(2)} \in \Omega_3^{(2)}$	Pink	$c(\vec{t}_0) < -(\alpha_4^{(2)})^{-1}$

The flip move at black vertexes leaves the divisor invariant. The flip move at white vertexes may transform trivial divisor points into untrivial divisor points. In the following lemma we label $\Omega_l, l \in [4]$, the ovals involved in the flip move.

Lemma 11.2. *The effect of the flip move at white vertexes (M2) on the divisor* If \mathcal{N}'_2 is obtained from \mathcal{N}'_1 via a flip move (M2) at a pair of trivalent white vertexes. Let $\mathcal{D}(\mathcal{N}'_l)$ either be the vacuum or dressed network divisor for $l = 1, 2$. Then

- (1) the number of ovals is invariant: $g(2) = g(1)$;
- (2) the number of untrivial divisor points is invariant in every oval except possibly at the ovals involved in the move. In the ovals $\Omega_l, l \in [4]$ the parity of the number of divisor points before and after the move is invariant: $\nu_l^{(2)} - \nu_l^{(1)} = 0 \pmod{2}, l \in [4]$;
- (3) $\mathcal{D}(\mathcal{N}'_2) = \left(\mathcal{D}(\mathcal{N}'_1) \setminus \{\gamma_1^{(1)}, \gamma_2^{(1)}\} \right) \cup \{\gamma_1^{(2)}, \gamma_2^{(2)}\}$, where $\gamma_l^{(s)}, l = 1, 2$, is the pole on $\Gamma_l^{(s)}$, the copy of \mathbb{CP}^1 associated to each white vertex involved in the flip move on $\mathcal{N}'_s, s = 1, 2$;

The proof is omitted. In Figure 54 we show the position of the poles before and after the flip move [top-left], in function of the relative signs of the value of the (vacuum or dressed) wave function $\Psi_l^{(1)} \equiv \Psi_l^{(1)}(\vec{t}_0), l \in [4]$, at the double points of Γ . Faces f_l correspond to ovals Ω_l , the orientation of the edges in the graph at each vertex induces the local coordinates at each copy of \mathbb{CP}^1 in Γ . In Figure 54, $\Psi_l^{(2)}(\vec{t}_0) = \Psi_l^{(1)}(\vec{t}_0), l \in [4]$, the same color identifies the position of the poles before and after the move depending on sign relation of the wave-function at the double points. The divisor points in the initial configuration are

$$\gamma_1^{(1)} = \frac{\Psi_2^{(1)}(\vec{t}_0)}{\Psi_1^{(1)}(\vec{t}_0) + \Psi_2^{(1)}(\vec{t}_0)}, \quad \gamma_2^{(1)} = \frac{\Psi_1^{(1)}(\vec{t}_0) + \Psi_2^{(1)}(\vec{t}_0)}{\Psi_1^{(1)}(\vec{t}_0) + \Psi_2^{(1)}(\vec{t}_0) + \Psi_3^{(1)}(\vec{t}_0)},$$

and the divisor points after the flip move are

$$\gamma_1^{(2)} = \frac{\Psi_1^{(1)}(\vec{t}_0)}{\Psi_1^{(1)}(\vec{t}_0) + \Psi_3^{(1)}(\vec{t}_0)}, \quad \gamma_2^{(2)} = \frac{\Psi_2^{(1)}(\vec{t}_0)}{\Psi_1^{(1)}(\vec{t}_0) + \Psi_2^{(1)}(\vec{t}_0) + \Psi_3^{(1)}(\vec{t}_0)}.$$

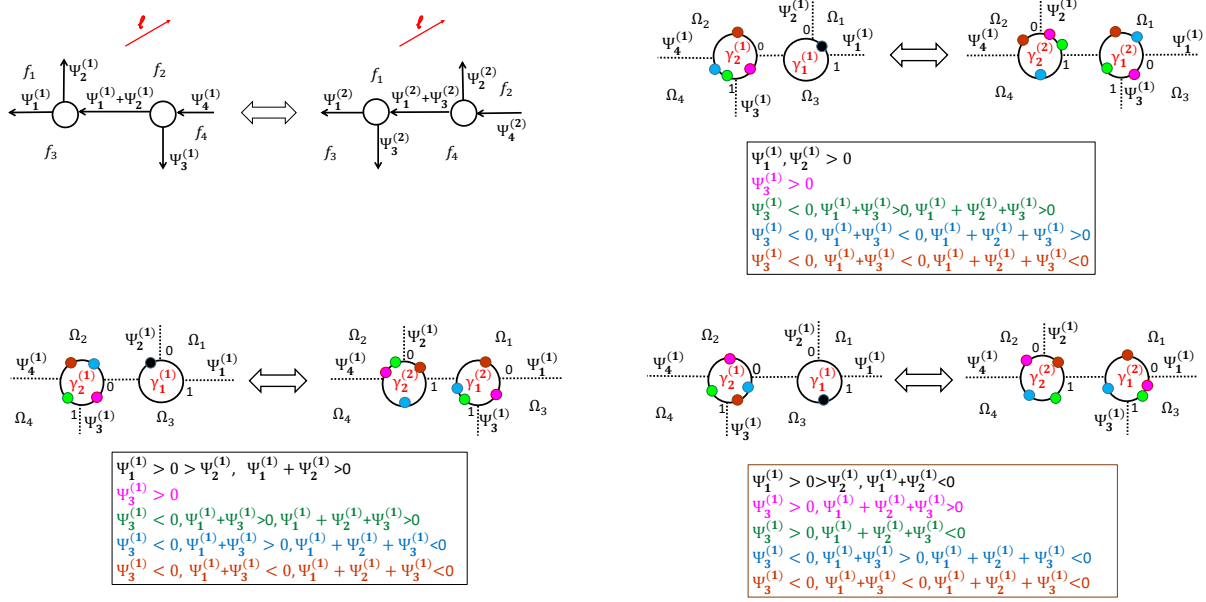


FIGURE 54. The effect of the flip move [top-left] on the possible configurations of effective (vacuum or) dressed poles [top-right],[bottom-left],[bottom-right].

The way the poles may change of position under the effect of the flip move is untrivial: they may move from an oval to another and untrivial divisor points may be transformed into trivial divisor points.

We remark that in the case of the dressed divisor not all combinations of signs are realizable at the finite ovals not containing Darboux sources or sinks. For instance in Figure 54[bottom,left], the blue case

$$\begin{aligned} &\Psi_2^{(1)}(\vec{t}_0), \Psi_3^{(1)}(\vec{t}_0) < 0 < \Psi_1^{(1)}(\vec{t}_0), \quad \Psi_1^{(1)}(\vec{t}_0), +\Psi_2^{(1)}(\vec{t}_0), \Psi_1^{(1)}(\vec{t}_0), +\Psi_3^{(1)}(\vec{t}_0) > 0, \\ &\Psi_1^{(1)}(\vec{t}_0), +\Psi_2^{(1)}(\vec{t}_0) + \Psi_3^{(1)}(\vec{t}_0) < 0, \end{aligned}$$

corresponds to

$$\gamma_1^{(1)}, \gamma_2^{(1)} \in \Omega_2, \quad \gamma_1^{(2)}, \gamma_2^{(2)} \in \Omega_4.$$

Moreover, if the edge vectors $E_1^{(1)}$ and $E_3^{(1)}$ are linearly dependent, while $E_2^{(1)}$, $E_1^{(1)}$ are linearly independent, then there exists a constant $c_{13} \neq 0$ such that $\Psi_3^{(1)}(\vec{t}) = c_{13}\Psi_1^{(1)}(\vec{t})$, for all \vec{t} . In

such case $\gamma_l^{(1)}$, $l = 1, 2$, and $\gamma_2^{(2)}$ are untrivial effective pole divisors while $\gamma_1^{(2)}$ is a trivial effective divisor pole, i.e. the normalized wavefunction is constant on the corresponding copy of \mathbb{CP}^1 .

The middle edge insertion removal (M3) does not affect the divisor configuration.

Lemma 11.3. The effect of (M3) on the divisor *If \mathcal{N}'_2 is obtained from \mathcal{N}'_1 via move (M3), then the number of ovals is invariant and the effective divisors before and after the move coincide.*

The parallel edge reduction eliminates an oval and a trivial divisor point. For notations we refer to Figure 55.

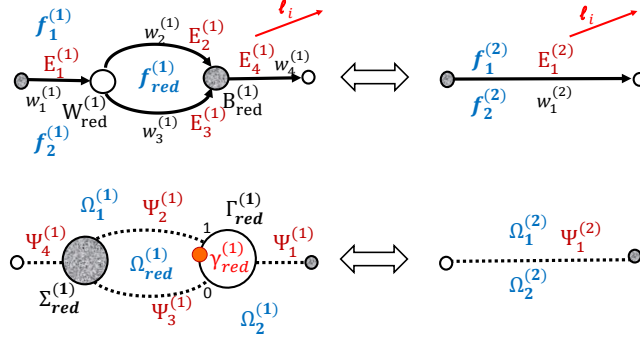


FIGURE 55. The parallel edge reduction [top] removes the effective vacuum or dressed pole $\gamma_{red}^{(1)}$ [bottom].

Lemma 11.4. The effect of (R1) on the divisor *If \mathcal{N}'_2 is obtained from \mathcal{N}'_1 via the parallel edge reduction (R1), then*

- (1) the number of ovals diminishes by one: $g(2) = g(1) - 1$;
- (2) the oval $\Omega_{red}^{(1)}$ corresponding to the face f_{red} , the components $\Gamma_{red}^{(1)}$, $\Sigma_{red}^{(1)}$ corresponding to the white and black vertices $W_{red}^{(1)}$, $B_{red}^{(1)}$ are removed by effect of the parallel edge reduction;
- (3) The trivial effective divisor point $\gamma_{red}^{(1)} \in \Gamma_{red}^{(1)} \cap \Omega_{red}^{(1)}$ is removed;
- (4) The positions of all other effective divisor points are not effected by the reduction.

In Figure 55 we show the effect of the parallel edge reduction. The relations between the edge vectors in the initial configuration

$$E_2^{(1)} = w_2^{(1)} E_4^{(1)}, \quad E_3^{(1)} = -w_3^{(1)} E_4^{(1)}, \quad E_1^{(1)} = w_1^{(1)} (E_2^{(1)} - E_3^{(1)}),$$

correspond to the following relations of the wavefunction in the initial configuration

$$\Psi_2^{(1)}(\vec{t}) = w_2^{(1)}\Psi_4^{(1)}(\vec{t}), \quad \Psi_3^{(1)}(\vec{t}) = -w_3^{(1)}\Psi_4^{(1)}(\vec{t}), \quad \Psi_1^{(1)}(\vec{t}) = w_1^{(1)}(\Psi_2^{(1)}(\vec{t}) - \Psi_3^{(1)}(\vec{t})), \quad \forall \vec{t},$$

so that the divisor point in $\Gamma_{\text{red}}^{(1)}$ is trivial

$$\gamma_{\text{red}}^{(1)} = -\frac{\Psi_3^{(1)}(\vec{t}_0)}{\Psi_2^{(1)}(\vec{t}_0) - \Psi_3^{(1)}(\vec{t}_0)} = \frac{w_3^{(1)}}{w_2^{(1)} + w_3^{(1)}}.$$

On both $\Gamma_{\text{red}}^{(1)}$ and $\Sigma_{\text{red}}^{(1)}$ the normalized wavefunction is independent of the spectral parameter and takes the value $\frac{\Psi_1^{(1)}(\vec{t})}{\Psi_1^{(1)}(\vec{t}_0)} \equiv \frac{\Psi_4^{(1)}(\vec{t})}{\Psi_4^{(1)}(\vec{t}_0)}$. After the reduction

$$E_1^{(2)} = E_1^{(1)}, \quad \Psi_1^{(2)}(\vec{t}) = \Psi_1^{(1)}(\vec{t}),$$

so that, for any \vec{t} , the normalized wavefunction keeps the same value after the reduction at the double point corresponding to such edge.

The dipole reduction (R2) corresponds to the removal of an edge carrying a null vector and leaves invariant the number of ovals and the position of the divisor point.

In the leaf reduction (R3) the only non-trivial case corresponds to the situation where the faces f_1, f_2 are distinct in the initial configuration. In this case we eliminate one oval and one divisor point.

Lemma 11.5. *The effect of (R3) on the divisor* If \mathcal{N}'_2 is obtained from \mathcal{N}'_1 via reduction (R3) and the faces f_1, f_2 be distinct. Let $\mathcal{D}(\mathcal{N}'_l)$ either be the vacuum or dressed network divisor for $l = 1, 2$. Then

- (1) the number of ovals diminishes by 1: $g(2) = g(1) - 1$;
- (2) $\mathcal{D}(\mathcal{N}'_2) = \mathcal{D}(\mathcal{N}'_1) \setminus \{\gamma_1^{(1)}\}$, where $\gamma_1^{(1)}$ is the pole on $\Gamma_1^{(1)}$ – the copy of \mathbb{CP}^1 associated to the white vertex involved in the reduction.

REFERENCES

- [1] S. Abenda. *On a family of KP multi-line solitons associated to rational degenerations of real hyperelliptic curves and to the finite non-periodic Toda hierarchy*, J.Geom.Phys. **119** (2017) 112–138.
- [2] S. Abenda, P.G. Grinevich. *Rational degenerations of M-curves, totally positive Grassmannians and KP-solitons*, arXiv:1506.00563 submitted.
- [3] E. Arbarello, M. Cornalba, P.A. Griffiths. *Geometry of algebraic curves. Volume II. With a contribution by Joseph Daniel Harris*, Grundlehren der Mathematischen Wissenschaften 268, Springer, Heidelberg, (2011) xxx+963 pp.

- [4] N. Arkani-Hamed, J.L. Bourjaily, F. Cachazo, A.B. Goncharov, A. Postnikov, J. Trnka. *Scattering Amplitudes and the Positive Grassmannian*, arXiv:1212.5605
- [5] N. Arkani-Hamed, J.L. Bourjaily, F. Cachazo, A.B. Goncharov, A. Postnikov, J. Trnka. *Grassmannian geometry of scattering amplitudes*, Cambridge University Press, Cambridge, (2016), ix+194 pp.
- [6] G. Biondini, S. Chakravarty. *Soliton solutions of the Kadomtsev-Petviashvili II equation*. Journal of Mathematical Physics, **47**, (2006), 033514; doi:10.1063/1.2181907.
- [7] M. Boiti, F. Pempinelli, A.K. Pogrebkov, B. Prinari. *Towards an inverse scattering theory for non-decaying potentials of the heat equation*, Inverse Problems **17** (2001) 937–957.
- [8] V. Buchstaber, A. Glutsyuk. *Total positivity, Grassmannian and modified Bessel functions*, arXiv:1708.02154.
- [9] S. Chakravarty, Y. Kodama. *Classification of the line-solitons of KP II*. J. Phys. A Math.Theor. **41** (2008), 275209.
- [10] S. Chakravarty, Y. Kodama. *Soliton solutions of the KP equation and application to shallow water waves*. Stud. Appl. Math. **123** (2009) 83-151.
- [11] L.A. Dickey. *Soliton equations and Hamiltonian systems*. Second edition. Advanced Series in Mathematical Physics, 26. World Scientific Publishing Co., Inc., River Edge, NJ, 2003. xii+408 pp.
- [12] A. Dimakis, F. Müller-Hoissen. *KP line solitons and Tamari lattices*, J. Phys. A **44** (2011), no. 2, 025203, 49 pp.
- [13] B.A. Dubrovin, *Theta functions and non-linear equations*, Russian Math. Surveys, **36**:2 (1981), 11–92.
- [14] B.A. Dubrovin, T.M. Malanyuk, I.M. Krichever, V.G. Makhankov. *Exact solutions of the time-dependent Schrödinger equation with self-consistent potentials*, Soviet J. Particles and Nuclei, **19**:3 (1988), 252–269.
- [15] B.A. Dubrovin, I.M. Krichever, S.P. Novikov. *Integrable systems*. Dynamical systems, IV, 177-332, Encyclopaedia Math. Sci., 4, Springer, Berlin, 2001.
- [16] B. A. Dubrovin, S.M. Natanzon. *Real theta-function solutions of the Kadomtsev-Petviashvili equation*. Izv. Akad. Nauk SSSR Ser. Mat. **52** (1988) 267-286.
- [17] V.Fock, A. Goncharov. *Moduli spaces of local systems and higher Teichmüller theory*, Publ.Math. I.H.E.S. **103** (2006), 1–211.
- [18] S. Fomin. *Loop-erased walks and total positivity*, Transactions of the AMS, **353**:9 (2001), 3563–3583.
- [19] S. Fomin, A. Zelevinsky. *Double Bruhat cells and total positivity*. J. Amer. Math. Soc. **12** (1999) 335-380.
- [20] S. Fomin, A. Zelevinsky. *Cluster algebras I: foundations*. J. Am. Math. Soc. **15** (2002) 497-529.
- [21] N.C. Freeman, J.J.C. Nimmo. *Soliton solutions of the Korteweg de Vries and the Kadomtsev-Petviashvili equations: the Wronskian technique*, Proc. R. Soc. Lond. A **389** (1983), 319–329.
- [22] F.R. Gantmacher, M.G. Krein. *Sur les matrices oscillatoires*. C.R. Acad. Sci. Paris **201** (1935) 577-579.
- [23] F.R. Gantmacher, M.G. Krein. *Oscillation Matrices and Kernels and Small Vibrations of Mechanical Systems*. (Russian), Gostekhizdat, Moscow- Leningrad, 1941, second edition 1950; German transl. as Oszillationsmatrizen, Oszillationskerne und kleine Schwingungen mechanischer Systeme, Akademie Verlag, Berlin, 1960; English transl. as Oscillation Matrices and Kernels and Small Vibrations of Mechanical Systems, USAEC, 1961, and also a revised English edition from AMS Chelsea Publ., 2002.

- [24] M. Gekhtman, M. Shapiro, A. Vainshtein. *Cluster algebras and Poisson geometry*. Mathematical Surveys and Monographs, 167. American Mathematical Society, Providence, RI, 2010. xvi+246 pp
- [25] I. M. Gel'fand, R. M. Goresky, R. D. MacPherson, V. V. Serganova. *Combinatorial geometries, convex polyhedra, and Schubert cells*. Adv. in Math. **63** (1987), no. 3, 301–316.
- [26] I.M Gel'fand and V.V. Serganova. *Combinatorial geometries and torus strata on homogeneous compact manifolds*. Russian Mathematical Surveys, **42** (1987), no. 2, 133–168.
- [27] A.B. Goncharov, R. Kenyon. *Dimers and cluster integrable systems*, Ann. Sci. Éc. Norm. Supér. (4) **46** (2013), no. 5, 747–813
- [28] P. Griffiths, J. Harris. *Principles of Algebraic Geometry*, John Wiley & Sons, 1978.
- [29] D.A. Gudkov. *The topology of real projective algebraic varieties*. Russ. Math. Surv. **29** (1974) 1-79.
- [30] A. Harnack. *Über die Vieltheiligkeit der ebenen algebraischen Curven*. Math. Ann. **10** (1876) 189-199.
- [31] R. Hirota. *The direct method in soliton theory*. Cambridge Tracts in Mathematics, 155. Cambridge University Press, Cambridge, 2004. xii+200 pp.
- [32] B.B. Kadomtsev, V.I. Petviashvili. *On the stability of solitary waves in weakly dispersive media*, Sov. Phys. Dokl. **15** (1970) 539-541.
- [33] S. Karlin. *Total Positivity, Vol. 1*. Stanford, 1968.
- [34] R. Kenyon, A. Okounkov, S. Sheffield. *Dimers and amoebae*, Ann. of Math. (2) **163** (2006), no. 3, 1019–1056
- [35] Y. Kodama. *Young diagrams and N -soliton solutions of the KP equation*, J Phys. A Math. Gen. **37** (2004), 11169–11190.
- [36] Y. Kodama. *KP solitons in shallow water* J. Phys. A: Math. Theor. **43** 2010, 434004.
- [37] Y. Kodama, L.K. Williams. *The Deodhar decomposition of the Grassmannian and the regularity of KP solitons*. Adv. Math. **244** (2013) 979-1032.
- [38] Y. Kodama, L.K. Williams. *KP solitons and total positivity for the Grassmannian*. Invent. Math. **198** (2014) 637-699.
- [39] I.M. Krichever. *An algebraic-geometric construction of the Zakharov-Shabat equations and their periodic solutions*. (Russian) Dokl. Akad. Nauk SSSR **227** (1976) 291-294.
- [40] I.M. Krichever. *Integration of nonlinear equations by the methods of algebraic geometry*. (Russian) Funkcional. Anal. i Priložen. **11** (1977) 15-31, 96.
- [41] I.M. Krichever. *Spectral theory of finite-zone nonstationary Schrödinger operators. A nonstationary Peierls model*, Functional Analysis and Its Applications, **20:3** (1986), 203–214
- [42] G. Lawler, *Intersections of random walks*, Birkhäuser, (1991).
- [43] G. Lusztig. *Total positivity in reductive groups*, Lie Theory and Geometry: in honor of B. Kostant, Progress in Mathematics **123**, Birkhäuser, Boston, (1994), 531–568.
- [44] G. Lusztig. *Total positivity in partial flag manifolds*, Representation Theory, **2** (1998), 70-78.
- [45] T.M. Malanyuk. *A class of exact solutions of the Kadomtsev-Petviashvili equation*. Russian Math. Surveys, **46:3** (1991), 225–227.

- [46] N. E. Mnëv *The universality theorems on the classification problem of configuration varieties and convex polytope varieties*, in *Topology and Geometry – Rohlin Seminar*, O. Ya. Viro ed., *Lecture Notes in Mathematics* **1346**, Springer, Heidelberg.
- [47] R. Marsh, K. Rietsch. *Parametrizations of flag varieties*, *Representation Theory*, **8**,(2004), 212–242.
- [48] V.B. Matveev. *Some comments on the rational solutions of the Zakharov-Shabat equations*. *Letters in Mathematical Physics*, **3** (1979), 503–512.
- [49] T. Miwa, M. Jimbo, E. Date. *Solitons. Differential equations, symmetries and infinite-dimensional algebras*. *Cambridge Tracts in Mathematics*, 135. Cambridge University Press, Cambridge, 2000. x+108 pp.
- [50] S.M. Natanzon. *Moduli of real algebraic surfaces, and their superanalogues. Differentials, spinors, and Jacobians of real curves*, *Russian Mathematical Surveys*, **54**:6 (1999), 1091–1147.
- [51] S.P. Novikov. *The periodic problem for the Kortewegde vries equation*, *Functional Analysis and Its Applications*, **8**:3 (1974), 236–246.
- [52] A. Postnikov. *Total positivity, Grassmannians, and networks.*, arXiv:math/0609764 [math.CO]
- [53] A. Postnikov, D. Speyer, L. Williams. *Matching polytopes, toric geometry, and the totally non-negative Grassmannian*. *J. Algebraic Combin.* **30** (2009), no. 2, 173-191.
- [54] K. Rietsch. *An algebraic cell decomposition of the nonnegative part of a flag variety*, *Journal of Algebra* **213** (1999), no. 1, 144-154.
- [55] M. Sato. *Soliton equations as dynamical systems on infinite-dimensional Grassmann manifold*. in: *Nonlinear PDEs in Applied Sciences (US-Japan Seminar, Tokyo)*, P. Lax and H. Fujita eds., North-Holland, Amsterdam (1982) 259-271.
- [56] I. Schoenberg. *Über variationsvermindende lineare Transformationen*, *Math. Zeit.* **32**, (1930), 321-328.
- [57] I.A. Taimanov. *Singular spectral curves in finite-gap integration*, *Russian Mathematical Surveys*, **66**:1 (2011), 107–144.
- [58] K. Talaska. *A Formula for Plücker Coordinates Associated with a Planar Network*, *IMRN*, **2008**, (2008), Article ID rnn081, 19 pages. doi:10.1093/imrn/rnn081
- [59] O. Ya. Viro. *Real plane algebraic curves: constructions with controlled topology* *Leningrad Math. J.* **1** (1990), no. 5, 1059–1134.
- [60] V.E. Zakharov, A. B. Shabat *A scheme for integrating the nonlinear equations of mathematical physics by the method of the inverse scattering problem. I*, *Funct. Anal. and Its Appl.*, **8** (1974), Issue 3, 226–235
- [61] Y. Zarmi. *Vertex dynamics in multi-soliton solutions of Kadomtsev-Petviashvili II equation*. *Nonlinearity* **27** (2014), 1499–1523.

DIPARTIMENTO DI MATEMATICA, UNIVERSITÀ DI BOLOGNA, P.ZZA DI PORTA SAN DONATO 5, I-40126 BOLOGNA
BO, ITALY

E-mail address: `simonetta.abenda@unibo.it`

L.D.LANDAU INSTITUTE FOR THEORETICAL PHYSICS, PR. AK SEMENOVA 1A, CHERNOGOLOVKA, 142432,
RUSSIA, PGG@LANDAU.AC.RU, LOMONOSOV MOSCOW STATE UNIVERSITY, FACULTY OF MECHANICS AND MATH-
EMATICS, RUSSIA, 119991, MOSCOW, GSP-1, 1 LENINSKIYE GORY, MAIN BUILDING,, MOSCOW INSTITUTE OF
PHYSICS AND TECHNOLOGY, 9 INSTITUTSKIY PER., DOLGOPRUDNY, MOSCOW REGION, 141700, RUSSIA.